Biogeochemical interactions and ecological consequences of sulfur in stands of wild rice

A Dissertation
SUBMITTED TO THE FACULTY OF THE
UNIVERSITY OF MINNESOTA
BY

Sophia LaFond-Hudson

IN PARTIAL FULFILLMENT OF THE REQUIREMENTS
FOR THE DEGREE OF
DOCTOR OF PHILOSOPHY

Advised by Nathan W. Johnson and John Pastor

May 2020

Acknowledgements

I would like to recognize the people who supported and encouraged this dissertation. This research would not have been possible without funding by Minnesota SeaGrant and the Fond du Lac Band of Lake Superior Chippewa. I am grateful to them for the opportunity to spend years deepening my understanding of manoomin, wild rice, *Zizania palustris.*

I would like to thank Chan Lan Chun and Jessica Savage for serving on my final committee and providing feedback on this dissertation. I would also like to thank Liz Austin-Minor and Sergei Katsev for serving as committee members for intermediary steps along the way. I appreciate all their work to strengthen my thinking and writing.

I would also like to extend my gratitude to Nancy Schuldt and Tom Howes for making sure my education extends beyond the science of *Zizania palustris* to include the cultural significance of manoomin. Likewise, I am grateful to Ed Swain for many conversations that reminded me of the larger context of my work and gave me insight into the ways science and policy can collaborate or collide. The encouragement from these three continually inspired and motivated my work on this project.

Thank you to my peers, fellow graduate students, and friends for supporting me throughout this journey by studying and writing together, talking through ideas, letting me practice presentations to them, and providing distractions from work when breaks were needed. Special thanks to Amber White, Dan Takaki, Jake Daire, and Marissa Castro for celebrating every major milestone and minor success along the way and listening or making me smile when things were hard. Likewise, I would like to thank my parents and brother for always believing in me and encouraging my ambitions while simultaneously ensuring I stay humble. I am extremely grateful for my husband, Zach, who not only listened to, but actively learned about my work while also providing the most incredible pep talks.

I also want to thank Brad Dewey for guiding me through setting up and caring for wild rice experiments, as well as volunteering to help with so many tedious tasks. I am convinced he is the world's leading expert on growing wild rice experimentally, and I am lucky to have learned more than a few things from him over the years.

Finally, and most importantly, I want to thank my advisors, Nate Johnson and John Pastor, whom I respect and admire deeply. I benefited greatly from John's experience and storytelling. I have learned so much from Nate's ability to communicate effectively with anyone, anywhere. They both balance their roles as critic and cheerleader exceptionally well. Their compassionately direct style of feedback pushed my science and writing beyond what I thought was possible. I remain impressed at their knack for seeing and articulating clearly the big picture. It has been a delight to learn from and with Nate and John; their mentorship will no doubt continue to influence the way I think and view the world.

Table of Contents

List of Tables

Dissertation

Appendix/Supplementary Information

List of Figures

Dissertation

Appendix/Supplementary Information

Chapter 1: Wild rice, treaty rights, and geochemistry

Wild rice (manoomin, *Zizania palustris*) grows extensively in shallow lakes and rivers of the upper Midwest and the western Great Lakes region of the United States and Canada, often forming vast monocultures covering tens or even hundreds of hectares on large lakes. Wild rice provides habitat for insects and fish, stabilizes sediment, and provides food for waterfowl and humans. Culturally, wild rice features prominently in many Ojibwe ceremonies as well as their migration story, which involved a prophesy that they should travel west until they found the food that grows upon the water (Fond du Lac Band of Lake Superior Chippewa, 2018). Archeologic evidence suggests that wild rice has been harvested in the region for at least 2000 years (Johnson, 1969; Yost and Blinnikov, 2011), and today both indigenous and non-indigenous people harvest its grain. The 1854 Treaty between the Lake Superior Chippewa and the United States granted the right of white settlers to settle in the land provided they did not interfere with ability of tribal members to hunt, fish, and gather on ceded territory.

Because populations of wild rice have been declining for several decades, these treaty rights are threatened and may lead to significant consequences on tribal health (Fond du Lac Band of Lake Superior Chippewa, 2018). Water level fluctuations and climate change have been identified as several threats to wild rice populations (*Natural Wild Rice in Minnesota*, 2008). Water level fluctuations during wild rice's floating leaf stage can either drown the plant in high water or remove physical support before the plant has constructed its own supportive tissues in low water. Climate change is related to water level fluctuations by intensifying storms and flood events, and creates problems for germination as winters warm, because seeds require four months below freezing.

Changes to surface water chemistry and sediment chemistry are another identified threat to wild rice, and the main topic of this dissertation. Because these changes originate primarily from pollution caused by industrial activities by settlers, they represent a threat to the cultural integrity of wild rice and a possible violation of treaty rights. Therefore, it behooves us to further our scientific understanding of the relationships between wild rice growth, life cycles, and population cycles and sediment geochemistry.

Several studies have examined correlations between surface water and sediment chemistry on wild rice (Lee, 2002; Lee and Stewart, 1983; Moyle, 1944). Moyle (1944) surveyed surface water chemistry and wild rice abundance of 200 lakes in Minnesota. He found that wild rice abundance declined as sulfate concentrations increased, large stands of wild rice did not occur when surface water sulfate concentrations exceeded 10 mg L^{-1}, and few, if any, individuals were present above 50 mg L^{-1}. As a result of his work, in 1973 the state of Minnesota adopted 10 mg L^{-1} sulfate as a protective water quality standard for wild rice waters (Specific Water Quality Standards for Class 4 Waters of the State; Agriculture and Wildlife). Later, sediment Eh was found to control wild rice productivity (Painchaud and Archibold, 1990). Work in other vegetated aquatic ecosystems showed that sulfide, the reduced form of sulfate present at low Eh, was responsible for die-offs of aquatic plants in a range of marine to freshwater environments, including *Thalassia testudinum* (turtlegrass), *Spartina alterniflora* (cordgrass) and *Stratiotes aloides* (water soldiers) (DeLaune et al., 1983; Lee and Dunton, 2000; Smolders et al., 2003). The objective of this dissertation is to elucidate some of the important biogeochemical interactions between wild rice and sulfur and the ecological consequences of these interactions for stability and health of wild rice populations.

Sulfide inhibits nutrient uptake in a variety of plants, both aquatic and terrestrial (Joshi et al., 1975; Koch et al., 1990; Koch and Mendelssohn, 1989; Martin and Maricle, 2015). The molecular mechanism for decreased nutrient uptake is that sulfide binds with iron in the electron transport chain, preventing ATP formation and inhibiting active processes, of which nutrient uptake is one (Allam and Hollis, 1972; Martin and Maricle, 2015). Nitrogen is the limiting nutrient in wild rice and is primarily taken up during seedling emergence and seed production (Grava and Raisanen, 1978; Sims et al., 2012). Mesocosm studies have showed that wild rice populations grown in elevated sulfate experienced high concentrations of porewater sulfide and were especially vulnerable during these life stages in which nitrogen uptake typically occurs (Pastor et al., 2017).

Iron may mitigate sulfide toxicity by decreasing sulfide activity in sediment in several ways. Reduction of iron oxides are thermodynamically more favorable than sulfate reduction. Thus, in sediments containing both iron oxides and sulfate, ferrous iron (the reduced form) should be present when sulfate is reduced. Ferrous iron and sulfide can combine to produce iron monosulfide (FeS) or pyrite (FeS_2), a solid phase with low aqueous activity. Despite the predictability of the sequence of electron acceptors used in anaerobic respiration, coincident iron reduction and sulfate reduction in close proximity has been documented, during which the subsequently produced sulfide reacts abiotically with nearby iron (hydr)oxides to produce reduced iron and elemental sulfur (Hansel et al., 2015). Field studies show that wetlands receiving high iron groundwater inputs have less sulfide impacts (Lamers et al., 2002).

The concept that surface water chemistry or sediment geochemistry affects the abundance and distribution of macrophyte species has been around for 100 years (Misra,

1938; Moyle, 1944; Pearsall, 1920); as mainly immobile organisms, plants are necessarily impacted by the geochemical conditions of their sediment, but they also employ mechanisms that control their geochemical environment. In order to understand how the geochemical environment affects wild rice, we need to also understand how wild rice influences its geochemical environment. Like many aquatic plants, wild rice has a conduit made from aerenchyma tissue that allows transport of oxygen and other gases between the atmosphere and the rhizosphere (Armstrong, 1980; T.D Colmer, 2003; Lai et al., 2012; Stover, 1928). Radial oxygen loss from roots creates an oxic zone at the root surface (Maisch et al., 2019; Schmidt et al., 2011; Van der Welle et al., 2007). Radial oxygen loss can have profound consequences for an ecosystem by altering the overall sediment redox potential and consequentially changing the interactions among all redox active species and species that react with redox active species. Oxygen released into the rhizosphere can stimulate nitrification and denitrification at the redox boundary adjacent to root surfaces (Reddy et al., 1989; Risgaard-Petersen and Jensen, 1997), causing a greater loss of N_2 to the atmosphere than in bare sediment. Radial oxygen loss promotes formation of iron oxides (Mendelssohn et al., 1995) which can adsorb phosphates in the adjacent sediment and on root surface iron oxides (Christensen and Sand-Jensen, 1998; Han et al., 2018), blocking uptake and creating a biologically unavailable sink for phosphorus. In ecosystems with large populations of aquatic plants oxygenating their rhizospheres, these nutrient dynamics controlled by radial oxygen loss can promote oligotrophic conditions within an ecosystem.

Porewater chemistry can fluctuate widely on diurnal time scales as rates of radial oxygen loss change with photosynthetic activity. Diurnal redox patterns in sediment

indicate that oxygenation of the rhizosphere is related in part to photosynthesis (Lee and Dunton, 2000; Ruiz-Halpern et al., 2008). Only a couple of studies have considered temporal patterns of oxygen release outside of diurnal fluctuations (Soana and Bartoli, 2013), so the seasonal and interannual time scales on which ROL varies, and the subsequent impacts to many other dissolved species, is not yet well understood. Temporal fluctuations in radial oxygen loss would greatly affect the redox conditions of sediment in a dense stand, leading to changes in toxic reduced compounds available to plants, including sulfide (Kinsman-Costello et al., 2015; Painchaud and Archibold, 1990).

Temporal variations in labile organic matter may also change the chemistry of macrophyte stands (Pulido et al., 2011), including wild rice. If labile organic matter inputs overwhelm the oxygen released by roots, the oxidized zone of sediment around the roots may be eliminated. Some aquatic plants release root exudates, small labile carbon compounds, from their roots into the rhizosphere during the growing season. Examples include siderophores that chelate iron for uptake by the plant, or compounds that stimulate microbial communities. Regardless of the function of root exudates, a notable consequence is that they provide labile carbon to sediment depths that generally contain more recalcitrant forms of carbon. One study observed increased sulfate reduction rates in a New England salt marsh dominated by *Spartina alterniflora* during periods of plant growth, followed by decreased rates during reproduction or infestation (Hines et al., 1989). This suggests sulfate reduction rates were controlled by root exudates released during growth, but not during reproduction or infestation when the plant needed to conserve nutrients. This is one of only a few studies that suggests sulfur geochemistry changes on time scales controlled by plant development.

Radial oxygen loss combined with iron may protect plants from sulfide, as together, iron and oxygen react to form iron oxides directly on root surfaces (Jorgenson et al., 2012; Mendelssohn et al., 1995) which may act as a redox buffer to protect against reduced species, especially sulfide (Povidisa et al., 2009; Ruiz-Halpern et al., 2008). Oxygen and ferrous iron gradients in saturated, vegetated sediment exist in opposite directions with high O_2 at root surfaces decreasing with distance away from the root and high Fe^{2+} in bulk sediment decreasing towards root surface, creating geochemical micro-niches and rhizosphere acidification due to iron oxidation (Maisch et al., 2019). In some cases, iron oxides do not completely prevent sulfide intrusion (Povidisa et al., 2009; Ruiz-Halpern et al., 2008). Iron oxides do not always cover the entire root surface and at night when photosynthesis ceases, lower rates of radial oxygen loss may allow sulfide to reduce iron oxides and enter roots (Lee and Dunton, 2000). Several studies have noted black roots forming on roots of white rice (Armstrong and Armstrong, 2005; Gao et al., 2003; Jacq et al., 1991; Sun et al., 2016), presumably iron sulfide. Sulfide-induced formation of suberin in the cell walls of roots forms a gas-impermeable layer that keeps dissolved sulfide out, but also prevents oxygen from being released (Armstrong and Armstrong, 2005). This barrier may lead to iron sulfide precipitation on the outside of the root surface, but because both oxygen and iron oxides can oxidize sulfide, the mechanism by which enough sulfide reaches the root surface to induce suberization is unclear. Iron sulfide is stable and unreactive, and therefore thought to be nontoxic to plants, but the consequences of an iron sulfide coating on the root surface has not yet been studied.

A life-cycle consequence of sulfide-inhibited nutrient uptake may be slower development. In nutrient limited conditions, plants, including wild rice, experience

ontogenetic drift (McConnaughay and Coleman, 1999; Sims et al., 2012) in which their phenology is delayed compared to plants growing without nutrient limitation. In some plant species, ontogenetic drift may give plants a competitive disadvantage compared to plants that grow faster. Wild rice tends to grow in monotypic stands with little competition from other species, but delayed development may adversely affect wild rice populations if they cannot cope with asynchronies in plant phenology and environmental conditions, such as temperature and length of daylight.

Even in the absence of elevated sulfate, wild rice experiences asynchronies between nitrogen supply in the sediment and nitrogen demand by the plant. Wild rice takes up nitrogen primarily during emergence from the water column and during seed production (Grava and Raisanen, 1978). Decomposition of litter can temporarily immobilize nitrogen resulting in delayed availability after the time period it was required by plants. This has been documented in terrestrial plants (de Jong and Klinkhamer, 1985; Knapp and Seastedt, 1986) as well as wild rice (Pastor and Walker, 2006; Walker et al., 2010). Years with high productivity produce large quantities of litter. The litter-microbe complex breaks down the litter and takes up nitrogen, causing lower availability of inorganic nitrogen. The decrease in available nitrogen for plants creates lower productivity until the nitrogen immobilized by the litter-microbe complex is mineralized. In wild rice, this litter-driven productivity cycle has a period of four years.

Although elevated sulfate produces sulfide, which inhibits nutrient uptake, sulfate addition to aquatic ecosystems increases nutrient availability, so although individual plants may be harmed by sulfide, we do not know how sulfate will interact with the population cycles driven by asynchronous immobilization of nitrogen. Sulfate provides

additional electron acceptors that can mineralize organic matter (Myrbo et al., 2017b; Smolders et al., 2003). Much of the work on the links between elevated sulfate and eutrophication, came out of the Netherlands when aquifer depletion led agriculture to switch their irrigation source to the Rhine River, which has much higher concentrations of sulfate than the aquifers did originally (Smolders et al., 2003). Additionally, as aquifers dried and were exposed to oxygen, pyrite was oxidized, increasing sulfate in groundwater as well. These increases in sulfate led to major declines in aquatic plant species sensitive to sulfide, especially rooted macrophytes, and increased plant species that tolerated eutrophic conditions, consisting mainly of floating species that do not root in the sediment. Increased alkalinity generated by sulfate reduction (Anderson and Schiff, 1987) provides abundant dissolved inorganic carbon which can be used by fast growing species to outcompete slower growing species (Lucassen et al., 2009). We know that sulfide inhibits nutrient uptake, but we do not yet know if increased nutrient availability from sulfate can compensate for decreased nutrient uptake and how this may affect asynchronous nutrient availability.

From a management perspective, we want to know how sulfur geochemistry impacts wild rice population dynamics and survival for purposes of conservation and restoration. This objective requires us to understand how wild rice physiology and life cycle patterns affect the fate of sulfur in wild rice beds during specific life stage transitions, life cycles, and population cycles. Experimentally, wild rice is a good model organism because its annual life cycle means that growth of roots and shoots start over each year. The life cycle of wild rice is well described, as is its plasticity in response to nutrient and light limitation (Grava and Raisanen, 1978; Sims et al., 2012). Prior work

has demonstrated that wild rice is sensitive to sulfide concentrations (Myrbo et al., 2017a; Pastor et al., 2017) and self-sustaining mesocosms are well-suited to studying interannual population dynamics (Pastor et al., 2017; Walker et al., 2010).

In this dissertation, I will start by describing mechanisms and timing of sulfide exposure to individual plants and sequentially expand the scope to the ways elevated sulfate affects the stability of interannual wild rice population cycles. Because the literature describes radial oxygen loss and iron oxides as processes that protect the root surface, I will demonstrate the mechanism of sulfide exposure in plants that have iron oxides but are known to be sensitive to sulfide. I will explain how this involves a plant-driven seasonal change in the root surface redox potential in Chapter 2, and in Chapters 2 and 3, I will explore the geochemical and ecological consequences of changes in sediment or root surface redox potential throughout the life cycle. In Chapter 4, I will show how life stages that are especially vulnerable to sulfide's effects can destabilize the biomass oscillations that occur in healthy, sustainable populations of wild rice as well as how iron and organic matter affect stability in the presence of elevated sulfate.

Chapter 2: Iron sulfide formation on root surfaces controlled by the life cycle of wild rice (*Zizania palustris*)

LaFond-Hudson, S., Johnson, N.W., Pastor, J., Dewey, B., 2018. Iron sulfide formation on root surfaces controlled by the life cycle of wild rice (Zizania palustris). Biogeochemistry 141, 95–106. https://doi.org/10.1007/s10533-018-0491-5
The final publication is available at www.springerlink.com

ABSTRACT

Iron sulfide plaques have been observed on roots of wild rice (*Zizania palustris*) and other wetland plants grown in sulfur-impacted freshwater ecosystems, but the mechanism of their formation and ramifications for plants have not been investigated. We exposed a model annual wetland plant, *Zizania palustris,* to elevated sulfate concentrations (3.1 mM) and quantified the development of iron-oxide and iron sulfide precipitates on root surfaces throughout the plant life cycle. During the onset of seed production, root surfaces amended with sulfate transitioned within one week from iron (hydr)oxide plaques to iron sulfide plaques. During the same week, Fe(III) decreased on roots of plants not amended with sulfate but FeS did not accumulate. Prior to FeS accumulation, sulfate-amended plants had taken up the same amount of N as unamended plants. After FeS accumulation, total plant nitrogen did not increase further on sulfate-amended plants, indicating a cessation in nitrogen uptake, whereas total plant N continued to increase in unamended plants. Sulfate-amended plants produced fewer and lighter seeds with less nitrogen than unamended plants. FeS precipitation on roots may be associated with elevated sulfide and inhibited nitrogen uptake before the end of the plant's life cycle, thus affecting the populations of this annual aquatic plant. We propose a mechanism by which a physiologically-induced decline in radial oxygen loss near the end of a plant's life cycle initiates a precipitous decline in redox potential at the root surface and in

adjacent porewater, initiating accumulation of iron sulfide plaques. These plaques could be an important locus for iron sulfide accumulation in wetland sediments.

INTRODUCTION

Introduction of sulfate to low-sulfate freshwater ecosystems and subsequent reduction to sulfide can induce eutrophication, enhance methyl mercury production, and decimate populations of sensitive aquatic plant species (Caraco et al. 1989, Gilmour et al. 1992, Smolders et al. 2003). Field observations have correlated elevated sulfide concentrations in sediment with population declines and decreased density of some aquatic plants (Myrbo et al. 2017, Pulido et al. 2012, Smolders et al. 2003). Black iron sulfide (FeS) plaques have been observed on the roots of aquatic plants grown with elevated sulfide in several sulfur addition experiments (Gao et al. 2003, Jacq et al. 1991, Koch and Mendelssohn 1989) including our outdoor mesocosm experiment with self-perpetuating wild rice (*Zizania palustris*) populations (Pastor et al. 2017); however, little is known about conditions conducive to iron sulfide precipitation on roots and the mechanism by which it occurs.

Roots of aquatic plants create redox interfaces that are hot spots for cycling of nitrogen, sulfur, iron, and other metals (Soana et al. 2015, Schmidt et al. 2011, Lee and McNaughton 2004). Many aquatic plants transport oxygen from the atmosphere to the roots through porous tissue called aerenchyma (Armstrong and Armstrong 2005). Radial oxygen loss from roots reacts with ferrous iron in sediment to form iron (hydr)oxide plaques at the interface of the oxidized root surface and the reduced sediment (Christensen and Sand-Jensen 1998, Mendelssohn and Postek 1982, Snowden and

Wheeler 1995). Together, radial oxygen loss and iron (hydr)oxide plaques provide a supply of electron accepting compounds at the root surface, hereafter referred to as an electron accepting buffer. This buffer may inhibit sulfide formation and precipitation in several ways. The release of oxygen by plant roots may reoxidize sulfide and inhibit sulfate reduction (Holmer et al. 1998). In addition, Fe(III) can oxidize sulfide, and the reduction of Fe(III) to Fe(II) may outcompete sulfate reduction (Roden and Wetzel 1996, Hansel et al. 2015). Others have observed increased FeS precipitation on roots and in sediments shortly after plant senescence (Jacq et al. 1991, Giblin and Howarth 1984), suggesting a decrease in the strength of the electron accepting buffer. However, the timing of sulfide interactions with iron on root surfaces, particularly in relation to the life cycle of the plants, remains largely unexplored.

To explore these processes, we subjected wild rice, *Zizania palustris*, an annual plant that forms large monotypic stands in the lakes and rivers of Minnesota, Wisconsin, northern Michigan, and Ontario, to enhanced sulfate concentrations. Although radial oxygen loss has not been directly quantified in wild rice, aerenchyma tissue, which transports oxygen to roots, have been observed and root surface iron oxides have been studied and documented in this species (Stover 1928, Jorgenson et al. 2012). In a previous mesocosm experiment with wild rice, increasing concentrations of porewater sulfide decreased vegetative biomass production only slightly, but strongly decreased annual seed production, leading to population declines in subsequent years (Pastor et al. 2017). Hydroponics experiments have demonstrated that sulfide reduces nutrient uptake in wetland plants (Joshi et al. 1975, Koch and Mendelssohn 1989) through inhibition of metallo-enzymes in the electron transport chain and subsequent inhibition of ATP

production required for nutrient transport (Allam and Hollis 1972, Koch et al. 1990, Martin and Maricle 2015). It is not well understood why the seed production life stage of wild rice is especially vulnerable to sulfide, but decreased seed production may be associated with the timing of favorable conditions for sulfate reduction and concomitant FeS accumulation on roots.

To identify the drivers of FeS formation on the root surfaces, we tested the hypothesis that surface water sulfate loading induces FeS formation on roots. To investigate the implications of FeS root plaques for nitrogen uptake during seed production, we explored the timing of FeS formation on wild rice roots. We exposed wild rice plants to elevated surface water sulfate and quantified the speciation of iron and sulfur on root surfaces and in rooting-zone porewater during reproductive life stages. Throughout the life cycle of the plant, we also monitored growth and seed production.

METHODS

Sediment was collected from Rice Portage Lake (MN Lake ID 09003700, 46.703810, -92.682921) on the Fond du Lac Band of Lake Superior Chippewa Reservation in Carlton County, Minnesota on 5/15/15 and placed in a 400 L polyethylene stock tank (High Country Plastics) where it was homogenized by shovel. Initial total carbon in the sediment was 14.8 ± 1.70 % and initial total nitrogen was 1.12 ± 0.13 % by dry weight. Eighty 4 L plastic pails were then filled with 3 L of the sediment. Each 4 L pail was placed inside a 20 L bucket that was filled with 12 L of groundwater from an on-site well to provide a 12-15 cm water column. In each pail, two seeds that were

harvested in 2014 from Swamp Lake on the Grand Portage Reservation (MN Lake ID 16000900, 47.951856, -89.856844) were planted on 5/15/15 (Julian day 135).

Forty randomly chosen buckets were amended with sulfate and forty were left unamended. On 6/3/15, the forty amended buckets received an aliquot of stock solution (5.15 g of Na_2SO_4 dissolved in 200 ml of deionized water) to result in 300 mg L^{-1} (3.1 mM) sulfate. We hereafter refer to all porewater, sediment, and plants in these buckets as "amended". This concentration is close to the EPA secondary standard for drinking water, 250 mg L^{-1} (2.6 mM), intended to prevent laxative effects and an unpleasant taste. Although northeastern Minnesota generally has sulfate concentrations less than 10 mg L^{-1} (0.1 mM), concentrations of sulfate higher than 2.6 mM are found in some Minnesota waters, either naturally from geologic sources or from anthropogenic inputs (Myrbo et al. 2017). A sulfate concentration of 3.1 mM caused wild rice populations to go extinct within five years in previous mesocosm experiments with the same sediment (Pastor et al. 2017). The overlying water was sampled twice throughout the trial and re-adjusted to 3.1 mM SO_4 by adding additional Na_2SO_4 stock solution on 7/10/15. Unamended buckets had an average surface water sulfate concentration of 0.15 ± 0.01 mM when sampled on 6/23/15, consistent with the concentration of sulfate in groundwater from the on-site well. This is only slightly above observations of Moyle (1944) that wild rice grows best in waters less than 10 mg L^{-1} sulfate. We hereafter refer to all porewater, sediment, and plants in these buckets as "unamended." Shoots were thinned on 6/23/15 to one plant per bucket. Shoot height ranged from 10-20 cm and the tallest, most robust shoot in each bucket was left in place.

The annual life cycle of wild rice begins with emergence from the sediment and water column in June, continues with vegetative growth in July, followed by flowering and seed production in August, and ends with the shedding of seeds and death of the plant from late August to late September. Seeds overwinter in the sediment until they germinate in May (Grava and Raisanen 1978, Sims et al. 2012). Four plants were harvested every two weeks from randomly chosen amended and unamended buckets beginning at the onset of flowering (7/9/15, day 190) and continuing to the onset of seed production (8/20/15, day 232), after which plants were harvested weekly until senescence (9/22/15, day 265). The first seeds were collected on 8/20/15 (day 232) but were unripe and not yet filled. Mature seeds were not produced until one week after the start of seed production (day 239). On the last sample date (day 265) seeds were collected but were unfilled. Stems and leaves were no longer green, indicating that the plants had senesced. Of the four amended replicates sampled on this date, two plants did not produce seeds. Thus, "mature seed production" refers to seeds produced between Julian days 239-253.

Each plant was removed from the sediment and immediately rinsed in buckets of deoxygenated water continuously bubbled with a rapid stream of nitrogen. If seeds were present, they were removed prior to sampling the plant and saved for separate analysis. While submerged in deoxygenated water, the stem was cut just above the root ball so that the shoots could be saved for mass and N analysis. The still submerged roots were then placed in jars full of deoxygenated water, which were immediately placed in a plastic bag flushed with nitrogen and transported to an oxygen-free glove box (Coy Lab Products, 97.5 % N_2, 2.5 % H_2). In the glove box, the roots were cleaned of sediment and all

organic matter except living wild rice roots prior to removing a 1-2 g section of wet root mass for AVS and iron analysis.

The plants and seeds were rinsed with deionized water and dried in paper bags for seven days at 65 °C. The dried plants were weighed, placed in polycarbonate vials with stainless steel balls, and shaken in a SPEX 800M mixer mill until the samples were in a powdered form. Seeds were counted, weighed, and powdered using the same method. The samples were transferred to glass vials and dried again overnight at 65 °C with caps loosely covering the vials. Samples were quantified for total N on an elemental analyzer coupled to a Finnigan Delta Plus XP isotope ratio monitoring mass spectrometer.

Sediment was collected at the beginning and end of the growing season. Immediately after sediment homogenization (5/15/15), five replicate samples were placed in jars and analyzed for AVS and simultaneously extracted iron. At the end of the growing season (9/22/15), a 7-cm diameter sediment core was collected from the top 10 centimeters of each bucket prior to root sampling. Jars were filled completely with sediment and placed in a plastic bag filled with nitrogen to prevent oxidation during transport to a glove box. In the glove box, sediment was homogenized and allocated for AVS and iron extraction.

From both sediment and roots, AVS and iron were extracted simultaneously from a 1-3 g wet sample (0.1-0.5 g dry) using 7.5 ml 1 N HCl for 4 hours using a modified diffusion method (Brouwer and Murphy 1994). During a room temperature acid incubation with gentle mixing, sulfide was trapped in an inner vial containing 3 ml Sulfide Antioxidant Buffer (SAOB) and subsequently quantified using a ThermoScientific sulfide ion-selective electrode with a detection limit of 0.01 mmol L^{-1}.

After the extraction, two aliquots of the 1 N HCl extracts were used for iron quantification. Ferrous iron was immediately quantified colorimetrically using the phenanthroline method on a HACH DR5000 UV-Vis spectrophotometer (Greenberg et al. 1992), and weak acid extractable iron (sum of Fe(II) + Fe(III) concentrations, hereafter referred to as "total extractable iron") was quantified using a Varian fast sequential flame atomic absorption spectrometer with an acetylene torch.

A subset of roots was tested for chromium(II)-reducible sulfur (CRS) to determine whether AVS included all total reduced inorganic sulfur on the roots. A diffusion-based CRS method was used, which can fully extract all amorphous iron sulfide and pyrite and can partially extract elemental sulfur (Burton et al. 2008). The same sampling apparatus was used for extraction of AVS and CRS (see Burton et al. 2008 Fig. 1 for a diagram of the sampling apparatus). Chromic acid for CRS analysis was prepared according to Burton et al. (2008). Inside an oxygen-free glove box, a section of root from a plant previously analyzed for AVS was placed in the analysis bottle. An inner vial containing SAOB was also placed inside the bottle prior to sealing. Bottles were removed from the glove box and injected with chromic acid with no oxygen exposure. CRS was extracted for 48 hours and quantified using a ThermoScientific sulfide ion-selective electrode.

One day prior to each root sampling date, the porewater was sampled for sulfide, sulfate, iron, and pH. First, pH was measured *in-situ* with a ThermoScientific Orion pH electrode at a depth of 5 cm below the sediment surface and 2 cm from the stem of the wild rice plant. Porewater was collected using 5-cm length, 2-mm diameter tension lysimeter filters (Seeberg-Elverfeldt et al. 2005) (Rhizons) attached with a hypodermic

needle to an evacuated, oxygen-free serum bottle sealed with a 20 mm thick butyl-rubber stopper (Bellco Glass, Inc). The entire filter end of the Rhizon was inserted vertically into the sediment just below the surface. The goal was to draw water from approximately the upper 5 cm of sediment without drawing surface water. The filter was placed with minimal jostling to avoid creating a cavity around the filter that would allow surface water to enter the sediment and contaminate the porewater. The Rhizon was placed approximately 2 cm away from the stem of the wild rice plant and on the opposite side from where pH was measured (Supplementary Fig. S1).

Porewater sulfide samples were drawn into 50-mL serum bottles preloaded with 0.2% 1 M ZnAc and 0.2% 6 M NaOH to preserve sulfide. Sulfide bottles were left to fill overnight, then stored at 4° C in the sealed serum bottles used for sample collection for approximately 30 days before sulfide was quantified. Samples for porewater sulfate analysis were withdrawn from sulfide sampling bottles and filtered through a Dionex 1cc metal cartridge and a 0.45 μm polyethersulfone filter approximately three months after they were collected. Porewater iron was collected in 8-mL serum bottles preloaded with 40% deionized water, 40% phenanthroline, 20% acetate buffer, and 1% concentrated hydrochloric acid. Iron bottles were filled until the solution turned light red, approximately ten minutes. If the solution turned red before 8 mL were collected, samples were diluted with deionized water to bring the total solution to 8 mL. Iron samples were quantified within two hours of sampling. Iron and sulfide in porewater were quantified colorimetrically using the phenanthroline and methylene blue methods, respectively, on a HACH DR5000 UV-Vis spectrophotometer (Greenberg et al. 1992). Sulfate was quantified using a Dionex ICS-1100 Integrated IC system (AS-DV

Autosampler) (Greenberg et al. 1992). The saturation index was calculated to determine if the porewater was saturated with respect to iron sulfide (equation 1, $K_{sp}=10^{-2.95}$) (Stumm and Morgan 1996). A positive saturation index indicates oversaturation and a thermodynamic force to drive precipitation, and a negative value indicates undersaturation (and potential dissolution).

$$SI = log\frac{[IAP]}{K_{sp}} \text{ where } IAP = \frac{[Fe^{2+}][HS^-]}{[H^+]} \qquad (1)$$

Geochemical parameters and measured attributes of plants were analyzed using repeated measures analysis of variance to determine differences between amended and unamended treatments over the course of the growing season. Analyses were performed with a repeated measures ANOVA because although individual plants were harvested on each date, each sampling date was not independent of the prior sample dates. A paired *t* test was used to determine differences between AVS and CRS concentrations on subsamples from the same roots. Analyses were performed using the statistical software SAS. Logarithmic transformations were used when data was non-normal. Data are available at the Data Repository for the University of Minnesota (https://doi.org/10.13020/D68W98).

RESULTS

Porewater sulfate and sulfide

Immediately before sulfate was added to amended buckets on Julian day 154, porewater sulfate concentrations were near 40 μmol L^{-1}. By the start of flowering (day 185), sulfate concentrations in amended porewater were over 1200 μmol L^{-1}, 30 times higher than the initial concentration (Fig 1). Sulfate concentrations continued to rise for the first 30 days of flowering (until day 217), peaking at nearly 2300 μmol L^{-1}. Over a four-week period (days 217-245) surrounding the onset of seed production, sulfate concentrations in amended porewater decreased by 86% to 315 μmol L^{-1}. Sulfate concentrations in unamended porewater were about 70 μmol L^{-1} at the start of flowering, roughly double the initial concentrations. Sulfate concentrations peaked at 230 μmol L^{-1} in unamended buckets on the same day as in amended buckets. During the same period that sulfate concentrations declined in amended porewater (days 217-245), sulfate concentrations in unamended buckets decreased by a similar proportion, 91%, to 20 μmol L^{-1}. Porewater sulfide did not differ between amended and unamended treatments (Supplementary Fig. S2). Concentrations averaged between 1 to 5 μmol L^{-1} during flowering and increased to an average of 8 to 17 umol L^{-1} at the start of seed production. Amended rhizospheres had a higher average sulfide concentration than unamended rhizospheres during seed production, but variability was high on the days porewater sulfide was elevated. Porewater sulfide concentrations decreased near the end of seed production and rose slightly at senescence.

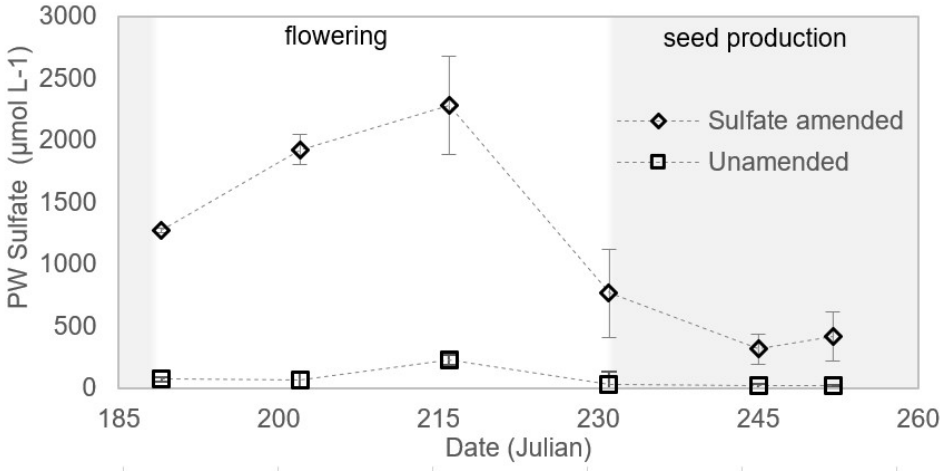

Figure 1. Seasonal measurements of porewater sulfate concentrations 2 centimeters from the root surface. Diamonds depict amended plants while squares depict unamended plants. Error bars show one standard deviation around the mean. Shading represents different life stages. Shading on left side of figure represents pre-flowering, unshaded represents flowering, and shading on right represents seed production.

Acid volatile sulfur on root surfaces

When grown in sediment with sulfate-amended overlying water (3.1 mM), amended plants developed a black coating on their root surfaces by the beginning of seed production on Julian day 231 (Fig. 2). The black precipitate started just above the root ball and extended along the entire length of the roots in the sediments. Adventitious roots that grew at the surface of the sediment, however, remained white, the natural color of wild rice root tissue. Unamended plants, grown in sediment with low concentrations of sulfate in overlying water (0.15 mM), developed amber coatings characteristic of iron (hydr)oxides over the same time period.

Figure 2. Photograph of sulfate-amended (left) and unamended (right) roots. Sulfate-amended (3.1 mM sulfate in surface water) root has black color extending from about 0.5 cm above the root ball down to the tips of the roots. Unamended (0.15 mM sulfate in surface water) root has amber color characteristic of iron (hydr)oxides, especially in the 2-3 cm below root ball. The photograph was taken during senescence in October, 2014 from a pilot experiment, but color is typical of roots in this experiment.

Roots of amended plants began accumulating AVS during the flowering stage (Julian days 190-230) of the life cycle (Fig 3a). The rate of AVS accumulation abruptly accelerated during the seed production stage (days 231-252) from approximately 2 µmol g^{-1} d^{-1} to over 15 µmol g^{-1} d^{-1}. During the seed production stage, amended roots accumulated up to 100 times more AVS than unamended roots, reaching a maximum mean concentration of 298 ± 74 µmol g^{-1} dw at the end of seed production. In contrast, AVS on unamended roots remained at 3.2 ± 1.7 µmol g^{-1} dw throughout the season (Fig 3b). Between the end of seed production and final senescence (day 265), AVS concentrations on amended roots remained elevated or decreased slightly.

Although AVS concentration in amended sediment increased by one order of magnitude over the life cycle (0.5 to 5 μmol g^{-1} dw, Supplementary Fig. S3), sediment contained approximately 50 times less AVS per gram than the roots. Concentrations of chromium reducible sulfur on both amended and unamended roots did not differ from AVS concentrations on the same roots during seed production, indicating that crystalline forms of FeS did not make up a significant proportion of reduced sulfur (paired *t* test, $p = 0.27$, $t = 0.63$, $n = 20$).

Iron speciation on root surfaces

During flowering, concentrations of Fe(III) and Fe(II) were similar between amended and unamended roots (Fig 3). During seed production, the redox state of iron was altered by the presence of sulfate. Concentrations of Fe(II) were much higher on amended roots compared to unamended roots ($p < 0.001$, $F = 19.1$, $df = 1, 31$), despite no significant difference in concentrations of Fe(III) between treatments. During the first week of seed production (between days 232 and 239), the concentration of ferric iron on amended roots decreased by 86%, from 233 ± 135 to 31.7 ± 30.4 μmol g^{-1} dw while ferric iron on unamended roots decreased by 67%, from 438 ± 208 to 144 ± 131 μmol g^{-1} dw. This abrupt reduction of Fe(III)) occurred the same week that the rate of net AVS accumulation increased on amended roots (Fig. 2). Following this transition, Fe(II) concentrations continued to increase (doubled) on amended roots but did not change on unamended roots.

Saturation index in porewater

Although the amended and unamended plants had significant differences in the speciation of solid-phase sulfur and iron on roots, the saturation index of FeS in the

sediment porewater 2 cm away from the roots was not affected significantly by sulfate amendment ($p = 0.177$, $F = 2.68$, $df = 1,4$) and remained, on average, near zero but mostly negative (-1.4 ± 0.3 to 0.1 ± 1.0) throughout the life cycle (Table S1).

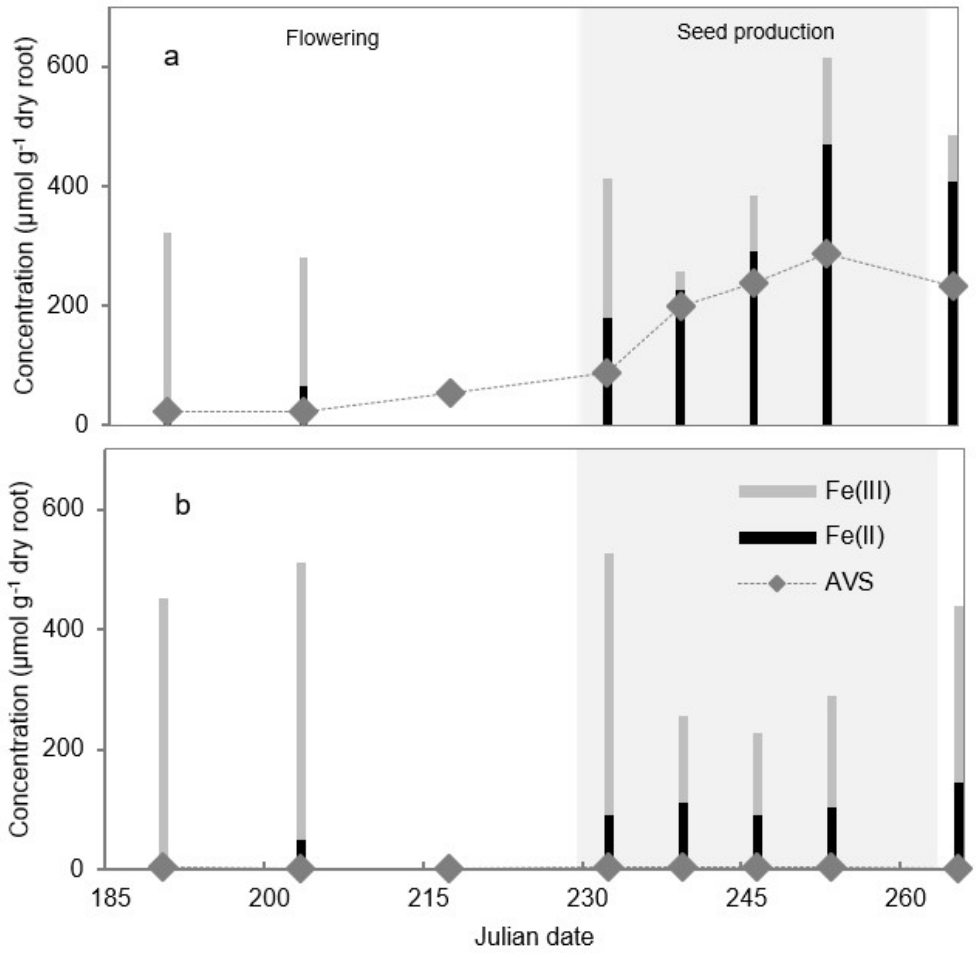

Figure 3. Seasonal variations in iron speciation and root AVS for (a) sulfate-amended and (b) unamended conditions, and effective E_H on root surfaces. The gray bars in panels a and b indicate ferric iron and the black bars represents ferrous iron. Root AVS concentrations are shown by gray diamonds. Error bars are omitted for clarity, but standard deviation is on average 33% of the mean.

Effects on plants

The transition of plants from the vegetative growth stage to the flowering and seed production stages of the life cycle coincided with the onset of a yellowing and senescence of leaves beginning the third week of August (around day 232). Amended

plants, all of which developed FeS plaques on roots, produced fewer seeds ($p = 0.067$, $F = 5.00$, $df = 1,6$, Fig 4) with less nitrogen ($p = 0.052$, $F = 5.84$, $df = 1,6$) and smaller mass ($p = 0.069$, $F = 4.88$, $df = 1,6$). During flowering, total plant N was similar between amended and unamended plants. But, during the subsequent seed production stage, total plant N continued to increase in the unamended plants, but not in the amended plants ($p = 0.084$, $F = 4.27$, $df = 1,6$).

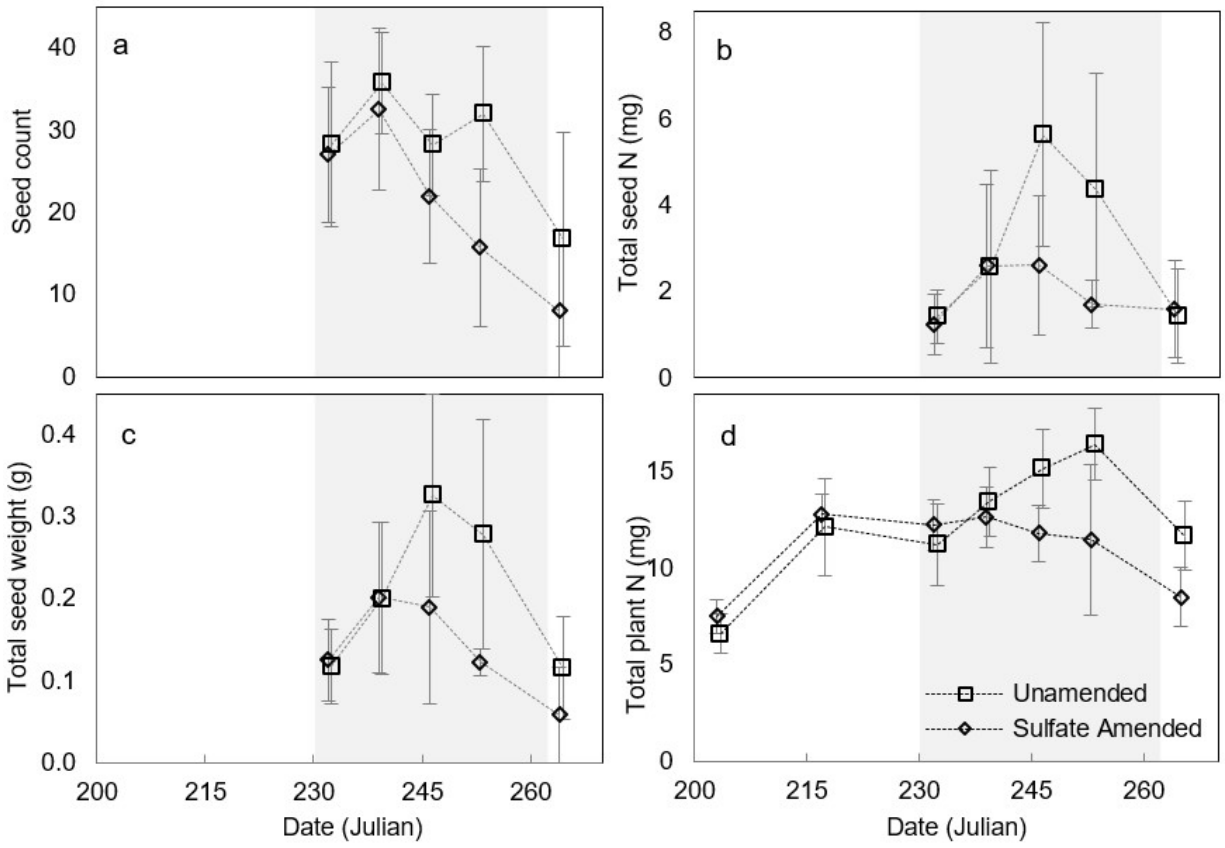

Figure 4. Plant response in sulfate-amended and unamended conditions; a) Seed count. b) Total seed mass. c) Total mass of nitrogen in seeds, d) Total plant nitrogen, calculated by summing nitrogen from seeds, stems, and leaves. Diamonds represent plants grown in surface water with 3.1 mM sulfate and squares represent unamended plants. The shaded background represents the seed production life stage. Error bars represent one standard deviation of four replicates.

DISCUSSION

We observed rapid shifts in sulfur and iron speciation at the surface of wild rice roots during the plant life cycle that differed depending on sulfate amendment. At the onset of leaf senescence and seed production, sulfate concentrations in the porewater decreased. This was followed shortly by decreased Fe(III) concentrations on the root surface as well as increased, but highly variable, dissolved sulfide concentrations in porewater. At this stage, solid phase-sulfide sulfide increased clearly and consistently on roots of amended plants, but not on unamended plants. The rapid development of FeS plaques was concomitant with the development of fewer filled seeds with lower nitrogen contents. Total plant nitrogen continued to increase in unamended plants but not in amended plants. The strong divergence between amended and unamended plants in total plant nitrogen and precipitation of FeS suggests a feedback between sulfur biogeochemistry on or near the root surface and plant nutrient uptake.

Sulfate amendments led to more reduced conditions and a more rapid development of iron sulfide precipitate on root surfaces, clearly confirming our hypothesis that surface water sulfate induces FeS accumulation on roots. In the absence of elevated sulfate, unamended plants filled out their seeds even when redox potential declined (Fig. 3, Supplementary Fig S4). In previous experiments with self-sustaining populations of wild rice (Pastor et al. 2017), elevated sulfate had little effect on total vegetative growth of adult plants but was associated with a decrease in the number and weights of seeds produced by mature plants at the late stages of the life cycle. FeS accumulates on roots during the last stages of wild rice's life cycle in which nitrogen taken up by the plant is allocated exclusively to panicles and seeds (Grava and Raisanen 1978, Sims et al. 2012). Porewater sulfide, which is known to decrease nitrogen uptake in

plants, increased simultaneously with FeS on roots of amended plants. However, porewater sulfide was variable and increased in both amended and unamended rhizospheres, whereas FeS only increased on amended roots. Nitrogen uptake continued through the seed production phase of unamended plants but not in amended plants, which contained FeS plaques. FeS on roots may be a symptom of elevated porewater sulfide or further exacerbate its effects; our experiment was not able to distinguish between these possibilities. Regardless, the presence of root surface FeS strongly suggests that during seed production, a plant-induced reversal in the flow of electrons occurred: from a net flow of e- accepting capacity away from the root, sustaining Fe(III) in the rhizosphere, to a net flow of e- towards the root, reducing Fe(III) and introducing S(II).

The decline in nitrogen uptake and seed production concomitant with the initiation of FeS plaque precipitation on roots and porewater sulfide accumulation may explain the disproportionate effect of sulfate on seeds compared with its negligible effect on cumulative vegetative biomass prior to flowering and seed production. We suggest that plants are especially vulnerable to sulfide during seed production, because a seasonal decrease in root surface redox potential is compromised by further sulfide-induced depletion of the electron accepting buffer capacity of iron (hydr)oxides. The oxidation states of the amended and unamended root surfaces diverged during the transition from flowering to seed production (Supplementary Fig. S4), suggesting that root surface redox potential is, in part, controlled by a physiological mechanism tied to the plant's life cycle.

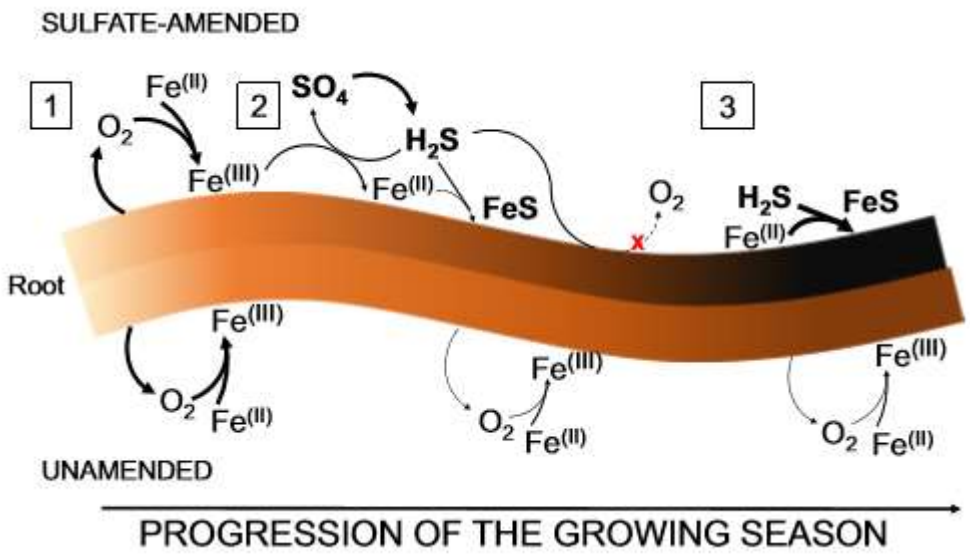

Figure 5. Proposed mechanism of iron sulfide formation on wild rice roots exposed to elevated sulfate concentrations. Reactions depicted above the root occur on sulfate-amended root surfaces, and reactions depicted below the root occur on unamended root surfaces. Roots are protected by iron (hydr)oxides [1], but these iron (hydr)oxides are reduced by sulfide [2]. Exposure of roots to sulfide may induce suberization, the thickening of root cell walls, which leads to decreased radial oxygen loss. Root surface anoxia accelerates the precipitation of iron sulfides [3]. In unamended roots, radial oxygen loss creates iron (hydr)oxides that remain present the entire growing season but decrease slightly in response to the life-cycle.

We hypothesize a pathway for how the living wild rice roots transition from iron (hydr)oxide plaques to iron sulfide plaques over the growing season (Figure 5). Initially, conditions in the rooting zone are oxic, likely from radial oxygen loss (Fig. 5, stage [1]), as evidenced by precipitation of iron (hydr)oxides that accumulate equally on both amended and unamended root surfaces. At this initial stage, the root is protected from the electrons contained in sulfide and other reduced species by an ongoing supply of electron accepting inputs, composed of both oxygen from roots and iron (hydr)oxide coatings on roots (Holmer et al. 1998, Roden and Wetzel 1996). Sulfide encountering the iron (hydr)oxide buffer is oxidized or precipitates with iron while the electron accepting

buffer is maintained. In amended conditions, some of this electron accepting buffer may be consumed (Fig. 5, stage [2]) during the flowering stage, allowing dissolved sulfide to penetrate nearer to the root surface. A decrease in radial oxygen loss near the onset of seed production, as vegetative growth ceases and leaves senesce, allows dissolved sulfide to reach the root surface. Sulfide exposure may further suppress radial oxygen loss by inducing suberization, the thickening of cell walls that prevents exchange of dissolved gases across the root (Armstrong and Armstrong 2005). After radial oxygen loss is suppressed, the electron accepting buffer capacity of iron (hydr)oxides can no longer be maintained and the remaining quantity of iron (hydr)oxides is then rapidly reduced due to a net decrease in the supply of electron acceptors to the rooting zone. A decrease in radial oxygen is likely tied to the end of the vegetative growth stage of the life cycle because both the amended and the unamended root surfaces simultaneously experience a loss of Fe(III) and a decline in porewater sulfate concentrations. Concentrations of root Fe(III) and porewater sulfate remained low in unamended plants for the rest of the growing season. But, as the amended root surface shifts toward reducing conditions, sulfide almost exclusively precipitates with reduced iron rather than being re-oxidized (Fig 5, stage [3]). In our amended buckets, rapid accumulation of root Fe(II), root AVS, and porewater sulfide occurred within a 1-2-week period during seed production immediately following the precipitous decline of porewater sulfate and root surface Fe(III). In unamended buckets, root Fe(II) and AVS did not accumulate further, and while porewater sulfide increased, it was highly variable.

The most likely explanation for a redox transition at both the unamended and amended roots is a decrease in radial oxygen loss at the end of the vegetative growth

stage when the leaves begin to senesce. Many mechanisms of rhizosphere oxidation have been described, including diffusion of atmospheric oxygen (Armstrong 1980), advection induced by temperature and vapor gradients (Dacey 1980) and Venturi-induced convection (Armstrong et al. 1992). Several studies have observed a correlation between light and rhizosphere oxygenation on diurnal time scales (Lee and Dunton 2000, Pedersen et al. 2004, Jensen et al. 2005), suggesting that some, if not most, radial oxygen loss may be photosynthetically derived. It has been previously suggested that accumulation of FeS occurs on white rice (*Oryza sativa*) roots only after plant senescence because dead roots no longer oxidize the rhizosphere (Jacq et al. 1991). However, as the plant approaches senescence, oxygen transport to the roots may decrease due to lower photosynthesis rates, subsequently slowing the regeneration of the electron accepting buffer of the root surface (Biswas and Choudhuri 1980). We observed a decrease in redox around the time that plants started to yellow and show early signs of senescence, consistent with a life-cycle-induced decline in radial oxygen loss.

Despite the rapid accumulation of FeS on roots in amended plants, the saturation index in sediment 2 cm from the roots remained relatively low, suggesting that the most severe decline in redox potential was confined to near the root surface. The Fe(II) in the FeS plaques may have come from the reduction of iron (hydr)oxides previously accumulated on the root surface. On the other hand, the sulfide in FeS plaques must have been supplied from a source external to the root. Although experimental conditions may have impacted the timing of sulfate intrusion to the rooting zone, porewater sulfate concentrations were already well above the half saturation constant for biological sulfate reduction at the start of flowering (Pallud and Van Cappellen 2006), making it unlikely

that the redox transition occurred from a delay in sulfate availability and reduction at the root surface. Once leaf senescence began, porewater sulfate concentrations (~2000 μmol L^{-1}) declined by more than 80% followed by rapid accumulation of porewater sulfide (from ~2 to 12 μmol L^{-1}) and AVS on the root surfaces (~300 μmol g^{-1}). Adjacent porewater sulfide was relatively low compared to the amount of sulfur in the porewater sulfate and root AVS pools. This suggests that a large amount of sulfur passes through the porewater sulfide pool very quickly, a scenario consistent with our proposed mechanism by which sulfide near the root surface is either oxidized by the electron accepting buffer or precipitated with Fe(II). Sediment AVS (5 μmol g^{-1}) was a larger component of overall solid-phase S accumulation due to its larger mass, but did not, apparently, experience the concentrated introduction of sulfide in the same way as roots. The rapid and concentrated accumulation of iron sulfide on roots in the setting of undersaturated porewater suggests an overwhelmingly plant-dominated geochemical niche very close to the root surface.

Beyond affecting wild rice populations, the mechanism behind the rapid accumulation of FeS on roots has implications for the fate of iron and sulfide in wetland sediments. Vegetated sediment in white rice paddies (Jacq et al. 1991) and in riparian wetlands containing *Phragmites australis* and *Zizania latifolia* (Choi et al. 2006) has higher concentrations of FeS than non-vegetated sediment. Significant accumulation of FeS on white rice roots has been observed after senescence (Jacq et al. 1991), likely because decaying root material stimulates iron and sulfate reduction. When roots coated with FeS decompose, the FeS becomes incorporated into the bulk sediment. Due to the concentrated introduction of both electron donors and acceptors to the subsurface, each

generation of an annual plant is effectively a "pump" for the incorporation of FeS precipitate into the sediment. In dense stands of aquatic plants, annual contributions of FeS from roots could significantly alter the geochemistry of the sediment within years to decades. If FeS plaques occur concomitantly with population declines in wetland plants, the plant-induced sulfur pump may only last a few generations but would have implications for changes in species composition in wetland plant communities. Understanding the rates of the distinctly plant-induced sulfur pump and the short- and long- term interactions of near-root processes with bulk sediment could help to predict how the distribution of wetland vegetation and sulfur accumulation change in response to a perturbation in surface water sulfate concentrations.

The results of this study may provide a mechanistic link between observed sulfide toxicity in lab hydroponic experiments (Koch et al. 1990, Koch and Mendelssohn 1989, Pastor et al. 2017) and empirical evidence of sulfur-induced population declines of wetland plants (Lamers et al. 2002, Myrbo et al. 2017, Pastor et al. 2017, Pulido et al. 2012, Smolders et al. 2003). Our observation that sulfur cycling is altered *during* the life cycle rather than after senescence allows for the possibility of rapid feedbacks between sediment and porewater geochemistry on the one hand and annual plant populations on the other. Understanding the timing of when electron accepting buffers are present or absent and how that correlates with the plant life cycle can provide insight into how populations of wild rice and other aquatic plant species will respond to perturbations in sulfur loading to ecosystems.

Chapter 3: Interactions between sulfide and reproductive phenology of an annual aquatic plant, wild rice, *Zizania palustris*

LaFond-Hudson, S., Johnson, N.W., Pastor, J., Dewey, B., 2020. Interactions between sulfide and reproductive phenology of an annual aquatic plant, wild rice (Zizania palustris). *Aquatic Botany* 164, 103230. https://doi.org/10.1016/j.aquabot.2020.103230

ABSTRACT

Aquatic plants live in anoxic sediments that favor formation of hydrogen sulfide, a known phytotoxin. We investigated how the phenology of reproductive life stages of wild rice (*Zizania palustris* Poaceae), an annual aquatic graminoid, is influenced by rooting zone sulfur geochemistry in response to elevated sulfate and sulfide. In addition, we characterized how redox conditions in the rooting zone change throughout reproduction to determine if they are tied to plant life stage. The redox conditions in sediment decreased just prior to flowering, and again just prior to seed production for all plants, allowing sulfide to accumulate at the root surface of sulfate-amended plants. Plants exposed to sulfide initiated seed production later than unamended plants. Sulfide appears to slow plant development in a way that gives the plant less time to allocate nutrients to seeds before senescence. The impact of sulfide in delaying reproductive life stages of wild rice and changing seasonal rooting zone biogeochemistry could extend to other plant species and additional chemical species that change mobility with redox potential, such as phosphate, manganese, mercury, and other metals.

INTRODUCTION

Many aquatic plants grow in sediments with low redox potential that favors formation of toxic reduced compounds like sulfide. To cope with these conditions, some aquatic plants transport oxygen to the roots through hollow aerenchyma tissue, release it into the rhizosphere, and form iron oxide plaques on root surfaces (T. D. Colmer, 2003; Jorgenson et al., 2012; Mendelssohn et al., 1995; Stover, 1928). The released oxygen and iron oxides may protect roots from dissolved sulfide species (Schmidt et al., 2011; Soana and Bartoli, 2013; Trolldenier, 1988; Van der Welle et al., 2007). Many wetland plants, including wild rice, are vulnerable to dissolved sulfide (Carlson et al., 1994; Koch and Mendelssohn, 1989; Lamers et al., 1998; Pastor et al., 2017). Wild rice (*Zizania palustris* Poaceae), an annual aquatic graminoid which forms large monotypic stands in lakes of the Western Lake Superior region, is especially sensitive during the seedling and seed production life stages, suggesting that the ability to withstand sulfide varies throughout their life cycle (LaFond-Hudson et al., 2018; Pastor et al., 2017).

Plants growing in nutrient limited conditions sometimes experience ontogenetic drift, a phenomenon in which morphological development through successive life stages is slowed (McConnaughay and Coleman, 1999; Sims et al., 2012). Because the allocation of biomass to different tissues changes throughout a plant's life cycle, delayed development has sometimes been misdiagnosed as morphological plasticity in experiments in which plants are normalized by date or age, rather than size or life stage (Coleman et al., 1994). Nitrogen is the limiting nutrient to wild rice (Sims et al., 2012) and its uptake is tied to specific life stages (Grava and Raisanen, 1978). About 30% of nitrogen is taken up during early vegetative growth, 50% is taken up during the growth of

the stem until flowering, and 20% is taken up during seed production (Grava and Raisanen, 1978). Dissolved sulfide inhibits nutrient uptake (Allam and Hollis, 1972; Koch et al., 1990; Martin and Maricle, 2015). If nitrogen uptake in wild rice is inhibited or slowed by sulfide, it may slow the rate at which the plant progresses through subsequent life stages and limit the quantity of N uptake available for seed production.

Near the end of an annual plant's life cycle when plants allocate resources from leaves into flowers and seeds, photosynthesis declines and radial oxygen loss from roots may also decrease, creating favorable conditions for reduction of iron oxides and sulfate (Schmidt et al., 2011). Several mechanisms for maintaining radial oxygen loss from roots have been described, including pressure gradients that actively pump oxygen from new leaves, through roots, to old leaves (Armstrong et al., 1992; Armstrong, 1980; Dacey, 1980); and production and transport as a byproduct of photosynthesis (Marzocchi et al., 2019). Although the exact mechanism of radial oxygen loss in wild rice is not yet known, the aforementioned mechanisms may be inhibited by the senescence of leaves during reproduction. We previously reported a decline in the redox potential of root surfaces during the seed production life stage (LaFond-Hudson et al., 2018). In plants grown in sediment without sulfur amendment, iron oxides plaques on root surfaces decreased, but in sulfate-amended plants, iron oxide plaques transitioned to iron sulfide, which further accumulated on root surfaces and coincided with production of fewer, smaller seeds with less nitrogen relative to unamended plants. In plants exposed to sulfide, the total uptake of nitrogen ceased during the onset of iron sulfide plaque formation and thickening while unamended plants continued to accumulate nitrogen in seeds (LaFond-Hudson et al., 2018). In this paper, we specifically explore the

relationship between sulfur geochemistry and phenology of life stages, as both may control each other through interactions that culminate in the redox potential of root surfaces. We use wild rice (*Zizania palustris,* Poaceae) as our model organism to investigate connections between sulfide and iron geochemistry in the rhizosphere and reproductive phenology and ontogeny. Because wild rice is an annual plant, the ontogeny of development is equivalent to the annual phenology. So in this case, the two words are synonymous, except that ontogeny has the connotation of development whereas phenology has the connotation of seasonality.

Wild rice is a culturally, economically, and ecologically important macrophyte that is harvested for its grain (Fond du Lac Band of Lake Superior Chippewa, 2018). An advantage of using an annual plant is the relatively simple life cycle; root and shoot growth starts over each year, photosynthesis declines and vegetative structures senesce during the transition from vegetative to reproductive life stages, and seeds are produced at the end of the growing season just prior to death. In addition, standard markers of transitions in life cycle stages for wild rice have been established in prior research in the context of nutrient limitation (Grava and Raisanen, 1978; Sims et al., 2012).

Motivated by acute and population-level impacts of sulfide on aquatic plants, we compare the ontogenetic progression of life stages with the development of iron sulfide plaques throughout the life cycle of wild rice. Sulfide may slow ontogenetic development, but plant life stage may in turn control rhizosphere redox conditions and the amount of sulfur present as reactive sulfide. To investigate these geochemical and phenological interactions, we quantify the timing and length of life stages and seed production along with the concurrent accumulation of iron sulfide plaques.

METHODS

Experimental design

Individual wild rice plants were grown outside in polyethylene buckets, 32 of which were amended with 300 mg L^{-1} sulfate and 32 of which were left unamended. Although many lakes and rivers in central and northern Minnesota have concentrations of sulfate lower than 10 mg L^{-1}, several current and former wild rice lakes and rivers have sulfate concentrations near or above 300 mg L^{-1}. Additionally, 300 mg L^{-1} is close to the EPA secondary standard for drinking water and is a concentration we have used in several prior sulfate-addition experiments with wild rice. Sediment was collected on 01-Jun-2016 from Rice Portage Lake (MN Lake ID 09003700, 46.7038, -92.6829) on the Fond du Lac Band of Lake Superior Chippewa Reservation in Carlton County, Minnesota. This lake is a productive and unpolluted wild rice lake with little or no settlement along its shores and its sediment is organic-rich mud. The sediment was not sieved, but thoroughly homogenized and loaded into 4 L plastic pails that were set inside 12 L buckets (see LaFond-Hudson et. al 2018) on 25-Jun-2016. Water was added from a nearby well (sulfate concentration ranging from 8 to 14 mg L^{-1}) to provide a 12-15 cm water column. Two wild rice seeds obtained from Rice Portage Lake were planted in each bucket on 26-Jun-2016 (Julian day 177). All buckets had at least one seedling by 28-Jun-2016 (day 179), and the less robust plant of the two was removed a week later. Half of the buckets had sodium sulfate added on 28-Jun-2016 and 05-Aug-2016 (days 179, 217) to maintain surface water sulfate concentrations of 300 mg L^{-1}. Plants remained outside for the entire duration of the experiment. Further details on the maintenance of buckets can be found in LaFond-Hudson et al. (2018).

Sampling methods

To compare changes in pace of progressions through the life cycle, we examined initiation of life stages from a subset of plants that completed their entire life cycle through seed production. We define initiation as the first date a plant was observed to be in a life stage. Life stages were identified visually and nondestructively according to the descriptions codified by Grava and Raisanen (1978) and further subdivided by Sims et al. (2012).

Our observations of the phenology of wild rice began with mid tillering, a life stage in which the main stem, the tiller, grows more than one leaf above the surface of the water (Table 1). Prior life stages include emergence of the seedling from sediment (life stage 0), the floating leaf stage (life stage 1), the first aerial leaf (life stage 2), and the formation of the tiller, the main stem that will eventually produce flowers and seeds (life stage 3). We started observations with mid tillering (life stage 4) because it is the last vegetative growth stage before reproductive life stages. After mid tillering, the internodes of the tiller elongate (jointing, life stage 5) and the panicles emerge (boot, life stage 6) in preparation for flowering (life stages 7-9). Flowering is broken into early (7), mid (8), and late (9) flowering by the proportion of flowers emerged and blooming. Once flowers have finished blooming, a seed hull develops and seed production begins (life stage 10). Filled seeds start to drop once they reach maturity (life stage 11), and senescence is reached once all seeds have dropped and leaves have turned completely yellow (life stage 12). Life stages of each plant and date were recorded eight times during the growing season.

When at least half of the plants were in a specific life stage, four sulfate-amended plants and four unamended plants in that life stage were destructively harvested to determine root surface geochemistry. When the plants entered the seed production life stage, harvests were made on three separate dates, each approximately a week apart, spanning the duration of the seed production life stage. Sampling at a more frequent temporal resolution during seed production enabled us to make detailed observations of the accumulation of iron sulfide (or lack thereof) on the roots during a potentially critical time for sulfide exposure.

Table 1. Descriptions of the life stages of wild rice and the range of dates for each life stage in which at least one *Zizania palustris* plant was observed (initially $n = 64$, followed by incrementally smaller sample sizes due to destructive sampling). Ranges are described for plants grown in water amended with 300 mg L^{-1} sodium sulfate or grown in water unamended, with background sulfate concentrations of ~8-14 mg L^{-1}. Life stages 1 through 3 pertain to seedling and early emergent stages that did not develop iron sulfide plaques on roots. Designation and description of life stages from Grava and Raisanen (1978) and Sims et al. (2012).

LIFESTAGE NAME	LIFESTAGE NUMBER	CHARACTERISTICS	DATES OBSERVED	
			Amended	Unamended
MID TILLERING	4	Tiller grows more than one leaf	210-235	210-222
JOINTING	5	Internodes elongate	210-240	210-240
BOOT	6	Panicles emerge from stems	235-249	235-245
EARLY FLOWERING	7	A few flowers bloom, some not yet emerged	235-245	235-245
MID FLOWERING	8	Most flowers bloom	235-249	235-245
LATE FLOWERING	9	Most panicles empty, few flowers still bloom	235-249	235-249
SEED PRODUCTION	10	Seed hull develops, seed filling occurs	240-263	235-263
SEED MATURITY	11	Filled, ripe seeds present, a few dropped	255-263	255-263
SENESCENCE	12	All seeds dropped, green tissues disappear	280	280

Biological and chemical analysis

On each sampling date, the same eight plants that were harvested were separated into aboveground vegetative tissue, seed tissue, and root tissue according to LaFond-Hudson et al. (2018). Vegetative tissue and seed tissues were dried for seven days at 65 °C and weighed. Total N concentrations were determined with a Thermo Electron Flash EA 1112 CHNS Analyzer. Fresh roots were analyzed for acid volatile sulfide (AVS) and weak acid extractable iron the same day plants were harvested, taking great care to avoid exposure to oxygen (LaFond-Hudson et al., 2018). Iron and acid volatile sulfur (AVS) were simultaneously extracted from entire roots using 1 M deoxygenated HCl for four hours. AVS was volatilized and trapped in a sulfide antioxidant buffer (SAOB) using a modified diffusion method (Brouwer and Murphy, 1994). AVS was quantified using a sulfide selective electrode. Iron was extracted into the 1 M HCl and analyzed for total extractable iron and Fe(II). Fe(III) was estimated from the difference between total iron and Fe(II). Total iron was quantified using a Varian fast sequential flame atomic absorbance spectrometer with an acetylene torch. Fe(II) was quantified on the day of extraction using the phenanthroline method on the spectrophotometer. After extraction, roots were dried at 38 °C for 24 hours to determine dry mass.

Data analysis

Data are publicly available in the Data Repository of University of Minnesota (DRUM) and can be accessed at https://conservancy.umn.edu/handle/11299/208579. We used a two-sample *t*-test to compare differences between sulfate-amended and unamended conditions for seed measurements and root sulfide. Because we sampled destructively to measure root surface sulfide and iron, dates for the initiation of early

reproductive life stages contain a larger sample size relative to the seed production life stage. Conclusions about the initiation of life stages between treatments are based only on the subset of plants that reached seed production in this experiment, and thus are not influenced by changes in sample size. For this subset of plants, we calculate the cumulative distribution of the date on which each life stage was initiated by summing the number of plants that are at or beyond the life stage. We also calculated the duration of seed stage for each plant in this subset using the difference between the first day we observed filled seeds and the first day we observed dropped or missing seeds. In many plants, seed production ended artificially early due to our destructive sampling design. In these cases, we used the harvest date as the end date in our calculation of duration and refer to the resulting value as "experimental duration". We investigated correlations between experimental duration and yield of seed production (seed count, seedhead mass, and seedhead nitrogen mass) to understand progression in seed development within the seed production life stage. We used these linear relationships to infer the seed yield at "true durations", which we define as the probable duration of seed production if plants were not harvested. For true duration, we use the average last date seeds were observed in parallel wild rice experiments. These parallel experiments occurred in the same year, used the same sediment and tested sulfate-addition but did not use non-destructive sampling (Table S1).

Effective redox potential at the root surface was calculated using a modified Nernst equation (Stumm and Morgan 2012).

(1) $p\varepsilon = p\varepsilon^{\circ} + \frac{1}{n} log \frac{\{ox\}}{\{red\}}$

(2) $p\varepsilon = 16 - 3pH + log \frac{\{Fe(III)\}}{\{Fe(II)\}}$

(3) $E_h* = \frac{2.3RTp\varepsilon}{F}$

While not strictly representative of the activity in solution, we use root surface Fe(III) and Fe(II) as a proxy for the activity of oxidized and reduced Fe in the rooting zone. Because the system is dynamic, root surface (solid-phase) quantities likely mirror the activity of iron in solution enough to draw general conclusions about the direction of the flow of electrons.

RESULTS

Sulfide effects on phenology

When life stage observations began (Julian day 210), unamended plants were ahead by nearly a full life stage (mean life stage of 4.5 ± 0.5 unamended compared with mean life stage of 3.8 ± 0.6 amended, $p < 0.01$, two-sample t test), indicating that vegetative growth life stages were delayed by sulfate amendment. Most amended plants initiated jointing later than unamended plants (mean Julian day 217 ± 9 unamended, mean Julian day 226 ± 9 amended, $p = 0.005$, $n = 17$), but both treatments initiated the boot stage at similar times (mean Julian day 237 ± 3 for both, Fig 6a, 6b). Because the boot stage occurs quickly, our temporal resolution may not have captured any differences in timing if they existed. From days 220-235, about half of the unamended plants initiated mid flowering, compared to only a quarter of amended plants (Fig 6c). During the same time frame, one third of unamended plants initiated seed production, compared to no amended plants (Fig. 6d). Eight days later, day 243, a comparable number of amended plants entered seed production. Amended plants entered seed production during a narrower range of time, with ~75% of plants reaching this life stage between days 240-250 (mean Julian day 247 ± 5), while the initiation of seed production was spread over a 2 week window for unamended plants (244 ± 7 days). Due to the destructive sampling required by our experimental design, we were unable to quantify the end date of seed production in this experiment, but we estimated the end date of seed production from parallel, non-destructive experiments involving sulfate-addition to wild rice mesocosms. The final date of seed collection was consistently close to day 260 for several years and experiments (Table S2). Using day 260 as the final date of seed production, we estimated

a 20% decrease in the true duration of seed production in amended plants compared to the unamended plants.

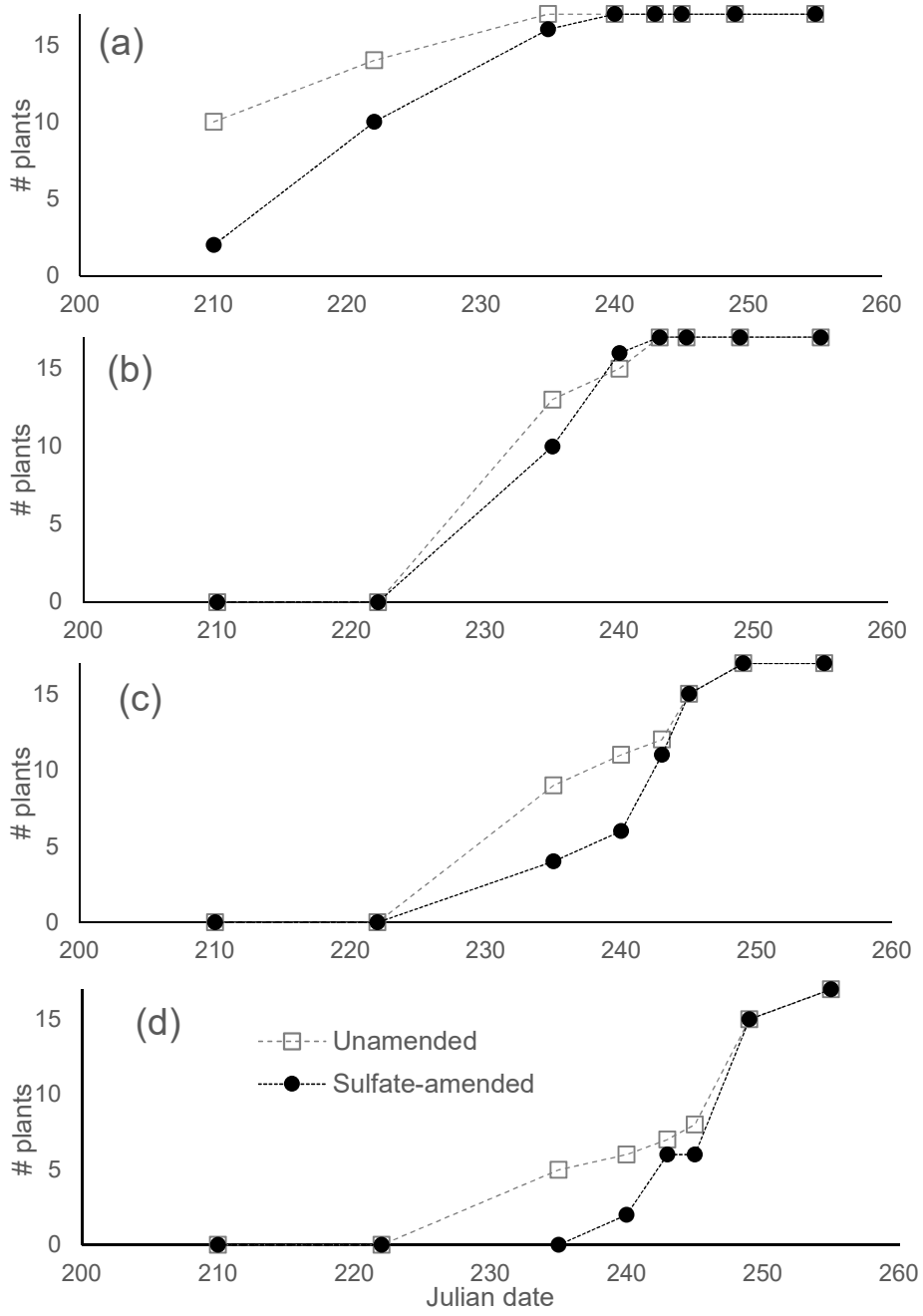

Figure 6. Cumulative frequency of sulfate-amended (300 mg L-1, filled circles) and unamended plants (open squares) that have initiated a) jointing, life stage 5, when internodes elongate just prior to reproduction, b) boot, life stage 6, when panicles emerge, c) mid flowering, life stage 8, when most flowers bloom, and d) seed production, life stage 10, when seed filling occurs.

Seed production and vegetative biomass

Sulfate amended plants produced 33% fewer seeds ($p = 0.03$), 50% less total seedhead mass ($p = 0.01$), and 40% total seedhead nitrogen ($p = 0.02$) compared to unamended plants (Table 2). Individual seeds were smaller by 33% ($p = 0.02$), but individual seed N mass did not differ significantly between treatments. Sulfate amended plants had lower vegetative biomass (leaves and stems) during late flowering ($p < 0.01$, $n = 4$), but not prior life stages (Fig. S5). The experimental duration of seed production, calculated from the difference between first day seeds were observed and the day the plant was destructively sampled, was positively correlated with more filled seeds ($p = 0.027$), greater seed mass ($p = 0.042$), and more seed nitrogen ($p = 0.012$, Fig. 7).

Table 2. Comparisons of acid volatile sulfide (AVS) concentration on root surfaces (μg g^{-1}) and of seed data in sulfate-amended (300 mg L^{-1}) and unamended conditions using a two-sample *t* test. AVS concentrations are compared during four reproductive life stages. The average for each treatment is reported with the standard deviation in parentheses ($n = 4$ for AVS during jointing, boot, and flowering; $n = 12$ for AVS during seed production, $n = 10$-12 for seed data; not all replicate plants had seeds)

Reproductive life stage	**Sulfate-amended**	**Unamended**	**P value**
Jointing	9.7 (± *3.7)*	0.6(± *0.3)*	***P* < 0.01**
Boot	64.9 (± *39.7)*	1.4 (± *0.2)*	***P* = 0.05**
Flowering (mid)	68.9 *(± 42.9)*	2.6 *(± 0.5)*	***P* = 0.03**
Seed production	144.8 *(± 61.6)*	3.3 *(± 0.8)*	***P* < 0.01**
Seed Measurements			
Filled seed count (# per plant)	10.5 *(± 7.3)*	16 *(± 7.1)*	***P* = 0.03**
Total seedhead mass (g)	0.14 *(± 0.07)*	0.28 *(± 0.16)*	***P* = 0.01**
Total seedhead N mass (mg)	3.05 *(± 1.36)*	4.93 *(± 2.28)*	***P* = 0.02**
Individual seed mass (mg)	11.1 *(± 3.27)*	15.26 *(± 4.75)*	***P* = 0.02**
Individual seed N mass (mg)	0.26 *(± 0.15)*	0.28 *(± 0.08)*	*P* = 0.38
Seed N%	2.28 *(± 0.63)*	1.89 *(± 0.48)*	*P* = 0.06

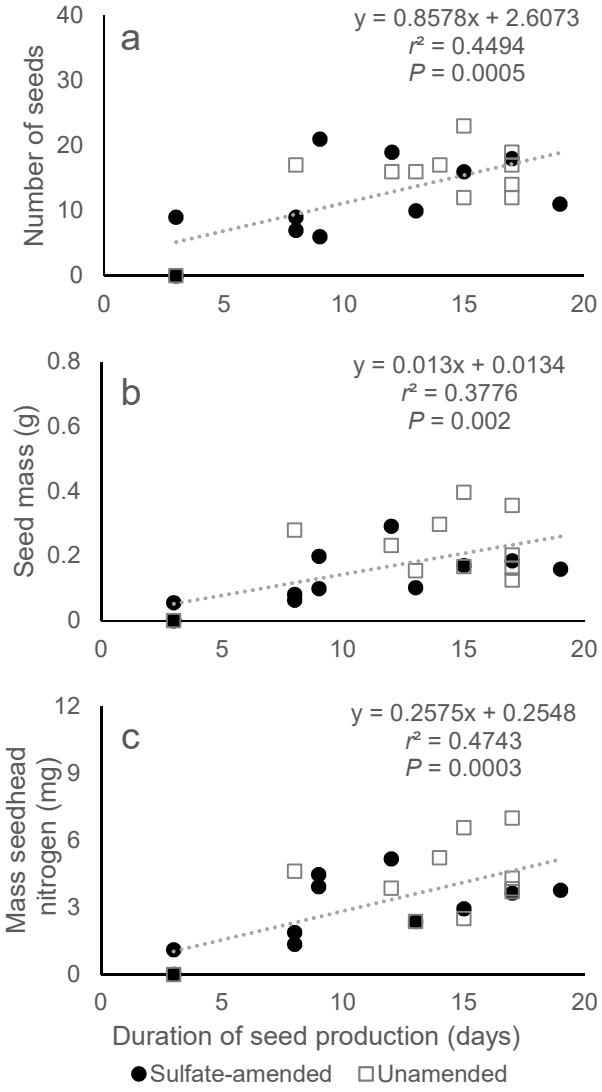

Figure 7. Relationship between the experimental duration of seed production (days) and a) filled seed count, b) seed mass (g), and c) seed nitrogen (mg). Filled circles indicate sulfate-amended plants (300 mg L^{-1}) and open squares indicate unamended plants. End dates of duration for each plant were determined either by the date they entered seed maturity or by harvest date if they were harvested before reaching seed maturity.

Root geochemistry

Concentrations of AVS on amended root surfaces were one to two orders of magnitude higher than on unamended root surfaces during jointing, boot, mid-flowering, and seed production (Table 2, Fig. S6). Porewater sulfate decreased from mid-flowering

until senescence, indicating that sulfate-amended plants were likely exposed to sulfide as a consequence of sulfate reduction (Fig. S7). On amended roots, AVS increased from about 10 μmol g^{-1} to about 65 μmol g^{-1} between jointing and boot. Concentrations of root surface sulfide then remained around 65 μmol g^{-1} until seed production. The AVS concentration doubled during seed production (life stages 10-11). On unamended roots, the concentration of sulfide steadily increased from 0.5 to 5 μmol g^{-1}, with the highest concentrations occurring during seed production. However, roots were not visibly black on unamended plants. Decreases in effective redox potential (E_h*), calculated from the ratio of Fe(III) to Fe(II) at root surfaces (Fig. 8, Fig. S8), occurred near both amended and unamended root surfaces between boot and jointing (life stage 5 to 6) and at the end of flowering (life stage 8 to 9). During seed production, the effective redox potential decreased more steeply at amended root surfaces.

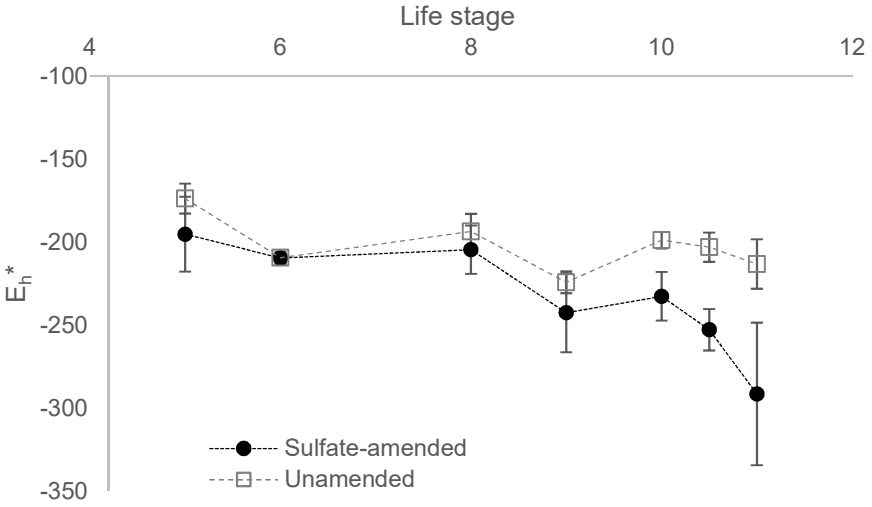

Figure 8. Effective redox potential calculated from Fe(III) and Fe(II) concentration on roots amended with sulfate (300 mg L^{-1}, filled circles) or left unamended (open squares). Error bars show one standard deviation (n = 4). Life stages were assigned as 10, 10.5, and 11 for Julian dates 252, 257, and 264 respectively to show chronological progression in E_h* during seed production and maturity.

DISCUSSION

The phenology of seed production was delayed in sulfate-amended plants, suggesting ontogenetic drift induced by sulfide. Across both amended and unamended conditions, seed mass, seed number, and N-mass correlated with length in the seed production life stage. In the presence of sulfate, delayed seed production and lower seed N-uptake both co-occurred with a precipitous drop in redox potential and rapid accumulation of sulfide on roots.

In a natural setting, plants with a delayed start to seed production would have to compensate by either increasing N uptake rate or delaying senescence until a later calendar date. In our experiment, sulfate-amended plants contained less seedhead nitrogen than unamended plants, so the N uptake rate likely did not increase much, if at all. Our experimental design, requiring destructive sampling during seed production, was unable to test the completion of the seed production life stage. To address these limitations, we examined average end dates of seed production in parallel wild rice experiments. The date of last seed collection happened at similar dates or even earlier dates for sulfate-amended plants in these other experiments (Table S2). Thus, it seems likely that sulfate-amended plants do not extend the seed production life stage to compensate for a delay in the initiation of seed production and have a shorter true duration of seed production. Because the seed production yield (number of filled seeds, seedhead mass, seedhead nitrogen) is positively and linearly correlated with experimental duration of seed production (Fig. 7), we suggest that the implications of delayed initiation without delayed completion of seed production are lower reproductive outputs by plants.

The curious timing of iron sulfide precipitation on root surfaces coincident with the beginning of seed production suggests that plants influence the geochemistry of the

sediments and that this influence changes during the plant's life cycle. The redox potential at the root surface, calculated from the ratio of Fe(III):Fe(II), decreased from jointing to boot (life stage 5-6), and again at the end of flowering (life stage 8-9). AVS concentrations increased on amended roots at the same life stages that redox declined. During seed production, the redox potential of amended and unamended plants diverged as the redox potential declined precipitously in amended plants. These decreases in redox potential reflect a net flow of electrons toward the plant root surfaces, suggesting a loss in the oxidizing capacity of the root surface. Transitions into new reproductive life stages are plausible times for plants to reallocate resources from photosynthetic tissues to reproductive tissues (Grava and Raisanen, 1978; McConnaughay and Coleman, 1999; Sims et al., 2012). Experiments with white rice (*Oryza sativa*), a closely related plant, have shown changes from iron oxide to iron sulfide in rhizosphere sediment as the plant entered flowering (Schmidt et al., 2011). We suggest that the change in redox conditions of the root surface at reproductive life stage transitions could be explained by a decrease in radial oxygen loss tied to the life stage of the plant, creating conditions conducive to iron sulfide formation in environments with elevated sulfur.

Plants concomitantly control and are controlled by sulfide. During vegetative growth life stages, plants maintain low sulfide in the rooting zone by releasing O_2 and accumulating Fe(III). However, at key reproductive life stage transitions, excess sulfide appears to overwhelm the plant's ability to oxidize the rhizosphere. The geochemical consequences of both life stage transition and excess sulfide is a precipitous drop in Fe(III):Fe(II) ratio and an accumulation of solid-phase sulfur on roots. The ecological consequences of life stage transitions in the presence of excess sulfide is a delay in

reproductive phenology and a decrease in N uptake to seeds. Slower development rates in the presence of sulfide may delay life stage transitions and the geochemical consequences of these life stage transitions for redox potential. Our experimental design was not able to directly determine if redox potential decreased at a later date due to delayed phenology in amended plants. However, our observations do provide evidence that the net effect of sulfide-induced ontogenetic drift is shortened and decreased seed production. This finding hints at a phenological mechanism underlying sulfide-induced inhibition of nitrogen uptake observed in prior work (LaFond-Hudson et al., 2018). Considering that seedlings also experience high mortality when exposed to sulfide, 50% less total seed mass in the presence of elevated sulfide may lead to rapid population declines, as has been previously observed in a mesocosm experiment (Pastor et al., 2017). Additionally, decreased density of plants in subsequent generations may lead to lower oxygen fluxes into sediment and exacerbate redox conditions that favor production of sulfide.

Sulfide limitation of nutrient uptake has been demonstrated in other plants (Koch et al., 1990; Martin and Maricle, 2015), as has ontogenetic drift ((McConnaughay and Coleman, 1999; Sims et al., 2012), so other freshwater annual aquatic plant populations may face similar reproductive challenges if exposed to sulfide. Additionally, sulfide and iron interact with nutrients besides nitrogen. Iron plaques can adsorb phosphorus and metals, controlling their availability for uptake (Christensen and Sand-Jensen, 1998; St-Cyr and Campbell, 1996). Reduction of iron plaques in the presence of sulfide may affect uptake of both macro- and micronutrients. Some studies have investigated changes in radial oxygen loss over the growing season in perennial aquatic plants (Soana and Bartoli

2013, 2014). However, because perennial plants may have different life-cycle patterns of radial oxygen loss, the ways sulfide might interact with phenology or reproduction of perennial aquatic plants remains unknown. Clarifying how sulfide interacts with nutrients in rhizospheres of both annual and perennial plants may be important for understanding how wetlands or vegetated littoral zones respond to elevated sulfide conditions on an ecosystem level.

Redox conditions at root surfaces are closely tied to wild rice phenology. Sulfide, through delaying phenology, has the potential to control the timing of changes in redox conditions. By changing the timing and duration of reproductive life stages, sulfide's effects on phenology likely plays a role in decreased survival of wild rice populations.

Chapter 4: Sulfur geochemistry impacts population oscillations of wild rice

INTRODUCTION

When sulfate diffuses from surface water into anoxic sediment, sulfide is produced and is toxic to aquatic plants (Koch and Mendelssohn, 1989; Lamers et al., 2013). Controlled mesocosm experiments have demonstrated how sulfide can eutrophy waters, eliminate sensitive macrophyte species, and decrease plant biomass (Geurts et al., 2009; Johnson et al., 2019; Lamers et al., 2001; Pastor et al., 2017). Bench scale experiments have determined that sulfide inhibits ATP production and causes root walls to thicken and thereby decrease root growth, water uptake and nutrient uptake (Allam and Hollis, 1972; Armstrong and Armstrong, 2005; Koch et al., 1990; Martin and Maricle, 2015). Because nitrogen uptake in plants requires ATP, sulfide exposure can inhibit nitrogen uptake.

The abundance of many macrophyte species, including wild rice, declines with elevated sulfate loadings and hence sulfide production (Carlson et al., 1994; DeLaune et al., 1983; Moyle, 1944; Myrbo et al., 2017a; Smolders et al., 2003). Wild rice (*Zizania palustris,* manoomin) is a culturally and ecologically important aquatic plant that grows in the western Great Lakes region and is harvested for its grain (Fond du Lac Band of Lake Superior Chippewa, 2018). Its simple annual life cycle makes it a good model organism to study the effects of sulfate and sulfide. We have demonstrated that when individual wild rice plants grow in elevated surface water sulfate, nitrogen uptake ceases as sulfide accumulates near roots and iron sulfide precipitates on them during seed production (LaFond-Hudson et al., 2020, 2018). Nitrogen is the limiting nutrient to wild rice (Sims et al., 2012) and inhibition of nitrogen uptake slows plant development and

shortens the duration of seed production (LaFond-Hudson et al., 2020). Mesocosm experiments show sulfate addition to mesocosms of wild rice decreased seedling survival and seed production within each year, leading to a decline in biomass and, at sulfate concentrations greater than 100 - 150 mg/L, eventually extinction of the mesocosm populations in as little as three years (Johnson et al., 2019; Pastor et al., 2017).

Although individual plant responses to sulfate have been well described, it remains unclear how the response to sulfate of individual plants translates to longer-term population dynamics. Asynchrony between litter decomposition and plant life cycles can drive oscillations in population biomass (Bergelson, 1990; Molofsky et al., 2000; Tilman and Wedin, 1991; Walker et al., 2010). Fresh litter immobilizes nitrogen, causing decreased biomass following a productive generation, and older litter mineralizes nitrogen, causing increased biomass, especially in conjunction with low plant density (Walker et al., 2006). Wild rice has stable oscillations of approximately 4-year periods due to delays in nitrogen mineralization caused by microbes immobilizing nitrogen in litter for at least one year (Pastor and Walker, 2006; Walker et al., 2010). Many studies have investigated sulfide toxicity to aquatic plants and populations, but none have investigated how sulfide-induced decreases in nitrogen uptake might interact with the litter-induced delays in nitrogen availability that are responsible for population oscillations. Here, we investigate how litter-driven population oscillations interact with sulfate geochemistry in wild rice through controlled mesocosm experiments that allow us to scale the individual plant physiology to the population scale for several generations while manipulating geochemical inputs.

Due to sulfide's high reactivity, it is difficult to predict the activity of sulfide in sediment from a given amount of sulfate in the overlying water (Pollman et al., 2017). The conversion of sulfate to sulfide occurs when sulfate acts as an electron acceptor in anaerobic heterotrophic microbial respiration. This redox reaction can be limited by either the electron acceptor, sulfate, or the electron donor, organic carbon. In sediment pore water, reduced iron binds with aqueous sulfide to form different forms of solid iron sulfide phases (FeS_x). Because iron precipitates aqueous sulfide out of solution, it is possible that addition of iron may improve the health of wild rice growing under high sulfate loads as it may do for sea grass (*Thalassia testudinum*) and a few other wetland plants (Lamers et al., 2002; Ruiz-Halpern et al., 2008; Van der Welle et al., 2007). Self-sustaining populations in controlled mesocosms are ideal to study how long-term interactions among iron, organic carbon, and sulfide become manifest in terms of population stability.

We herein explore interactions between sulfur geochemistry and stability of wild rice populations by investigating 1) the patterns of biomass oscillations in high sulfate and low sulfate conditions, and 2) geochemical factors that may enhance or alleviate sulfate's effects on biomass oscillations. We consider several possibilities for changes in biomass oscillation. First, biomass may continue to cycle stably over time with similar amplitude and frequency, but the overall mean may shift to a lower stable value in high sulfate concentrations (Fig 9a). Extinction occurs in this scenario if sulfate decreases the overall mean low enough that the cycles reach zero during one or more low points of the cycle. Secondly, the amount of biomass is initially similar in both low and high sulfate environments, but the mean of the cycle in high sulfate progressively decreases over time

until the population goes extinct (Fig 9b). These two possibilities are not mutually exclusive and the actual response may be a combination of the two. In the context of this conceptual model, we will also examine whether iron addition or litter removal change the patterns of biomass oscillations. We expect that iron may delay extinction of populations exposed to high sulfate. We expect litter removal to decrease sulfide production, but litter's effects may be more complex due to its role in driving biomass oscillations.

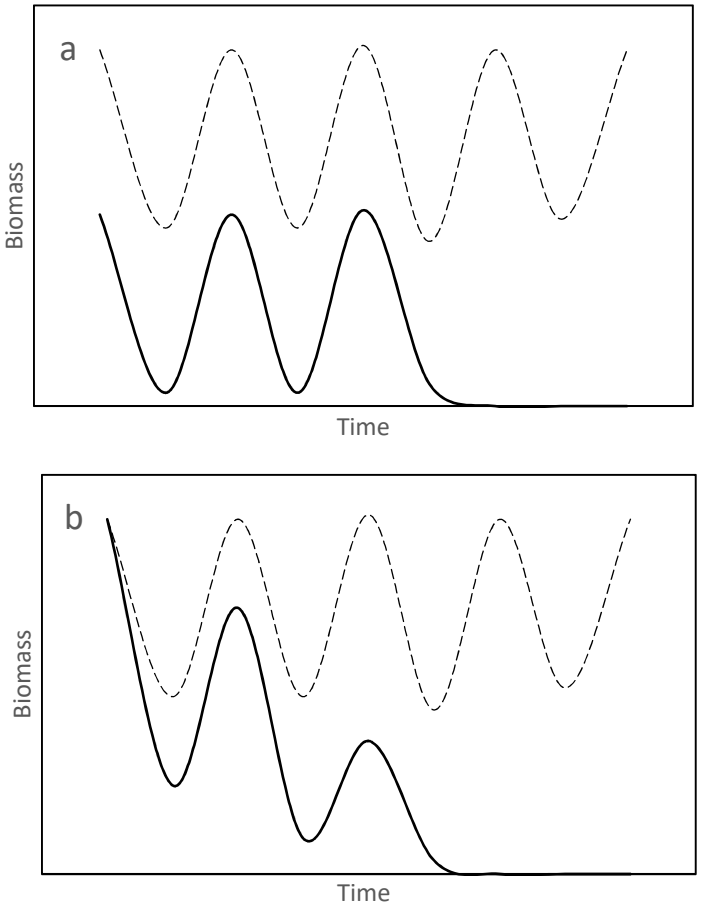

Figure 9. Potential effects of high sulfate loading on biomass oscillations (solid lines). Overall oscillation mean may be shifted lower (a), or oscillation mean may decrease with time (b) compared to low sulfate conditions (dashed lines).

METHODS

Experimental Design

The interactions of sulfate, iron, and carbon in wild rice sediment and their effect on wild rice population dynamics were studied using a factorial experiment. Forty polyethylene stock tanks (High Country Plastics 400L, 132x78x61 cm) were used to assemble the mesocosms. The sediment in the tanks was taken from Rice Portage Lake (MN Lake ID 09003700, 46.7038, -92.6829) on the Fond du Lac Band of Lake Superior Ojibway Reservation in Carlton County, Minnesota (Table 3). This lake is a productive wild rice lake with little surrounding development and its sediment has been used successfully to grow wild rice in previous experiments (Pastor et al 2017). Sediment was homogenized before it was added to the tanks. Fifty liters of sediment were placed in each tank, resulting in a sediment depth of about 10 centimeters. Water levels were maintained at 22 cm with a drain standpipe during precipitation and well water additions to account for evaporation.

Five replicates were created for each of eight different treatments. For high-sulfate treatments, enough sodium sulfate was added to the surface water to bring the sulfate concentration to 300 mg L^{-1}. Surface water sulfate concentrations were tested weekly and sodium sulfate was added to maintain concentrations at 300 mg L^{-1} as required through the growing season for the duration of the experiment. The low-sulfate tanks were filled with water from an on-site well with concentrations around 10 mg L^{-1} and received no additional sulfate additions except for precipitation, which averaged 2.3 ±1.5 mg/L sulfate. The sulfate concentrations in the low-sulfate tanks averaged around 10 mg L^{-1} over several years (Pastor et al. 2017). The low sulfate conditions for our experiment are still higher than the median sulfate concentration of Minnesota wild rice

waters, 1.8 mg L^{-1} (Myrbo et al., 2017a), but we used this concentration as a lower limit because it represents Minnesota's protective sulfate standard for wild rice waters. At 300 mg L^{-1}, our high sulfate treatment is close to the EPA's secondary standard for sulfate in drinking water (250 mg L^{-1}) and represents surface water concentrations of a few lakes and rivers in Minnesota that contain wild rice (Myrbo et al., 2017a). Iron-amended treatments only received iron at the beginning of the experiment. Iron-amended tanks received two times the total amount of iron found in the sediment (96 g Fe^{2+} added to each tank). Iron (II) chloride was dissolved in anoxic water and added directly into the sediment through PVC standpipes during the first field season. Samples of pore water iron were taken several times over the course of the first field season in ten points distributed across the tank to ensure that the iron loading distributed evenly. Non-iron tanks did not receive any added iron, but the sediment initially contained about 77 μmol g^{-1} dry weight. In carbon-amended tanks, leaf litter produced by the wild rice was left in the tank and was removed from the non-carbon tanks. Initial carbon content of the sediment was 14.8 ± 1.7% by dry weight.

Sampling & Analysis

To test whether iron addition and litter removal affected the iron and sulfur geochemistry of the mesocosms, the sediments of all 40 tanks were sampled for porewater iron, sulfide, and pH twice a year, during emergence of seedlings and during seed production or senescence. The sampling procedure used 5 cm length Rhizons attached to an evacuated serum bottle (Seeberg-Elverfeldt et al., 2005). The filter end of the Rhizon was inserted so that the entire filter was just below the sediment surface, drawing water from sediment approximately 0 to 5 cm deep. The filter was placed

vertically into the sediment with minimal jostling to avoid creating a cavity around the filter that would allow surface water to enter the sediment and contaminate the pore water. The Rhizon was placed at least 10 cm from the edge of the tank and at least 2 cm from the stem of a root. To minimize disturbing the sediment, one Rhizon was installed in each tank for the duration of sampling, and sample bottles were swapped out after the first bottle was filled. Bottles used to collect samples for sulfide were preloaded with 0.2% concentrated sodium hydroxide and 0.2% 1 M zinc acetate. Rhizons attached to sample bottles with a hydpodermic needle remained in position overnight to fill sample bottles.

In 2019, passive diffusion samplers (peepers) were installed in the tanks during vegetative growth (July) and seed production (September) to obtain porewater measurements from discrete depths in the top six centimeters of sediment. The peepers were placed in deionized water that was bubbled with nitrogen for one week prior to installation (Johnson et al., 2019). The peepers were transported to mesocosms in degassed water and installed in three tanks for each treatment. Each peeper contained four wells, the top of which was in the flocculant litter layer at the sediment surface and the bottom of which was approximately six centimeters below the sediment surface. Two weeks after peepers were installed, each peeper was removed and quickly placed in a large, resealable plastic bag with nitrogen gas to keep porewater anoxic during porewater extraction. Approximately 6 ml of porewater from each well was extracted with a syringe and allocated for sulfide and iron measurements in preloaded vials. A separate aliquot was used to measure pH within 30 seconds.

Iron and sulfide were quantified colorimetrically using the phenanthroline and methylene blue methods, respectively, on a HACH DR5000 UV-Vis spectrophotometer (Federation and Association, 2005). Sulfate was quantified using a Dionex ICS-1100 Integrated IC system (AS-DV Autosampler). The pH of the pore water was measured by placing a calibrated ThermoScientific Orion pH electrode in porewater immediately after it was extracted from peepers.

Biological sampling and analysis

Seedlings usually began to germinate around mid-May. Once seedlings were 3-5 centimeters above the sediment, they were counted every two or three days to determine mortality before they reached the surface of the water column. Seedlings that became unrooted and floated to the water surface were counted separately as "floaters" and removed. When seedlings grew to the water surface, populations in each mesocosm were thinned to approximately 30 plants per tank, which is the optimal density to limit competition and minimize overlapping rhizospheres (Lee, 2002). Total germination was calculated by counting the number of floaters, thinned seedlings, and plants remaining at the end of the growing season. Because we thinned plants, we were unable to directly record post-germination survival. Instead, we estimated potential survival by adding the number of thinned plants and the number of plants remaining at the end of the growing season. This estimate may be artificially high, as it assumes all thinned plants would have survived, and thus it provides a conservative estimate of the effects of sulfide on survival. In August, as plants began to flower, six plants from each tank were randomly selected and tagged. Seed data was collected from these six plants and extrapolated to the total number of plants in the tank. Seeds from the remaining plants were left in the tank to

reseed the sediment for the next year. Seeds were sorted into filled or unfilled by visual inspection, counted, and dried at 65 ºC and weighed to determine seed mass. After all plants had completely senesced in October, all aboveground biomass was removed, dried at 65 ºC and weighed. For plants receiving the litter treatment, dried biomass was returned to the tank by the end of October of each year.

Data analysis

Interannual porewater trends were analyzed from Rhizon data, meaning they represent instantaneous porewater concentrations taken from the top 5 cm of sediment. The porewater data collected via peepers during the final year of the experiment were collected after two weeks of deployment in the sediment, and at discrete depth intervals (~2cm). The porewater data collected from peepers were examined to understand how porewater sulfide to iron ratios and saturation with respect to FeS were changed five years after geochemical manipulation. Repeated measures ANOVAs were used to determine the effect of time, sulfate addition, iron addition, and litter removal on biological traits and porewater measurements.

The cumulative effects of sulfate on the annual life cycle and interannual population cycles were examined by examining at the relationships between prior and subsequent life stages, and by examining the dependence of changes in biomass on the biomass produced during the previous year. To examine how addition of sulfate affected the progression of subsequent stages of the life cycle, we regressed potential survival against germination, biomass against potential survival, population seed mass against biomass, and germination the subsequent year against population seed mass separately for the high and low sulfate conditions.

To test the propensity of the population to oscillate in high and low sulfate conditions, we regressed the change in biomass (biomass(t) – biomass(t-1)) over the biomass from the previous year (biomass(t)). A negative slope of this regression indicates that high productivity one year leads to lower productivity the following year and, conversely, that years with low productivity are followed by years with higher productivity (Walker et al., 2010). The slope of this line is effectively an eigenvalue, and -1 is a critical value indicating a Hopf bifurcation giving birth to stable limit cycles. A slope of -1 or steeper indicates propensity for stable oscillations, while a slope between -1 and 0 indicates dampened oscillations. Dampened oscillations will eventually converge on a stable value, which may include zero (extinction). Additionally, we compare the proximity of measurements to a line representing the extinction boundary condition, $y = -x$. This line represents the scenario in which the loss of biomass from one year to the next is equal to the amount of biomass produced the previous year. Therefore, no production occurs the following year when the system is at this boundary condition.

For ANOVA analysis, zeros were removed in the geochemistry data, but not in the biological data. Using zeros in biological data made variance large in high sulfate conditions, making it harder to detect differences between treatments using ANOVAs. However, averages calculated including zeros (extinction of the population) represent the effects of high sulfate more accurately than removing zeros.

RESULTS AND DISCUSSION

Geochemical context

The initial sulfide to iron ratio in the porewater was 0.0015 (Table 3). Our sulfate amendments to the surface water increased porewater sulfate, sulfide, and pH. Porewater sulfide is often a small pool with rapid turnover, making it challenging to draw conclusions about sulfate reduction activity based on concentrations alone. Iron amendment increased porewater ferrous iron concentrations and decreased pH. However, only sulfate amendment increased the saturation index with respect to FeS (Fig 10, Table S3, Table S4).

Table 3. Initial bulk sediment physical and chemical characteristics. Sulfide was measured from initial sediment and porewater iron is an average from fall measurements in tanks unamended with iron.

Porosity	0.87
Bulk density	0.29 g cm^{-3}
Percent solids	30
Solid-phase acid volatile sulfide (AVS)	0.346 µmol/g +/- 0.054
Solid-phase extractable iron	76.7 µmol/g +/- 5.1
Solid-phase ferrous iron	65.2 µmol/g +/- 4.8
Porewater sulfide	0.659 ± 0.239 µmol/L
Porewater ferrous iron	435 ± 200 µmol/L
Initial solid phase S:Fe ratio	0.00450
Initial porewater ΣS^{2-} :Fe^{2+} ratio	0.0015

After five years, porewater profiles of iron and sulfide were sampled using passive diffusion samplers to examine depth profiles and equilibrium porewater concentrations of iron and sulfide during vegetative growth (July) and seed production (September) (Table S4, Fig. S9). High sulfate treatments had a sulfide to ferrous iron ratio of ~1-100 in porewater. Low sulfate conditions had a sulfide to ferrous iron ratio of <0.01-0.1 (Fig S11). The sulfide to iron ratio in low sulfate conditions increased after five

years likely because Rice Portage lake, the source of sediment used in the experiment, has sulfate concentrations ~1 mg L^{-1}, so our low sulfate experimental conditions elevated sulfate by an order of magnitude above the sediment's natural porewater concentrations. Both high and low sulfate conditions contained sulfide and iron concentrations that favored precipitation of FeS (saturation index > 0, Figure 10). In low sulfate conditions, naturally elevated levels of iron led to saturation of FeS, whereas, in high sulfate conditions, experimental inputs of sulfate leading to elevated sulfide raised the ion activity product further above equilibrium saturation.

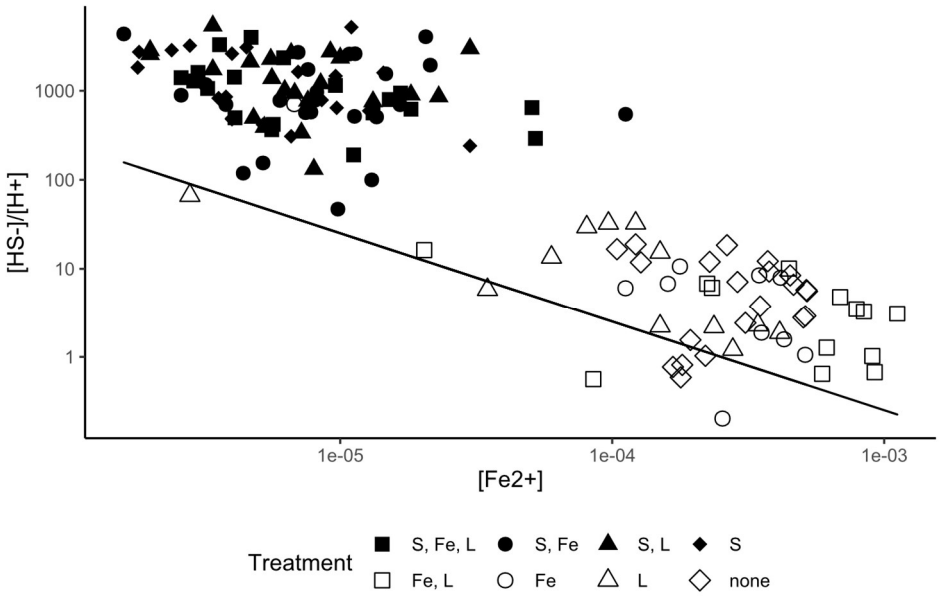

Figure 10. Comparison of ferrous iron and sulfide concentrations (mol L^{-1}) in sediment porewater after five years of sulfate and iron amendment and litter removal. Data points represent porewater measurements collected at the sediment surface, 2 cm, 4 cm, and 6 cm deep using peepers. Data from July and September are both included. The line depicts the ion activity product of saturation for iron sulfide (log IAP = -3.2).

Geochemical effects on growth and recruitment

All measured traits of wild rice growth and reproduction changed with time (Table 4) as expected based on prior work describing natural oscillations of wild rice populations (Pastor and Walker, 2006; Walker et al., 2010). Sulfate addition affected all measured traits of wild rice growth (Table 4) corroborating recent work on sulfide toxicity in wild rice populations (Johnson et al., 2019; Pastor et al., 2017).

Table 4. Wild rice growth and reproduction (repeated measures ANOVA) in high sulfate and low sulfate conditions for 2014-2019.

TRAIT	YEAR	SULFATE	IRON	LITTER	INTERACTIONS
Germination	***P* < 0.001**	***P* < 0.001**	*P* = 0.13	***P* = 0.03**	
Potential survivors	***P* < 0.001**	***P* < 0.001**	***P* = 0.03**	*P* = 0.11	
Vegetative biomass	***P* < 0.001**	***P* < 0.001**	*P* = 0.71	*P* = 0.67	
Population seed mass	***P* < 0.001**	***P* < 0.001**	*P* = 0.96	*P* = 0.27	
Filled seed ratio	***P* < 0.001**	***P* < 0.001**	***P*= 0.004**	*P* = 0.50	
Mass per filled seed	***P* < 0.001**	***P* < 0.001**	***P* = 0.03**	*P* = 0.36	
		High sulfate conditions			
Germination	***P* < 0.001**	**--**	*P* = 0.17	*P* = 0.14	
Potential survivors	***P* < 0.001**	**--**	***P* = 0.001**	*P* = 0.45	**Fe x L, P = 0.04**
Vegetative biomass	***P* < 0.001**	**--**	*P* = 0.80	*P* = 0.83	
Population seed mass	***P* < 0.001**	**--**	*P* = 0.29	*P* = 0.67	**Fe x Year P = 0.03**
Filled seed ratio	***P* < 0.001**	**--**	***P* = 0.01**	*P* = 0.33	
Mass per filled seed	***P* < 0.001**		*P = 0.09*	*P* = 0.17	
		Low sulfate conditions			
Germination	***P* < 0.001**	**--**	*P* = 0.29	*P = 0.09*	
Potential survivors	***P* < 0.001**	**--**	*P* = 0.20	*P* = 0.20	
Vegetative biomass	***P* < 0.001**	**--**	*P* = 0.79	*P* = 0.51	
Population seed mass	***P* < 0.001**	**--**	*P* = 0.42	*P* = 0.29	
Filled seed ratio	***P* = 0.004**	**--**	*P* = 0.19	*P* = 0.62	
Mass per filled seed	***P* < 0.001**		*P* = 0.20	*P* = 0.67	

Germination

The number of seeds that germinated was similar in both high and low sulfate conditions during the first year of the experiment but diverged thereafter. In high sulfate conditions, the number of seeds that germinated decreased by about 66% from 2015-2019

and was not affected by litter removal (Fig 11, Table 4). After 2015, the mean germination shifted well below that of low sulfate. Germination in high sulfate appeared to have two-year cycles consisting of decline followed by partial, but not complete recovery, looking similar to a combination of the hypotheses depicted in Fig 9. In low sulfate conditions, the number of germinated seeds increased by about 50% between 2015 and 2019 (Fig 11). On average, about twice as many seeds germinated in 2017 as any other year. Litter removal increased germination by as much as 60 seedlings, but only in low sulfate conditions ($p = 0.09$, Table 4).

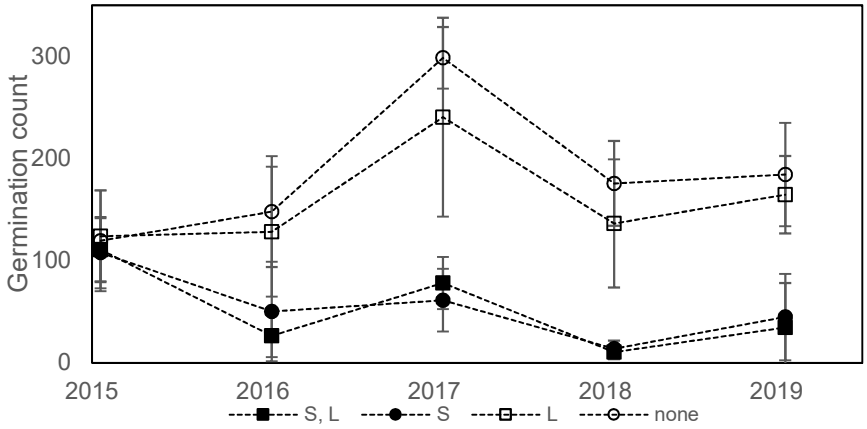

Figure 11. Effect of litter (squares, litter present; circles, litter removed) on the number of germinated seedlings under low sulfate conditions, 10 mg L^{-1}, (empty symbols), and high sulfate conditions, 300 mg L^{-1} (filled symbols). Error bars depict one standard deviation ($n = 10$)

Plant potential survival

Plant potential survival was similar in all populations in 2015, but then declined in high sulfate conditions and increased or remained relatively constant in low sulfate conditions. In high sulfate conditions, the number of potential survivors dropped precipitously between the 2nd and 3rd generations of the experiment (2015-2016) from 100 to ~4-25, except for populations that received an iron amendment and had litter

removed (Fig 12a). Populations in elevated sulfate that also received iron amendment usually had a higher number of potential survivors compared to populations that did not receive iron (Fig. 12a, Table 4), although the magnitude of iron's effect varied from year to year. Iron's beneficial effect on potential survival was most prevalent in 2016, when populations receiving iron were 3-20x higher than populations without iron. Large variance within treatments made it challenging to distinguish consistent effects of litter. In low sulfate conditions, the average number of potential survivors ranged from 100-250 (Fig 12b). Neither iron nor litter was consistently associated with increased potential survival in low sulfate conditions (Table 4).

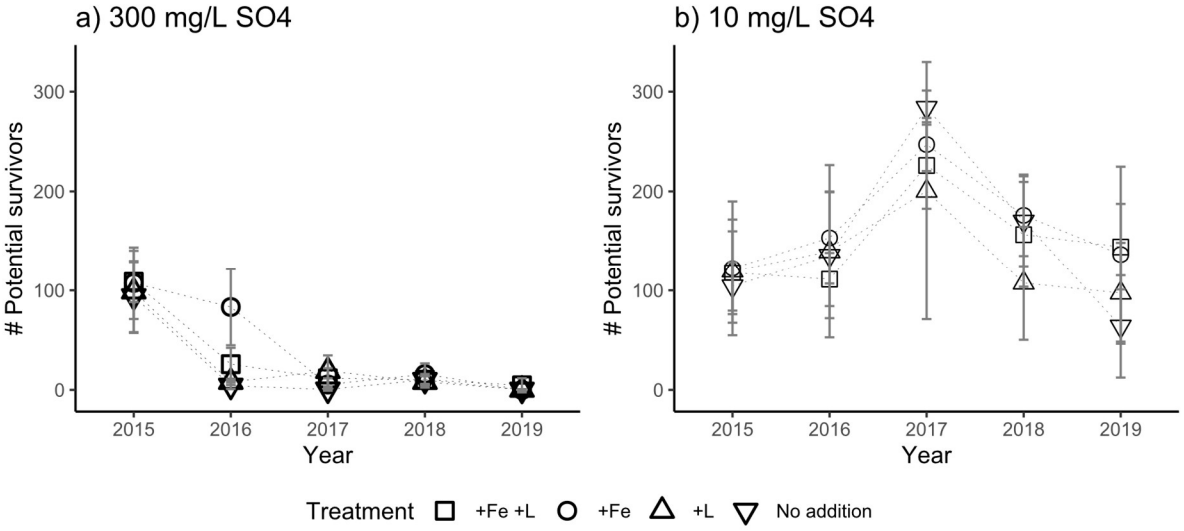

Figure 12. The effect of iron and litter on the number of potential surviving plants in a) high sulfate conditions, 300 mg L^{-1}, and b) low sulfate conditions, 10 mg L^{-1}, over six generations. Error bars represent one standard deviation around the mean (n = 5).

Seeds

In high sulfate conditions, the proportion of filled seeds declined from 80% to nearly zero (Fig 13a). Five to seven sulfate-amended populations out of 20 produced no seeds at all in 2016 and 2017. By 2019, only three sulfate-amended populations out of 20 produced any seeds. Sulfate-amended populations that received iron amendment had a

20% higher filled seed ratio for 2015-2017 (p = 0.001, Table 4), but the effect of iron diminished in 2018 and by 2019 the proportion of filled seeds in both populations with and without iron was less than 0.1. Litter did not affect seeds in high sulfate conditions. In low sulfate conditions, the proportion of filled seeds fluctuated between 0.75 and 0.9 and was not affected by iron or litter (Fig 13b, Table 4).

The average mass per filled seed was increased by iron (p = 0.03) when both high and low sulfate conditions were considered together. In high sulfate, average mass per filled seed decreased from about 25 mg to about 4 mg over six years (Fig 13c) but experienced the largest decline in the sixth year. Iron increased the average mass of individual seeds by approximately 40% in 2016 and continued to increase the average mass by 20-30% until 2019 (p = 0.09, Table 4). In low sulfate conditions, individual seed mass increased from about 30 mg to 40 mg and was relatively unaffected by litter and iron.

Like the filled seed ratio and average individual seed mass, population seed mass declined in high sulfate and remained roughly constant in low sulfate. Although both filled seed ratio and average mass per filled seed were increased in populations receiving sulfate and iron amendments, compared to populations receiving sulfate only (p = 0.01, p = 0.09 respectively), the population seed mass was not consistently increased by iron amendment (Table 4). In low sulfate conditions, seed mass was between 15-20 g except in 2018, when population seed mass increased above 30 g (Fig 13f). This increase in population seed mass during 2018 was not paralleled by increases in filled seed ratio or individual seed mass, indicating that it results from an increase in the number of seeds produced by the population.

Interpretation of seed data for high sulfate conditions is complicated because populations generally produce a small number of plants with a large seed mass due to reduced competition as populations approach extinction. In the latter half of the experiment, each year's average represents a combination of many populations with low seed mass and a few populations with very high seed mass (Fig 13e).

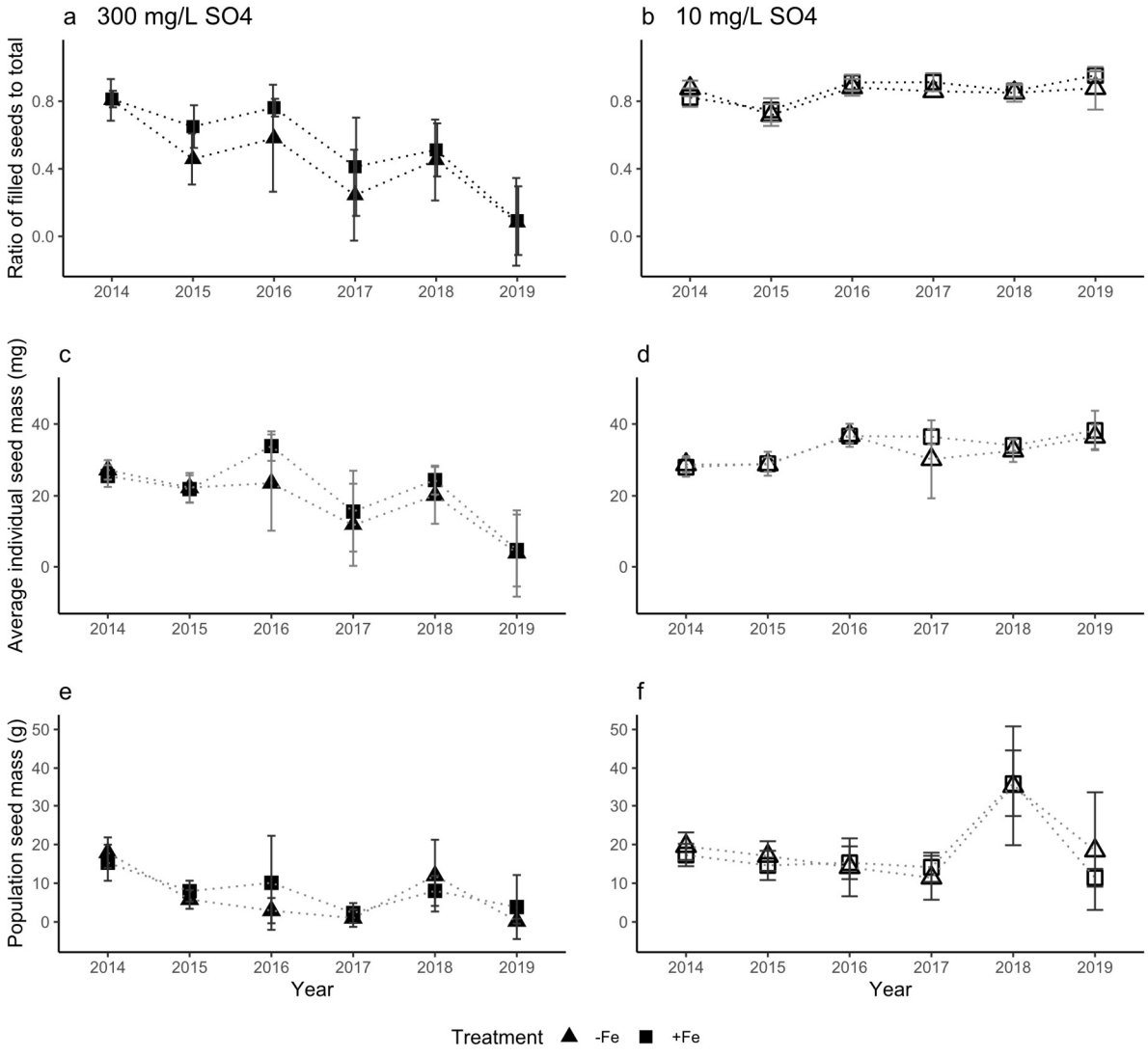

Figure 13. Effect of iron on filled seed ratio (a,b), average seed mass (c,d), and population seed mass (e,f) in high sulfate conditions (300 mg/L sulfate, a,c,e) and low sulfate conditions (10 mg/L, b,d,f). Squares depict populations that received an iron amendment, and triangles depict populations that did not receive additional iron. Error bars represent one standard deviation around the mean (n = 10).

Biomass

In high sulfate conditions, biomass steadily declined from about 45 g to extinction (Fig 14). In 2017, four years into the experiment, eight out of the 20 populations receiving high sulfate loadings produced no biomass regardless of iron addition and litter removal. Seven populations recovered, possibly from the germination of seeds from previous years buried in the sediment, and produced biomass in 2018, but by 2019, 16 out of these 20 populations produced no biomass. In low sulfate conditions, populations showed a stable three-year cycle of biomass (Fig 14) that oscillated between about 30-75 g on average. In both high and low sulfate conditions, populations produced their maximum biomass in 2018. In high sulfate conditions, this was surprising given that germination was very low in 2018. Biomass was not consistently influenced by iron and litter (Table 4).

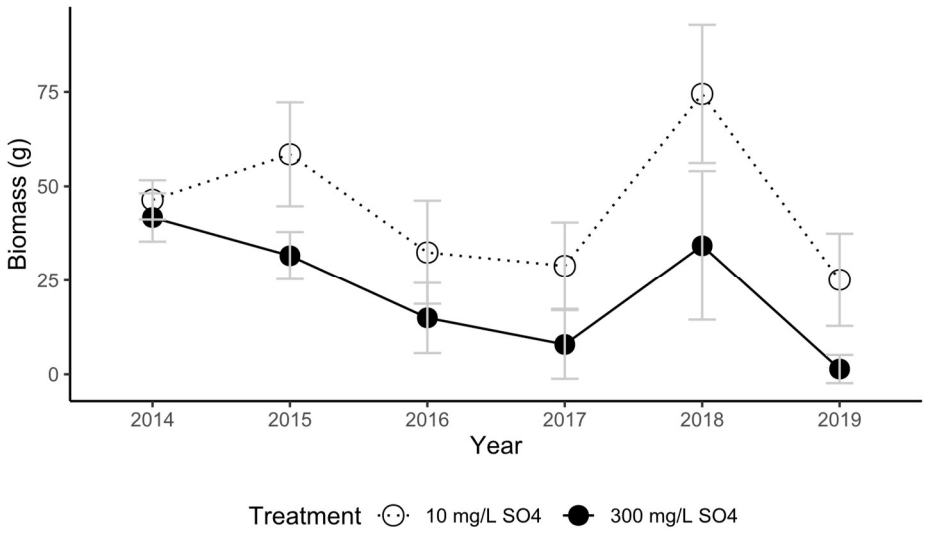

Figure 14. Annual average vegetative biomass (g) in populations grown in high sulfate (300 mg L^{-1}, filled circles) and low sulfate (10 mg L^{-1}, empty circles) in the overlying water. Error bars depict one standard deviation around the mean (n = 20).

Iron amendments appear to have marginally alleviated some of the effects of sulfide, but not consistently enough to delay extinction. In our high sulfate conditions, we maintained sulfate concentrations in the surface water 30x higher than the low sulfate conditions, while we only added 3x iron addition for the first growing season out of concern for Fe^{2+} toxicity. Our results demonstrated only occasional or temporary evidence of iron alleviating effects of sulfide on wild rice populations. We did not find evidence of litter affecting populations differently in high and low sulfate conditions.

In low sulfate conditions, litter removal did not change biomass oscillations, because root litter drives the biomass oscillations (Pastor and Walker, 2006). In high sulfate conditions, we expected that returning the litter would increase organic carbon available for microbial sulfate reduction, and subsequently increase sulfide and decrease biomass. We did not observe evidence of decreased biomass in treatments with litter returned. We did not measure mass of root litter or nitrogen concentration in root litter, but decreases in both root growth and nitrogen uptake in response to sulfate loadings have been documented in white rice, a physiologically similar plant (Armstrong and Armstrong, 2005; Koch et al., 1990). If root growth was inhibited in elevated sulfate and shoot litter was removed, the amount of nitrogen recycled in litter may have successively decreased. Low availability of nitrogen in root litter in addition to decreased uptake caused by sulfide would result faster declines in potential survival, biomass, and seed production (Figs 12-14). Further work could consider how sulfide influences the mass and N content of root litter and how that affects biomass oscillations.

Interannual effects

When changes in biomass are regressed against the biomass of the previous year, population oscillations can be examined for stability (Walker et al., 2010). If the slope of this regression is less than -1 (steeper), the population undergoes stable oscillations. If the slope is between -1 and 0, the population undergoes dampened oscillations that will eventually converge on a stable point. In low sulfate conditions, biomass oscillations are stable, as indicated by the slope of -1.24 for years 2015-2018 (Fig 15a) and consistent biomass (t-1) of between 25 and 75 g. Using the regression from 2015-2018 data, one four-year period of the productivity cycle for wild rice, the changes in population biomass for individual populations from 2018 to 2019 fall on or near the linear model. These findings are consistent with previous studies that show wild rice undergoes litter-driven productivity cycles. Although litter was removed in half of the low sulfate populations, these populations still cycled, potentially because root litter has a higher concentration of nitrogen and is more recalcitrant, causing it to drive oscillations more than the relatively more labile shoot litter (Walker et al., 2010).

In high sulfate conditions, a slope of -0.9 for year 2015-2018 indicates dampened oscillations (Fig 15b). Biomass decreased every year except for 2018, when the populations partially recovered. The change in biomass from 2018 to 2019 was not well predicted by the linear model from 2015-2018 data. Instead, almost all points fell on the line $y = -x$, indicating that populations lost the entirety of the biomass produced the previous year (Fig 15b). Rather than shifting the average biomass of the cycle to a lower, stable value (hypothesis Fig. 9a), the trajectory of biomass over time appears to decrease in the presence of sulfate (hypothesis Fig. 9b).

In low sulfate concentrations, biomass peaked in 2015 and 2018. In high sulfate concentrations, biomass decreased rather than peaking in 2015. Because we only have six years of data for a population that normally oscillates on 3-4 year periods, and most populations went extinct during that time period, it is difficult to determine whether populations are experiencing dampened oscillations or whether another mechanism suppressed the 2015 peak or created a peak in 2018 for high sulfate conditions.

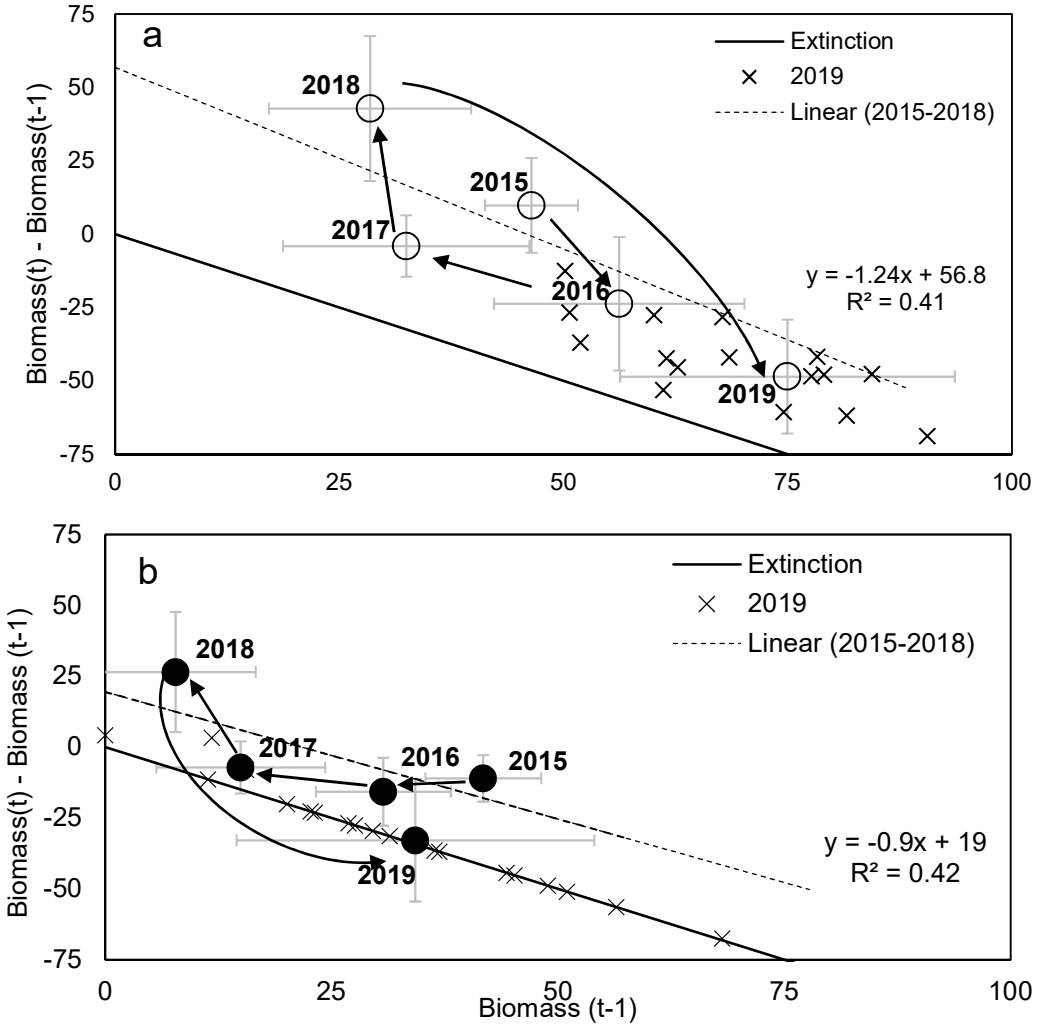

Figure 15. The relationship between the change in biomass to the previous year's biomass in a) 10 mg L^{-1} sulfate and b) 300 mg L^{-1} sulfate. Biomass is measured in grams. The slope represents the eigenvalue. A negative slope with a magnitude larger than 1 indicates stable oscillations and a negative slope with magnitude between 0 and -1 indicates dampened oscillations.

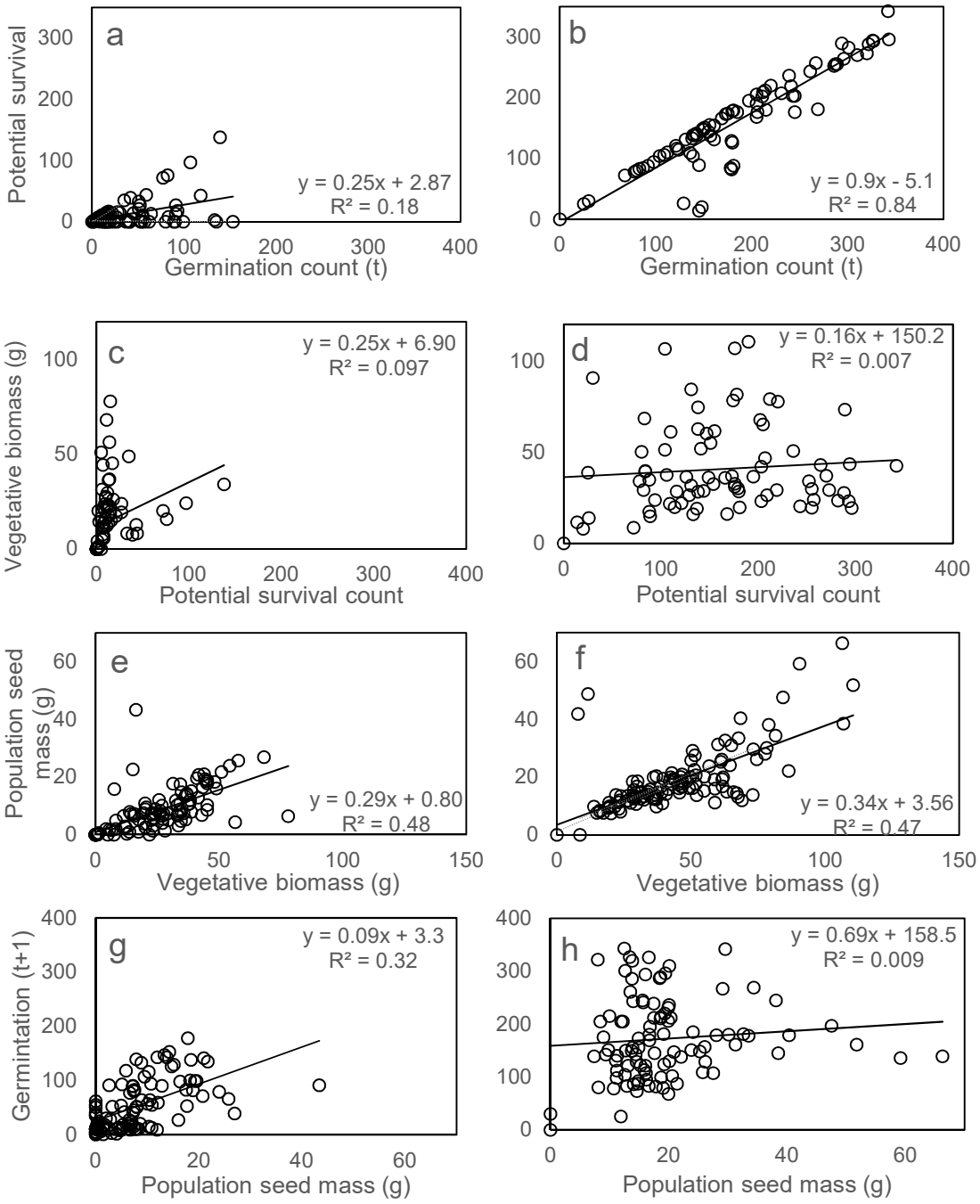

Figure 16. The correlation of four major population traits with the trait that occurs next in the life cycle; a, b) germination and potential survival, c,d) potential survival and vegetative biomass, e,f) vegetative biomass and seed biomass, and g,h) seed biomass and germination the subsequent year. These correlations are examined in high sulfate conditions (300 mg L^{-1}, a, c, e, g) and low sulfate conditions (10 mg L^{-1}, b, d, f, h). Trends are examined for data from 2014-2019.

It is clear from the divergence in the average biomass quantity in our experimental tanks that sulfur decreases wild rice population biomass. While some evidence of the mechanisms of the means by which sulfur impacts rice life stages has been gleaned in prior experiments (seedling emergence from the water column, Pastor et al., 2017; N-uptake/delays, LaFond-Hudson et al., 2020, 2018), here we investigate explicitly how sulfur geochemistry affects the progression of life stages within a population.

Here we examine the relationship between consecutive life stages (broadly speaking) in high and low sulfate conditions (Fig 16). First, in high sulfate conditions, the correlation between germination and potential survival is not strong, the slope is low on average, and the slope varies between individual years (Fig 16a). In low sulfate conditions, germination is highly correlated with potential survival and the slope is 0.9, indicating potential survival of nearly all germinated plants (Fig 16b). The relationship between potential survivors and vegetative biomass is unpredictable in high and low sulfate, possibly due to density-size relationships, but low sulfate populations usually have more potential survivors and higher biomass (Fig. 16c, 16d). Vegetative biomass is well correlated with seed mass, with R^2 coefficients ~0.5, in both high and low sulfate (Fig. 16e, 16f). However, the slopes predict that for every gram of vegetative biomass in high sulfate, 0.29 g of seed mass is produced, while in low sulfate, 0.34 g of seed mass is produced. Because vegetative biomass in low sulfate conditions is, on average, nearly twice as high as vegetative biomass in high sulfate conditions, the population seed mass is more than double that found in low sulfate conditions. Finally, the total population seed mass is correlated with the number of germinated seedlings the subsequent year in high

sulfate, whereas in low sulfate, the population seed mass does not appear to affect germination the following year (Fig. 16g, 16h). Populations exposed to low sulfate rarely produced less than ten grams of seed mass, whereas many populations in high sulfate produced less than ten grams of seeds, particularly in later years. This suggests there may be a threshold value for seed mass, above which additional seed mass does not matter. The average mass of a single seed is approximately 30 mg, so to produce 30 plants, the number of plants in our mesocosm that maintains optimal density, the population is required to produce only approximately one gram of seeds assuming that all seeds germinate and survive. However, the slope of the relationship between seed mass and germination is 0.09 in the presence of elevated sulfate, suggesting that maintenance of a population of 30 plants requires approximately ten grams.

Elevated sulfate drives interannual biomass trajectories towards extinction by disproportionately impairing potential survival and seed production. Our findings are consistent with previous work on sulfide toxicity to wild rice. According to previous hydroponics experiments, sulfide does not decrease germination, but prior mesocosms experiments indicated that seedling survival and seed production are the life stages most vulnerable to sulfide (Pastor et al., 2017). Nitrogen uptake mainly occurs during June as seedlings are emerging from the water surface and during late August, early September as the plants produce seeds (Grava and Raisanen, 1978), so the life stages controlled by sulfide are the life stages during which wild rice takes up the majority of its nitrogen. Examination of the progression of life stages shows that sulfate disrupts the correlation between germination and potential survival the most (Fig 16). Our examination of the correlation between vegetative biomass and seed production may capture the process of

nutrient translocation from leaves to seeds, but because plants take up additional nitrogen from the sediment during seed production, this analysis does not fully capture the sensitivity of reproduction to sulfide. However, we previously demonstrated that nitrogen uptake is inhibited during seed production at similarly high sulfate concentrations (LaFond-Hudson et al., 2020, 2018). Sulfide may also disproportionately affect seedling survival and seed production because photosynthetic rates may be lower during seedling growth than mid-season growth, and photosynthesis likely slows when plants begin to translocate nutrients to seeds during reproduction, resulting in lower radial oxygen loss from plant roots to oxidize sulfide.

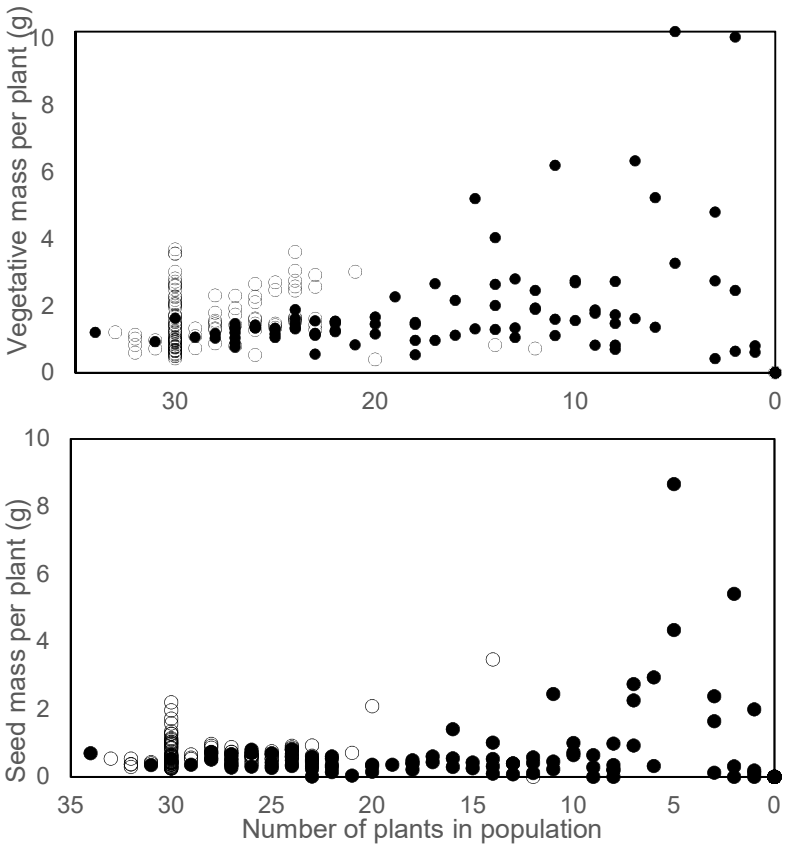

Figure 17. The change in individual plant mass and seed mass per plant as the number of plants per population approaches extinction. Filled circles indicate populations exposed to high sulfate (300 mg L^{-1}) and empty circles indicate populations exposed to low sulfate (10 mg L^{-1}).

Additional observations

We have noticed an unusual temporal pattern in sulfate-amended populations as they approach extinction. As the number of plants in the population declines to less than 10 plants, some plants are unusually large with vegetative and seed biomasses double or triple that of the average individual biomass (Fig 17a, b). Generations with these few, but large, plants are usually followed by extinction the following year, regardless of the total number of generations elapsed prior to extinction. These very large plants resulted in very high variance in biomass and seed measurements just prior to extinction. The increased variance made it difficult to interpret our repeated measures ANOVAs, potentially concealing the effect of variance due to iron amendment or litter removal.

We suggest a couple hypotheses for this curious pattern, starting with a simple ecological explanation. As the density of plants in a population decreases, competition between individuals is reduced (Lee, 2002). If the pool of nutrients available to individual plants increases enough, it may outweigh the inhibitory effects of sulfide on nutrient uptake. Another possibility, which may act in conjunction with reduced competition, is that sulfate addition increases decomposition and eutrophication (Lamers et al., 1998). In another wild rice mesocosm study, using the sediment from the same source, sulfate depletion from the surface water was correlated with increased DOC, nitrogen, and phosphorus concentrations in the surface water (Myrbo et al., 2017b). It seems plausible that both an increase in available nutrients and a decrease in competition would lead larger plants that survive to have greater seed mass. The subsequent extinction of the population the following year may be related to immobilization of nutrients in the biomass produced by these large plants. Many populations were productive in 2018, and

most went extinct in 2019. Several populations went extinct earlier (2016-2017), but recovered in 2018, possibly because the nitrogen contained in the litter was mineralized to plant-available ammonium and possibly because of delayed germination of seeds two-years old or older that had been stored in the sediment. We do not know whether or for how long sulfate-amended populations will continue to oscillate in conditions in which low points of the cycle reach zero. Further studies could explore whether this pattern occurs in other populations exposed to elevated sulfate or eutrophic conditions.

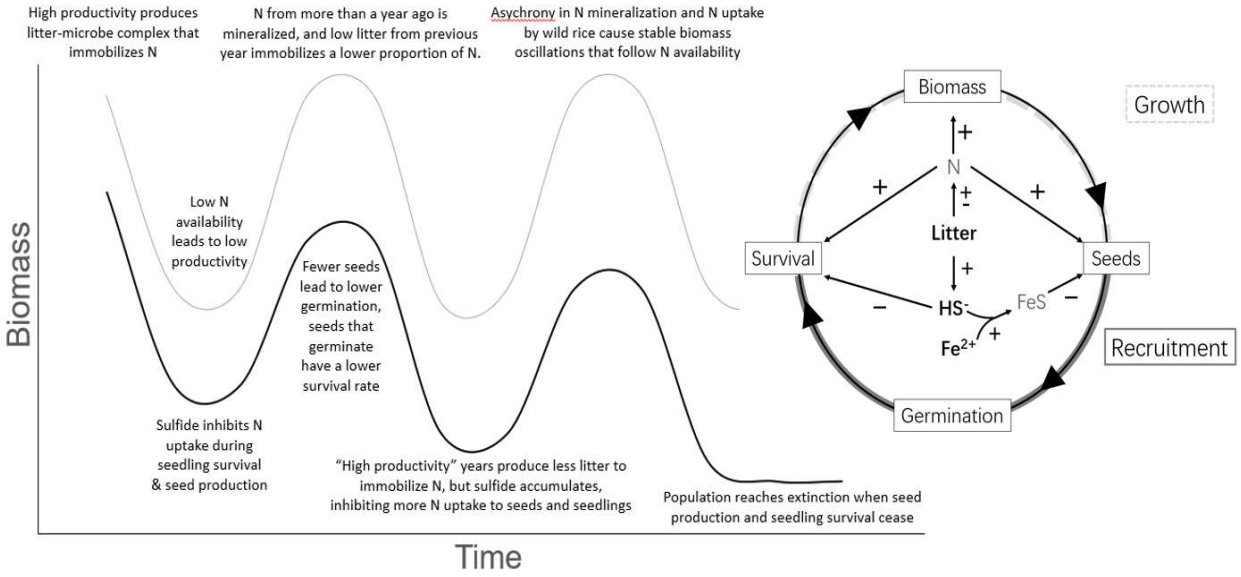

Figure 18. Diagram explaining how nitrogen, litter, sulfur and iron affect the wild rice life cycle and interannual biomass cycles.

CONCLUSION

The hypothesized cumulative effect of geochemistry on wild rice populations is depicted in Figure 18. In low sulfate conditions, high biomass production one year leads to large of amount of litter that immobilize nitrogen and decrease nitrogen availability the following year. The lower nitrogen availability then creates competition among seedlings for scarce nitrogen. Biomass production and seed production are also lowered as a result

of lower available nitrogen. As root litter slowly decays, it releases nitrogen the subsequent year (t+2), and thereby increases seedling survival, biomass, and seed production. These delays in nitrogen release from litter demonstrate that litter has alternating positive and negative effects on the wild rice life cycle. When sulfate is added to the system, production of sulfide directly decreases seedling survival and seed production. At the levels of experimental sulfate addition we used, apparently sulfur impacts are larger than the effects from changes to N availability, causing the populations to quickly decrease. When decreased seedling survival and seed production is sustained due to constant sulfate loading, germination and biomass both decrease. Iron precipitates sulfide into stable, unreactive iron sulfide, alleviating some of the effects of sulfide on seedling survival and seed production. However, unless iron concentrations are continued at levels sufficient enough to precipitate most of the sulfide, its beneficial effects on wild rice populations appear marginal.

Our work suggests that geochemical context should be considered when studying population cycles. Litter-driven cycles have already been demonstrated in other plant species, both terrestrial and aquatic. We have demonstrated that sulfate addition can decrease the productivity of wild rice within one generation and over several generations; sulfide toxicity overpowers the stable litter-driven cycles, driving the populations to extinction. Extinction of wild rice occurs despite evidence that sulfate can increase mineralization of organic matter and increase nutrient availability. The ways these geochemical mechanisms affect population cycles will likely depend on the individual's life cycle patterns and the patterns of the population cycle, factors that may be informed by understanding the natural history of species. Perhaps other species more tolerant of

sulfide will benefit from increased nutrient availability. Understanding how populations respond to geochemical conditions will improve efforts to understand community composition, competition, conservation, and restoration.

Chapter 5: Concluding thoughts

Micro-biogeochemical processes occurring at steep redox gradients surrounding roots have implications cascading into population stability. Accumulation of sulfide on the root surface during seed production occurred concomitantly with inhibited nitrogen uptake in wild rice at a time when the plant needed nitrogen to fill out seeds. In addition to inhibiting nitrogen uptake, sulfide also delayed reproductive life stages (and possibly earlier life stages), but did not delay senescence, causing seed production to be shortened. On a population scale, decreased seed production in elevated sulfate led to lower germination rates. Compounding this, fewer seedlings survived, leading to an overall decline in biomass over six years. Populations in low sulfate went through stable productivity oscillations characteristic of wild rice, whereas populations in high sulfate declined to extinction.

Iron sulfide accumulation on roots occurred only in the presence of elevated sulfate, but conditions with low sulfate also showed evidence of a change in redox potential at the root surface during seed production. This redox shift in both high and low sulfate conditions suggests the geochemical mechanism of iron sulfide accumulation on roots is controlled by plant mechanisms, likely a decrease in the oxygen released by roots when the plant enters reproductive life stages. Plant phenological control of geochemistry is described by a few other studies in aquatic ecosystems that observed changes in radial oxygen loss and sulfur geochemistry on timescales corresponding to the life cycle of the dominant vegetation (Hines et al., 1989; Soana and Bartoli, 2013). The consequence of phenological control of geochemistry is that geochemical conditions may be especially harmful during certain life stages, and the extent of toxicity experienced during these life

stages can control the overall response of the population. In the case of wild rice, we saw that the shortening and inhibiting of nitrogen uptake during seed production by sulfide was responsible, along with decreased seedling survival, for destabilization and extinction of the population in just a few generations. Further modeling could tell us how life stage fitness affects subsequent life stage fitness and the sensitivity of each of these life stage relationships to sulfide. We tested sulfate concentrations well above normal for natural systems that support healthy wild rice, but evidence suggests that cumulative loading of lower sulfate concentrations can lead populations to extinction, but at a slower rate (Johnson et al., 2019).

Our experiments with wild rice did not clearly illustrate when iron alleviates sulfide availability and subsequent toxicity, and when it does not. Iron increased potential plant survival and several seed traits including filled seed ratio and individual seed mass, but iron did not increase the population biomass or seed mass, indicating that its ameliorating effects were not enough to prevent a population decline. Field studies show that sulfide's effect on vegetation is mitigated in aquatic ecosystems receiving iron-rich groundwater inputs (Lamers et al., 2002; Ng et al., 2017). Our bucket and mesocosm experiments removed any mechanisms involving groundwater hydrodynamics and chemical inputs. The small amount of iron added, relative to the amount of sulfate added, may have minimized iron's effects on sulfide and plants. In contrast to studies that suggest iron protects plants from sulfide, our experiments showed that iron precipitated with sulfide on root surfaces, an event associated with decreased nitrogen uptake by the plant. Because ferrous iron can be toxic at high concentrations and because iron oxides at the root surface were reduced during the transition into seed production, perhaps toxic

effects also occur from elevated ferrous iron during a sulfide-induced precipitous decline in redox potential. Root surface geochemistry during transitions from oxic to anoxic conditions bear further study.

The drivers of fluctuating oxygen and organic matter concentrations in the rhizosphere are also poorly understood. Much work on radial oxygen loss has focused on quantifying locations of oxygen release (apical meristems, root hairs, etc.) and amount of oxygen released. Some work has quantified diurnal variations in radial oxygen loss and associated geochemical patterns, but patterns of radial oxygen loss throughout the growing season of plants are not well described, let alone the drivers of these patterns. The extent of rhizosphere oxidation likely also depends on the amount and lability of organic matter present to consume rhizosphere oxygen. One study observed increased sulfate reduction rates during growth of *Spartina alterniflora* and decreased rates when growth stopped (Hines et al., 1989). They attribute this geochemical pattern to growth-related root exudates. Although this contrasts our results in which sulfide accumulated when the plant stopped growing, this may be due to differing physiology between the two species. In addition to having biological phenology, plants may also have geochemical phenology, patterns of release of elements or compounds into their environment. Release of both oxygen and DOC from roots are dependent upon plant physiology, which is governed by its developmental stage. Understanding the geochemical phenology of keystone species may lead to better success in restoring aquatic plants in habitats dealing with contaminants.

The conclusions of this dissertation and other work preceding it make clear the mechanisms behind the population declines of wild rice at elevated levels of sulfate. In

the context of wild rice conservation and restoration, both surface water and sediment chemistry are important, but natural resource managers should consider that geochemical conditions in the surface water and bulk sediment often do not reflect the geochemical conditions at the root surface. This introduces challenges in monitoring, as the best way to sample root surface chemistry is to sacrifice plants. Electrodes that can be placed at the root surface may provide a nondestructive alternative but using these in the field provides other challenges such as identifying when the electrode is at the root surface and accessing roots in sediment under a water column several feet deep. Another challenge in restoration is that we do not well understand how sulfate's effects may compound other threats to wild rice. Climate change is a concern for wild rice as it increases intensity of storms and floods that may uproot plants. If sulfate inhibits root growth in wild rice as it does in white rice, plants may uproot more easily. Floods may dilute and flush sulfate out of a wild rice ecosystem, though more frequent wetting and drying could mobilize sulfide stored in anoxic riparian soils. Increased temperatures and CO_2 concentrations may increase photosynthesis and radial oxygen loss, but they may also increase release of DOC from the roots and increase rates of sulfate reduction. Besides climate change, invasive species also threaten wild rice. Invasive species may have less sensitivity to sulfide or different patterns of radial oxygen loss that give them a competitive advantage in wild rice ecosystems experiencing sulfate stress.

Although the practicality of this research for conserving and restoring wild rice is apparent, these findings have broader applications. Understanding interactions of radial oxygen loss, nutrient uptake, precipitation of minerals on root surfaces, and asynchronies in mineralization can inform phytoremediation efforts and the efficiency of constructed

treatment wetlands. As humans continue to perturb biogeochemical cycles, understanding the mechanisms by which elements are transformed in natural vegetated aquatic environments is crucial for understanding ecosystem resilience and change. The key to succeeding in any of these endeavors is to understand deeply both the geochemical mechanisms and the plant physiology, life history, and population dynamics. The natural history of plants is tightly intertwined with its geochemical context; the two cannot be fully understood separately.

Bibliography

Allam, A.I., Hollis, J.P., 1972. Sulfide inhibition of oxidases in rice roots. Phytopathology 62, 634–639.

Anderson, R.F., Schiff, S.L., 1987. Alkalinity Generation and the Fate of Sulfur in Lake Sediments. Can. J. Fish. Aquat. Sci. 44, s188–s193. https://doi.org/10.1139/f87-294

Armstrong, J., Armstrong, W., 2005. Rice: Sulfide-induced Barriers to Root Radial Oxygen Loss, Fe2+ and Water Uptake, and Lateral Root Emergence. Ann Bot 96, 625–638. https://doi.org/10.1093/aob/mci215

Armstrong, J., Armstrong, W., Beckett, P.M., 1992. Phragmites australis: Venturi- and humidity-induced pressure flows enhance rhizome aeration and rhizosphere oxidation. New Phytologist 120, 197–207. https://doi.org/10.1111/j.1469-8137.1992.tb05655.x

Armstrong, W., 1980. Aeration in Higher Plants, in: Woolhouse, H.W. (Ed.), Advances in Botanical Research. Academic Press, pp. 225–332. https://doi.org/10.1016/S0065-2296(08)60089-0

Bergelson, J., 1990. Life After Death: Site Pre-Emption by the Remains of Poa Annua. Ecology 71, 2157–2165. https://doi.org/10.2307/1938629

Brouwer, H., Murphy, T.P., 1994. Diffusion method for the determination of acid-volatile sulfides (AVS) in sediment. Environmental Toxicology and Chemistry 13, 1273–1275. https://doi.org/10.1002/etc.5620130808

Carlson, J., Yarbro, L.A., Barber, T.R., 1994. Relationship of Sediment Sulfide to Mortality of Thalassia Testudinum in Florida Bay. Bulletin of Marine Science 54, 733–746.

Christensen, K.K., Sand-Jensen, K., 1998. Precipitated iron and manganese plaques restrict root uptake of phosphorus in Lobelia dortmanna. Can. J. Bot. 76, 2158–2163. https://doi.org/10.1139/b98-181

Clesceri, L.S., Association, A.P.H., 2005. Standard Methods for the Examination of Water & Wastewater. American Public Health Association.

Coleman, J.S., McConnaughy, K.D.M., Ackerly, D.D., 1994. Interpreting phenotypic variation in plants. TREE 9, 187–191.

Colmer, T.D, 2003. Long-distance transport of gases in plants: a perspective on internal aeration and radial oxygen loss from roots. Plant, Cell & Environment 26.

Colmer, T. D., 2003. Aerenchyma and an Inducible Barrier to Radial Oxygen Loss Facilitate Root Aeration in Upland, Paddy and Deep-water Rice (Oryza sativa L.). Ann Bot 91, 301–309. https://doi.org/10.1093/aob/mcf114

Dacey, J.W.H., 1980. Internal Winds in Water Lilies: An Adaptation for Life in Anaerobic Sediments. Science 210, 1017–1019.

de Jong, T.J., Klinkhamer, P.G.L., 1985. The negative effects of litter of parent plants of Cirsium vulgare on their offspring: autotoxicity or immobilization? Oecologia 65, 153–160. https://doi.org/10.1007/BF00379212

DeLaune, R.D., Smith, C.J., Patrick, W.H., 1983. Relationship of Marsh Elevation, Redox Potential, and Sulfide to Spartina alterniflora Productivity. Soil Science Society of America Journal 47, 930–935. https://doi.org/10.2136/sssaj1983.03615995004700050018x

Federation, W.E., Association, A.P.H., 2005. Standard methods for the examination of water and wastewater.

Fond du Lac Band of Lake Superior Chippewa, 2018. Expanding the Narrative of Tribal Health: The Effects of Wild Rice Water Quality Rule Changes on Tribal Health. Health Impact Assessment 68.

Gao, S., Tanji, K., Scardaci, S., 2003. Incorporating straw may induce sulfide toxicity in paddy rice. California Agriculture 57, 55–59.

Geurts, J.J.M., Sarneel, J.M., Willers, B.J.C., Roelofs, J.G.M., Verhoeven, J.T.A., Lamers, L.P.M., 2009. Interacting effects of sulphate pollution, sulphide toxicity and eutrophication on vegetation development in fens: A mesocosm experiment. Environmental Pollution 157, 2072–2081. https://doi.org/10.1016/j.envpol.2009.02.024

Grava, J., Raisanen, K.A., 1978. Growth and Nutrient Accumulation and Distribution in Wild Rice 1. Agronomy Journal 70, 1077–1081. https://doi.org/10.2134/agronj1978.00021962007000060044x

Han, C., Ren, J., Wang, Z., Yang, S., Ke, F., Xu, D., Xie, X., 2018. Characterization of phosphorus availability in response to radial oxygen losses in the rhizosphere of Vallisneria spiralis. Chemosphere 208, 740–748. https://doi.org/10.1016/j.chemosphere.2018.05.180

Hansel, C.M., Lentini, C.J., Tang, Y., Johnston, D.T., Wankel, S.D., Jardine, P.M., 2015. Dominance of sulfur-fueled iron oxide reduction in low-sulfate freshwater sediments. The ISME Journal 9, 2400–2412. https://doi.org/10.1038/ismej.2015.50

Hines, M.E., Knollmeyer, S.L., Tugel, J.B., 1989. Sulfate reduction and other sedimentary biogeochemistry in a northern New England salt marsh: Salt marsh

biogeochemistry. Limnol. Oceanogr. 34, 578–590. https://doi.org/10.4319/lo.1989.34.3.0578

Jacq, V.A., Prade, K., Ottow, J.C.G., 1991. Iron Sulphide Accumulation in the Rhizosphere of Wetland Rice (Oryza sativa L.) as the Result of Microbial Activities, in: Berthelin, J. (Ed.), Developments in Geochemistry, Diversity of Environmental Biogeochemistry. Elsevier, pp. 453–468. https://doi.org/10.1016/B978-0-444-88900-3.50049-7

Johnson, E., 1969. Archeological Evidence for Utilization of Wild Rice. Science 163, 276–277.

Johnson, N.W., Pastor, J., Swain, E.B., 2019. Cumulative Sulfate Loads Shift Porewater to Sulfidic Conditions in Freshwater Wetland Sediment. Environmental Toxicology and Chemistry 38, 1231–1244. https://doi.org/10.1002/etc.4410

Jorgenson, K.D., Lee, P.F., Kanavillil, N., 2012. Ecological relationships of wild rice, Zizania spp. 11. Electron microscopy study of iron plaques on the roots of northern wild rice (Zizania palustris). Botany 91, 189–201. https://doi.org/10.1139/cjb-2012-0198

Joshi, M.M., Ibrahim, I.K.A., Hollis, J.P., 1975. Hydrogen sulfide: Effects on the physiology of rice plants and relation to straighthead disease. Phytopathology 65, 1165–1170.

Kinsman-Costello, L.E., O'Brien, J.M., Hamilton, S.K., 2015. Natural stressors in uncontaminated sediments of shallow freshwaters: The prevalence of sulfide, ammonia, and reduced iron. Environmental Toxicology and Chemistry 34, 467–479. https://doi.org/10.1002/etc.2801

Knapp, A.K., Seastedt, T.R., 1986. Detritus Accumulation Limits Productivity of Tallgrass Prairie. BioScience 36, 662–668. https://doi.org/10.2307/1310387

Koch, M.S., Mendelssohn, I.A., 1989. Sulphide as a Soil Phytotoxin: Differential Responses in Two Marsh Species. Journal of Ecology 77, 565–578. https://doi.org/10.2307/2260770

Koch, M.S., Mendelssohn, I.A., McKee, K.L., 1990. Mechanism for the hydrogen sulfide-induced growth limitation in wetland macrophytes. Limnology and Oceanography 35, 399–408. https://doi.org/10.4319/lo.1990.35.2.0399

LaFond-Hudson, S., Johnson, N.W., Pastor, J., Dewey, B., 2020. Interactions between sulfide and reproductive phenology of an annual aquatic plant, wild rice (Zizania palustris). Aquatic Botany 164, 103230. https://doi.org/10.1016/j.aquabot.2020.103230

LaFond-Hudson, S., Johnson, N.W., Pastor, J., Dewey, B., 2018. Iron sulfide formation on root surfaces controlled by the life cycle of wild rice (Zizania palustris). Biogeochemistry 141, 95–106. https://doi.org/10.1007/s10533-018-0491-5

Lai, W.-L., Zhang, Y., Chen, Z.-H., 2012. Radial oxygen loss, photosynthesis, and nutrient removal of 35 wetland plants. Ecological Engineering 39, 24–30. https://doi.org/10.1016/j.ecoleng.2011.11.010

Lamers, L.P.M., Dolle, G.E.T., Van Den Berg, S.T.G., Van Delft, S.P.J., Roelofs, J.G.M., 2001. Differential responses of freshwater wetland soils to sulphate pollution. Biogeochemistry 55, 87–101. https://doi.org/10.1023/A:1010629319168

Lamers, L.P.M., Falla, S.-J., Samborska, E.M., Dulken, I.A.R. van, Hengstum, G. van, Roelofs, J.G.M., 2002. Factors controlling the extent of eutrophication and toxicity in sulfate-polluted freshwater wetlands. Limnology and Oceanography 47, 585–593. https://doi.org/10.4319/lo.2002.47.2.0585

Lamers, L.P.M., Govers, L.L., Janssen, I.C., Geurts, J.J., Van der Welle, M.E., Van Katwijk, M.M., Van der Heide, T., Roelofs, J.G., Smolders, A.J., 2013. Sulfide as a soil phytotoxin—a review. Front. Plant Sci. 4. https://doi.org/10.3389/fpls.2013.00268

Lamers, L.P.M., Tomassen, H.B.M., Roelofs, J.G.M., 1998. Sulfate-Induced Eutrophication and Phytotoxicity in Freshwater Wetlands. Environ. Sci. Technol. 32, 199–205. https://doi.org/10.1021/es970362f

Lee, K.-S., Dunton, K.H., 2000. Diurnal changes in pore water sulfide concentrations in the seagrass Thalassia testudinum beds: the effects of seagrasses on sulfide dynamics. Journal of Experimental Marine Biology and Ecology 255, 201–214. https://doi.org/10.1016/S0022-0981(00)00300-2

Lee, P.F., 2002. Ecological relationships of wild rice, Zizania spp. 10. Effects of sediment and among-population variations on plant density in Zizania palustris. Can. J. Bot. 80, 1283–1294. https://doi.org/10.1139/b02-118

Lee, P.F., Stewart, J.M., 1983. Ecological relationships of wild rice, Zizania aquatica. 2. Sediment – plant tissue nutrient relationships. Can. J. Bot. 61, 1775–1784. https://doi.org/10.1139/b83-186

Lucassen, E.C.H.E.T., Spierenburg, P., Fraaije, R.G.A., Smolders, A.J.P., Roelofs, J.G.M., 2009. Alkalinity generation and sediment CO2 uptake influence establishment of Sparganium angustifolium in softwater lakes. Freshwater Biology 54, 2300–2314. https://doi.org/10.1111/j.1365-2427.2009.02264.x

Maisch, M., Lueder, U., Kappler, A., Schmidt, C., 2019. Iron Lung: How Rice Roots Induce Iron Redox Changes in the Rhizosphere and Create Niches for Microaerophilic Fe(II)-Oxidizing Bacteria. Environ. Sci. Technol. Lett. 6, 600–605. https://doi.org/10.1021/acs.estlett.9b00403

Martin, N.M., Maricle, B.R., 2015. Species-specific enzymatic tolerance of sulfide toxicity in plant roots. Plant Physiology and Biochemistry 88, 36–41. https://doi.org/10.1016/j.plaphy.2015.01.007

Marzocchi, U., Benelli, S., Larsen, M., Bartoli, M., Glud, R.N., 2019. Spatial heterogeneity and short-term oxygen dynamics in the rhizosphere of Vallisneria spiralis: Implications for nutrient cycling. Freshwater Biology 64, 532–543. https://doi.org/10.1111/fwb.13240

McConnaughay, K.D.M., Coleman, J.S., 1999. Biomass Allocation in Plants: Ontogeny or Optimality? A Test Along Three Resource Gradients. Ecology 80, 2581–2593. https://doi.org/10.1890/0012-9658(1999)080[2581:BAIPOO]2.0.CO;2

Mendelssohn, I.A., Kleiss, B.A., Wakeley, J.S., 1995. Factors controlling the formation of oxidized root channels: A review. Wetlands 15, 37–46. https://doi.org/10.1007/BF03160678

Misra, R.D., 1938. Edaphic Factors in the Distribution of Aquatic Plants in the English Lakes. Journal of Ecology 26, 411–451.

Molofsky, J., Lanza, J., Crone, E.E., 2000. Plant litter feedback and population dynamics in an annual plant, Cardamine pensylvanica. Oecologia 124, 522–528. https://doi.org/10.1007/PL00008877

Moyle, J.B., 1944. Wild Rice in Minnesota. The Journal of Wildlife Management 8, 177–184. https://doi.org/10.2307/3795695

Myrbo, A., Swain, E.B., Engstrom, D.R., Wasik, J.C., Brenner, J., Shore, M.D., Peters, E.B., Blaha, G., 2017a. Sulfide Generated by Sulfate Reduction is a Primary Controller of the Occurrence of Wild Rice (Zizania palustris) in Shallow Aquatic Ecosystems. Journal of Geophysical Research: Biogeosciences 122, 2736–2753. https://doi.org/10.1002/2017JG003787

Myrbo, A., Swain, E.B., Johnson, N.W., Engstrom, D.R., Pastor, J., Dewey, B., Monson, P., Brenner, J., Dykhuizen Shore, M., Peters, E.B., 2017b. Increase in Nutrients, Mercury, and Methylmercury as a Consequence of Elevated Sulfate Reduction to Sulfide in Experimental Wetland Mesocosms: SO_4 Reduction Mobilizes N, P, C, and Mercury. Journal of Geophysical Research: Biogeosciences 122, 2769–2785. https://doi.org/10.1002/2017JG003788

Natural Wild Rice in Minnesota, 2008. . Minnesota Department of Natural Resources.

Ng, G.-H.C., Yourd, A.R., Johnson, N.W., Myrbo, A.E., 2017. Modeling hydrologic controls on sulfur processes in sulfate-impacted wetland and stream sediments. Journal of Geophysical Research: Biogeosciences 122, 2435–2457. https://doi.org/10.1002/2017JG003822

Painchaud, D.L., Archibold, O.W., 1990. The effect of sediment chemistry on the successful establishment of wild rice (Zizania palustris L.) in northern Saskatchewan water bodies. Plant Soil 129, 109–116. https://doi.org/10.1007/BF00032402

Pastor, J., Dewey, B., Johnson, N.W., Swain, E.B., Monson, P., Peters, E.B., Myrbo, A., 2017. Effects of sulfate and sulfide on the life cycle of Zizania palustris in hydroponic and mesocosm experiments. Ecological Applications 27, 321–336. https://doi.org/10.1002/eap.1452

Pastor, J., Walker, R.D., 2006. Delays in nutrient cycling and plant population oscillations. Oikos 112, 698–705. https://doi.org/10.1111/j.0030-1299.2006.14478.x

Pearsall, W.H., 1920. The Aquatic Vegetation of the English Lakes. Journal of Ecology 8, 163–201. https://doi.org/10.2307/2255612

Pollman, C.D., Swain, E.B., Bael, D., Myrbo, A., Monson, P., Shore, M.D., 2017. The Evolution of Sulfide in Shallow Aquatic Ecosystem Sediments: An Analysis of the Roles of Sulfate, Organic Carbon, and Iron and Feedback Constraints Using Structural Equation Modeling. Journal of Geophysical Research: Biogeosciences 122, 2719–2735. https://doi.org/10.1002/2017JG003785

Povidisa, K., Delefosse, M., Holmer, M., 2009. The formation of iron plaques on roots and rhizomes of the seagrass Cymodocea serrulata (R. Brown) Ascherson with implications for sulphide intrusion. Aquatic Botany 90, 303–308. https://doi.org/10.1016/j.aquabot.2008.11.008

Pulido, C., Lucassen, E.C.H.E.T., Pedersen, O., Roelofs, J.G.M., 2011. Influence of quantity and lability of sediment organic matter on the biomass of two isoetids, Littorella uniflora and Echinodorus repens. Freshwater Biology 56, 939–951. https://doi.org/10.1111/j.1365-2427.2010.02539.x

Reddy, K.R., Patrick, W.H., Lindau, C.W., 1989. Nitrification-denitrification at the plant root-sediment interface in wetlands. Limnology and Oceanography 34, 1004–1013. https://doi.org/10.4319/lo.1989.34.6.1004

Risgaard-Petersen, N., Jensen, K., 1997. Nitrification and denitrification in the rhizosphere of the aquatic macrophyte Lobelia dortmanna L. Limnology and Oceanography 42, 529–537. https://doi.org/10.4319/lo.1997.42.3.0529

Ruiz-Halpern, S., Macko, S.A., Fourqurean, J.W., 2008. The effects of manipulation of sedimentary iron and organic matter on sediment biogeochemistry and seagrasses in a subtropical carbonate environment. Biogeochemistry 87, 113–126. https://doi.org/10.1007/s10533-007-9162-7

Schmidt, H., Eickhorst, T., Tippkötter, R., 2011. Monitoring of root growth and redox conditions in paddy soil rhizotrons by redox electrodes and image analysis. Plant Soil 341, 221–232. https://doi.org/10.1007/s11104-010-0637-2

Seeberg-Elverfeldt, J., Schlüter, M., Feseker, T., Kölling, M., 2005. Rhizon sampling of porewaters near the sediment-water interface of aquatic systems. Limnology and Oceanography: Methods 3, 361–371. https://doi.org/10.4319/lom.2005.3.361

Sims, L., Pastor, J., Lee, T., Dewey, B., 2012. Nitrogen, phosphorus and light effects on growth and allocation of biomass and nutrients in wild rice. Oecologia 170, 65–76. https://doi.org/10.1007/s00442-012-2296-x

Smolders, A.J.P., Lamers, L.P.M., Hartog, C. den, Roelofs, J.G.M., 2003. Mechanisms involved in the decline of Stratiotes aloides L. in The Netherlands: sulphate as a key variable. Hydrobiologia 506, 603–610. https://doi.org/10.1023/B:HYDR.0000008551.56661.8e

Soana, E., Bartoli, M., 2014. Seasonal regulation of nitrification in a rooted macrophyte (Vallisneria spiralis L.) meadow under eutrophic conditions. Aquat Ecol 48, 11–21. https://doi.org/10.1007/s10452-013-9462-z

Soana, E., Bartoli, M., 2013. Seasonal variation of radial oxygen loss in Vallisneria spiralis L.: An adaptive response to sediment redox? Aquatic Botany 104, 228–232. https://doi.org/10.1016/j.aquabot.2012.07.007

St-Cyr, L., Campbell, P.G.C., 1996. Metals (Fe, Mn, Zn) in the root plaque of submerged aquatic plants collected in situ: Relations with metal concentrations in the adjacent sediments and in the root tissue. Biogeochemistry 33, 45–76.

Stover, E.L., 1928. The Roots of Wild Rice Zizania Aquatica L. The Ohio Journal of Science 28, 7.

Sun, L., Zheng, C., Yang, J., Peng, C., Xu, C., Wang, Y., Feng, J., Shi, J., 2016. Impact of sulfur (S) fertilization in paddy soils on copper (Cu) accumulation in rice (Oryza sativa L.) plants under flooding conditions. Biol Fertil Soils 52, 31–39. https://doi.org/10.1007/s00374-015-1050-z

Tilman, D., Wedin, D., 1991. Oscillations and chaos in the dynamics of a perennial grass. Nature 353, 653–655. https://doi.org/10.1038/353653a0

Trolldenier, G., 1988. Visualisation of oxidizing power of rice roots and of possible participation of bacteria in iron deposition. Zeitschrift für Pflanzenernährung und Bodenkunde 151, 117–121. https://doi.org/10.1002/jpln.19881510209

Van der Welle, M.E.W., Niggebrugge, K., Lamers, L.P.M., Roelofs, J.G.M., 2007. Differential responses of the freshwater wetland species Juncus effusus L. and Caltha palustris L. to iron supply in sulfidic environments. Environmental Pollution 147, 222–230. https://doi.org/10.1016/j.envpol.2006.08.024

Walker, R., Pastor, J., Dewey, B.W., 2006. Effects of wild rice (Zizania palustris) straw on biomass and seed production in northern Minnesota. Can. J. Bot. 84, 1019–1024. https://doi.org/10.1139/b06-058

Walker, R.E.D., Pastor, J., Dewey, B.W., 2010. Litter Quantity and Nitrogen Immobilization Cause Oscillations in Productivity of Wild Rice (Zizania palustris L.) in Northern Minnesota. Ecosystems 13, 485–498. https://doi.org/10.1007/s10021-010-9333-6

Yost, C.L., Blinnikov, M.S., 2011. Locally diagnostic phytoliths of wild rice (Zizania palustris L.) from Minnesota, USA: comparison to other wetland grasses and usefulness for archaeobotany and paleoecological reconstructions. Journal of Archaeological Science 38, 1977–1991. https://doi.org/10.1016/j.jas.2011.04.016

Appendix

CHAPTER 2

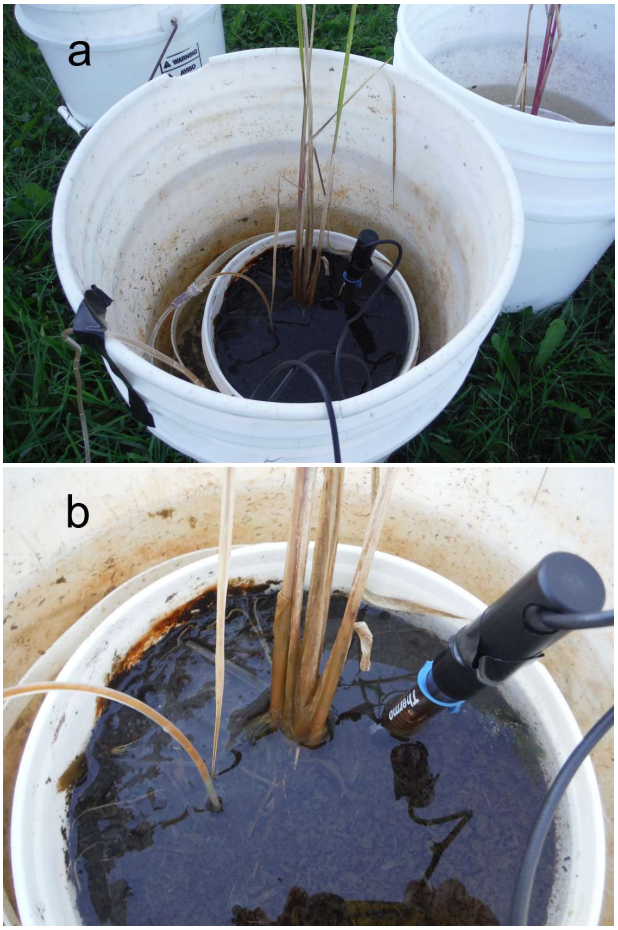

Figure S1. Bucket setup and sampling procedure. Two rice seeds were planted in a 4 L pail filled with 3 L sediment placed inside a 20 L bucket filled with 12 L of well water to create a water column height of 12-15 cm above the sediment surface (a). Buckets were thinned to one plant once shoots reached a height of 10-20 cm. Porewater was sampled the day before harvest 2 cm from the stem (b). A Rhizon was inserted vertically into the sediment to draw out porewater into a sealed, vacuumed serum bottle. On the opposite side of the stem, pH was sampled with an electrode.

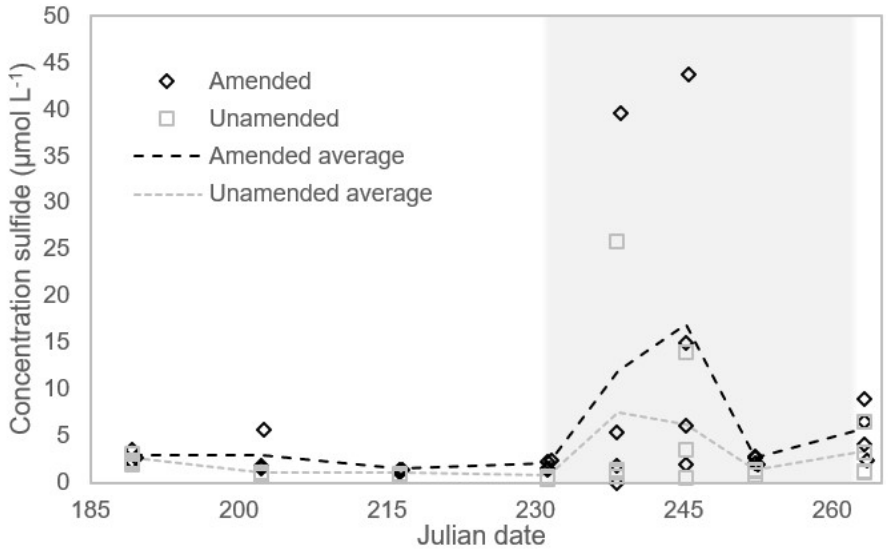

Figure S2. Seasonal measurements of porewater sulfide concentrations 2 centimeters from the root surface. Diamonds depict individual measurements for amended plants while squares depict individual measurements for unamended plants. Shading represents different life stages. Shading on left side of figure represents pre-flowering, unshaded represents flowering, and shading on right represents seed production.

Table S1. Average and standard deviation of the porewater saturation index for FeS in sulfate-amended and unamended porewaters. The K_{sp} value (Stumm and Morgan 1996) used was $10^{-2.95}$.

Date (julian)	Sulfate-amended	Unamended
177	-1.436 ± 0.228	-1.436 ± 0.228
190	-0.282 ± 0.346	-0.175 ± 0.354
203	-0.390 ± 0.189	-1.061 ± 0.204
232	-0.560 ± 0.195	-0.802 ± 0.242
239	0.099 ± 0.969	-0.232 ± 0.435
245	-0.140 ± 0.580	-0.410 ± 0.837
256	-0.302 ± 0.376	-0.365 ± 0.333
263	-0.199 ± 0.198	-0.597 ±0.581

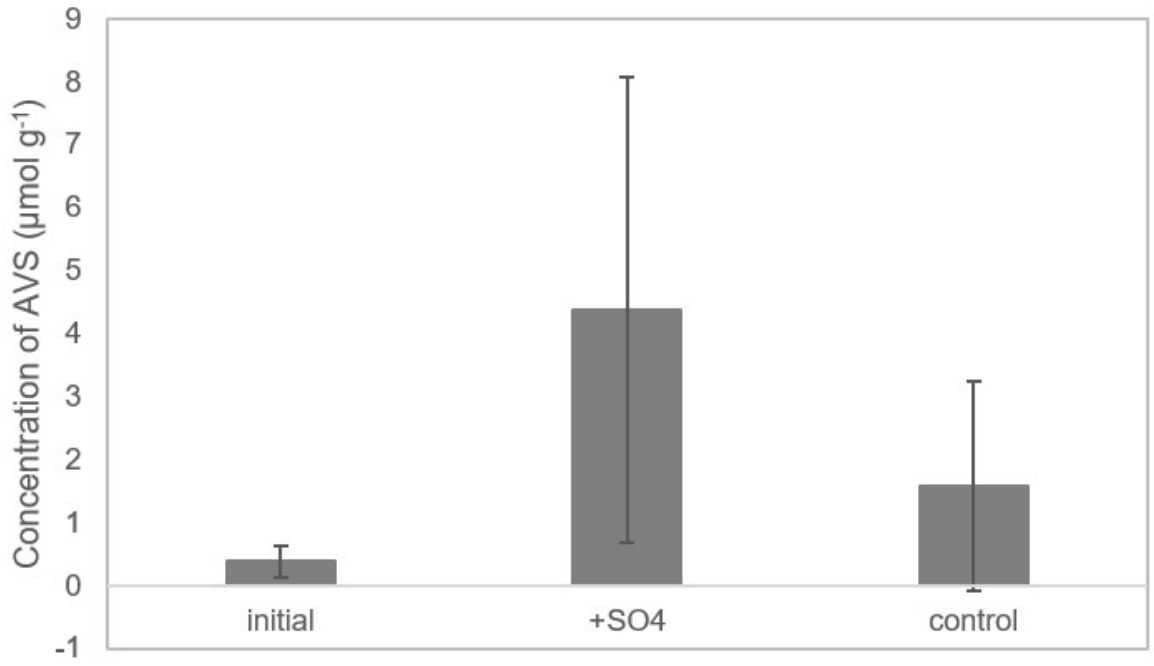

Figure S3. Bulk sediment concentrations of acid volatile sulfide (AVS) at the beginning of the growing season (initial; Julian date 149) and at the end (Julian date 264) after being exposed to surface water sulfate concentrations of either 3.1 mM (+SO4) or 0.15 mM (unamended). Error bars show the standard deviation (initial *n*=5, amended *n*=4, unamended *n*=2).

An effective redox potential for the root surface (E_H^*) was estimated throughout the growing season using root surface concentrations of Fe(III) and Fe(II). It was assumed that root Fe(III) iron oxides are reduced to dissolved ferrous iron (1) which mostly precipitates with sulfide back onto the root surface. Redox potentials are typically calculated from equations (2) and (3) using the activity of dissolved species (Stumm and Morgan 1996), but in our effective redox potential we used the concentrations of solid phase iron on root surfaces (Supplementary fig S4). While solid-phases do not represent the electron activity of a system as well as dissolved phases, the oxidation state of iron and sulfur in solid phases can indicate the redox state that led to their development.

$$FeOOH + 3H^+ + e^- \rightarrow Fe^{2+} + 2H_2O \quad (1)$$

$$p\varepsilon = 16 - 3pH + log\frac{Fe(III)}{Fe(II)} \quad (2)$$

$$E_H^* = \frac{2.3RTp}{F} \quad (3)$$

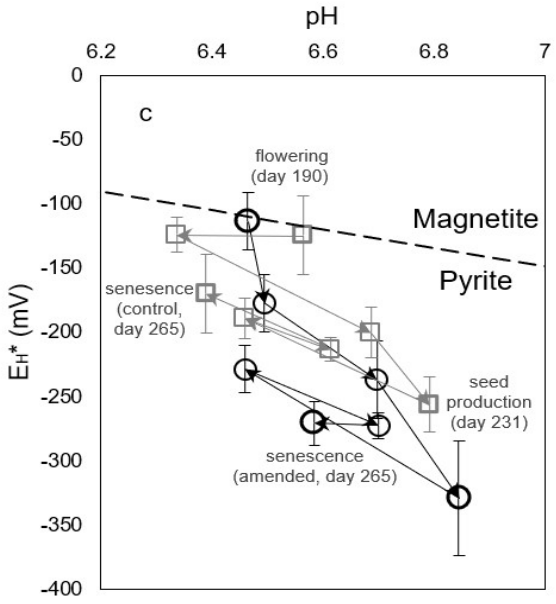

Figure S4. E_H^* (effective E_H) calculated from ferric and ferrous iron concentrations on root surfaces and pH. E_H^* is represented by black circles for amended conditions and by gray squares for unamended conditions. Arrows show the progression of E_H^* over time. Error bars represent one standard deviation of four replicates.

In both amended and unamended roots, at the observed circumneutral pH conditions, E_H^* began near the thermodynamic magnetite/pyrite boundary (Stumm and Morgan 1996), but decreased into the region of stability of FeS as the growing season progressed, especially for the amended roots. At the start of flowering, E_H^* was about -120 mV on both amended and unamended root surfaces. Throughout flowering and the beginning of seed production, E_H^* decreased and was consistently 50-75 mV lower in amended conditions. By senescence, E_H^* had decreased by 50 mV on unamended roots and by 150 mV on amended roots.

Additional methods

One day before plants were destructively sampled, porewater sulfide, porewater sulfate, porewater iron, and porewater pH were measured. Porewater was sampled using 5 cm length Rhizons attached to a vacuumed serum bottle sealed with a butyl rubber stopper. Sulfide and iron were quantified within 24 hours by spectrophotometer using the methylene blue method and phenanthroline method respectively on a HACH DR5000 UV-Vis spectrophotometer (Clesceri and Association, 2005) Porewater for sulfate analysis was filtered through a Dionex OnGuard II M cartridge and a 0.45 μm polyethersulfone filter and stored at 4 °C. Samples were quantified using a Dionex ICS-1100 Integrated IC system (AS-DV Autosampler) (Clesceri and Association, 2005).

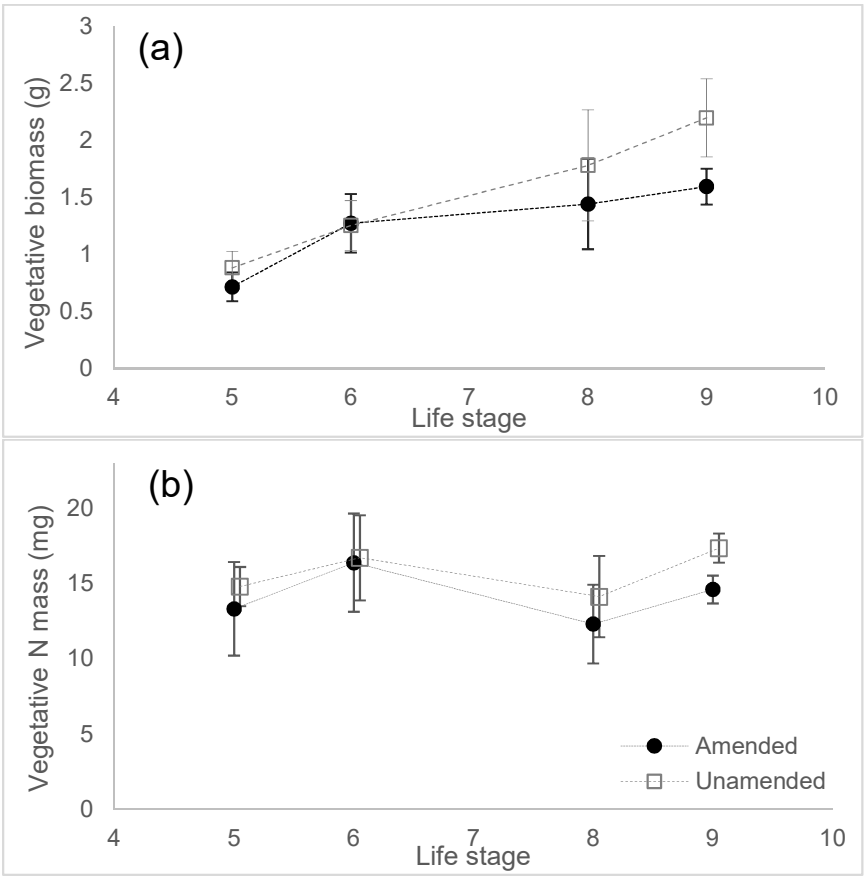

Figure S5. Average biomass (a) and vegetative nitrogen mass (b) of aboveground wild rice tissue during life stages prior to seed production. Nitrogen mass was determined by multiplying the dry weight by the N%. Error bars represent one standard deviation (n = 4).

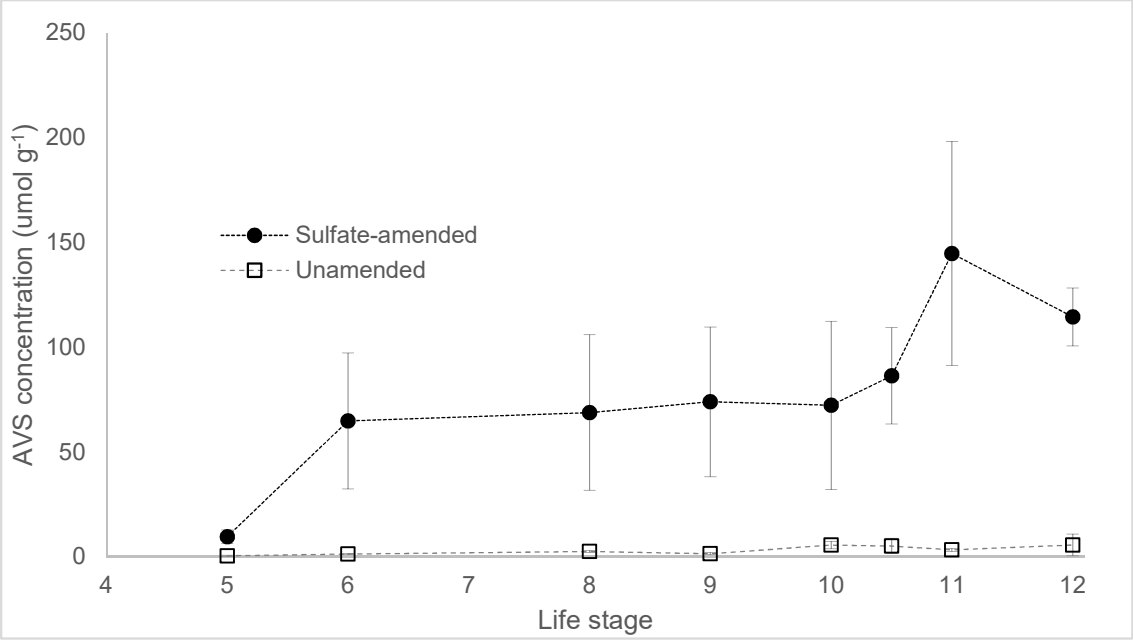

Figure S6. Average concentrations of root surface sulfide (AVS) on wild rice amended with sulfate (300 mg L^{-1}) or left unamended. Each point represents the average of four plants harvested from the same life stage. Error bars show one standard deviation.

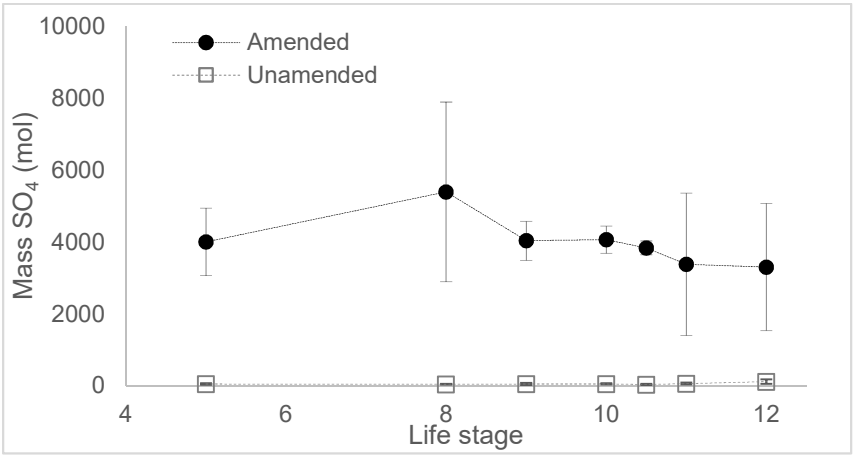

Figure S7. Average mass of sulfate in amended and unamended buckets containing plants throughout the life cycle of wild rice (n = 4). Error bars show one standard deviation.

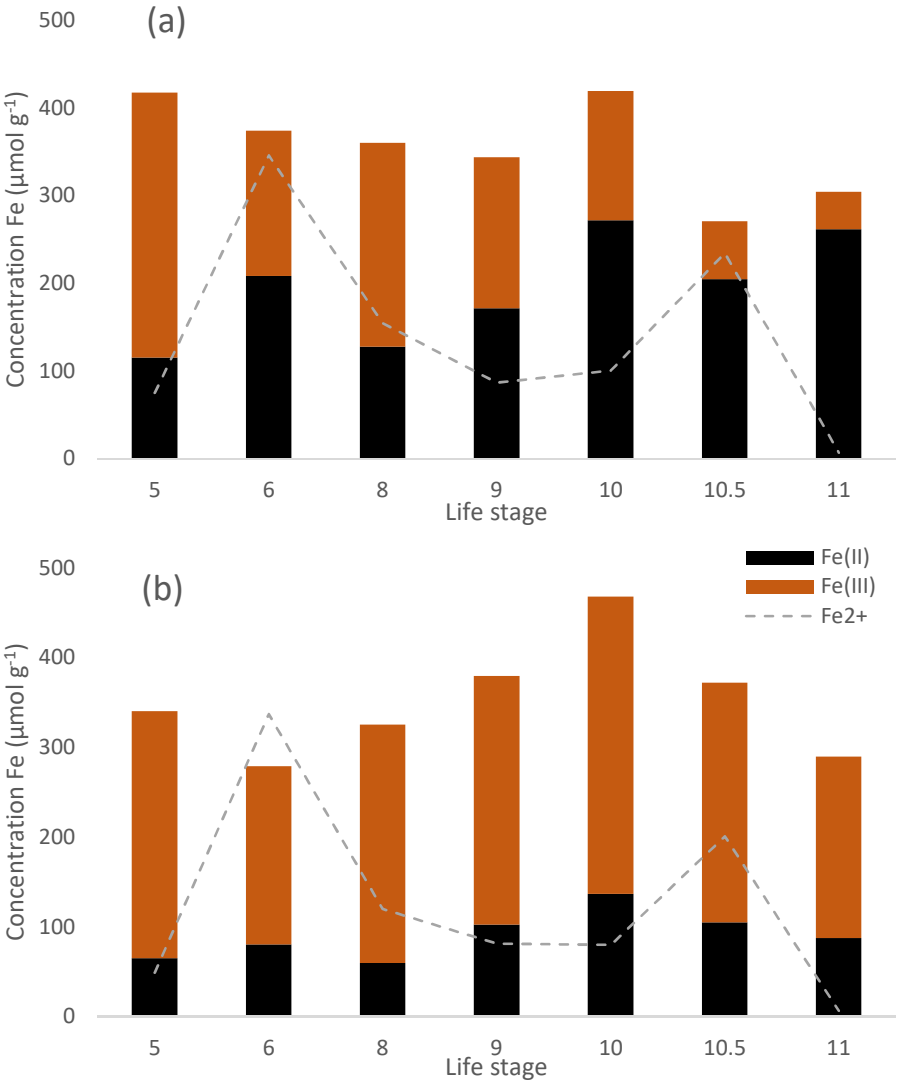

Figure S8. Speciation and average concentration of Fe(II) and Fe(III) on root surfaces of wild rice in amended plants (a) and unamended plants (b) (*n*=4). Error bars are omitted for clarity.

Table S2. ANOVAs comparing the date of last seed collection in mesocosm experiments (methods not described) with sulfate amendments to overlying water. Mesocosm experiment #1 is described in Pastor et al. 2017. Mesocosm experiment #2 will be described in Chapter 4. Average dates are given with standard deviations below.

Experiment	**Julian date of last seed collection**					***p* value**
Sulfate treatment	0 ppm	50 ppm	100 ppm	150 ppm	300 ppm	
Mesocosm # 1 (2016)	261.6 *± 6.7*	259.4 *± 7.0*	256.5 *± 7.0*	257.0 *± 6.6*		$p = 0.018$
Mesocosm # 2 (2016)	261.7 *± 6.0*				259.3 *± 6.7*	$p = 0.047$
Mesocosm # 2 (2017)	264.9 *± 4.8*				258.0 *± 9.7*	$p = 0.002$

Assuming seed production ends approximately day 260:

Unamended true duration: 260-244 = 16,

Amended true duration: 260-247 = 13,

Amended plant seed production ~20% shorter than unamended

Table S3. Geochemistry ANOVAs using rhizon measurements. Porewater chemistry was sampled using rhizons.

VARIABLE	YEAR	SULFATE	IRON	LITTER
PW sulfide (fall)	**P < 0.001**	P = 0.19	P = 0.41	P = 0.63
PW sulfide (spring)	P = 0.09	**P < 0.001**	P = 0.82	P = 0.83
PW iron (fall)	**P < 0.001**	P = 0.75	**P < 0.001**	P = 0.81
PW iron (spring)	**P < 0.001**	P =0.11	**P = 0.005**	P = 0.29
PW pH (fall)	**P < 0.001**	**P < 0.001**	**P <0.001**	P = 0.31
PW pH (spring)	**P < 0.001**	**P < 0.001**	**P <0.001**	P = 0.77
SI of FeS (fall)	**P < 0.001**	**P < 0.001**	P = 0.12	P = 0.27
SI of FeS (spring)	**P < 0.001**	**P <0.001**	P = 0.57	P = 0.18
PW SO4 (spring)	**P < 0.001**	**P <0.001**	P = 0.98	P = 0.98
PW SO4 (fall)	P = 0.14	**P = 0.002**	P = 0.49	P = 0.85

Table S4. Geochemistry ANOVAs using peeper measurements in 2019.

VARIABLE	SULFATE	IRON	LITTER
PW sulfide	**P < 0.001**	P = 0.53	P = 0.64
PW iron	**P < 0.001**	**P < 0.001**	P = 0.16
PW pH	**P < 0.001**	P =0.64	P = 0.57
SI of FeS	**P < 0.001**	P = 0.19	P = 0.96

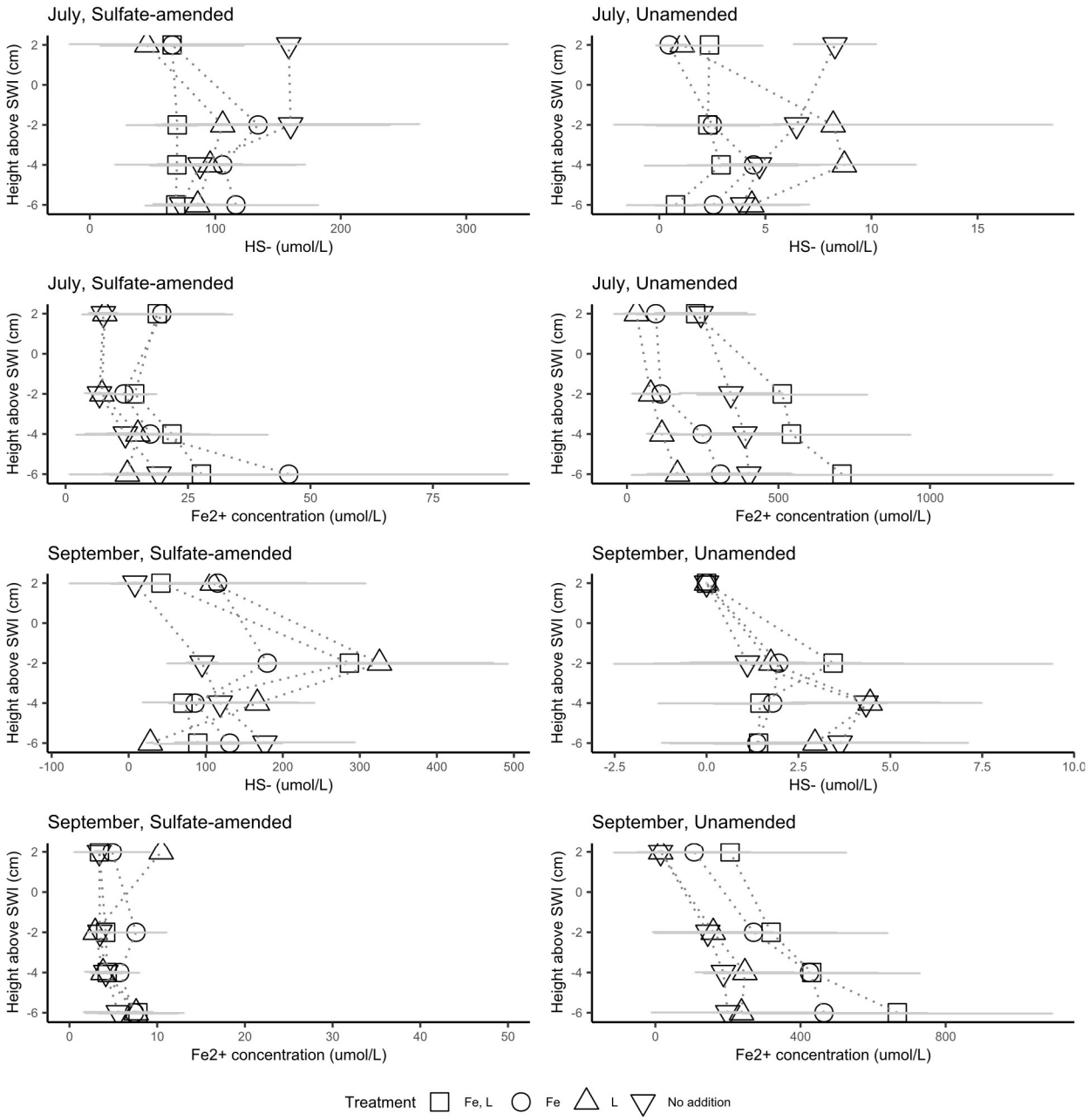

Figure S9. Depth profiles of iron and sulfide concentrations measured with peepers in July and September 2019, during the fifth generation of wild rice.

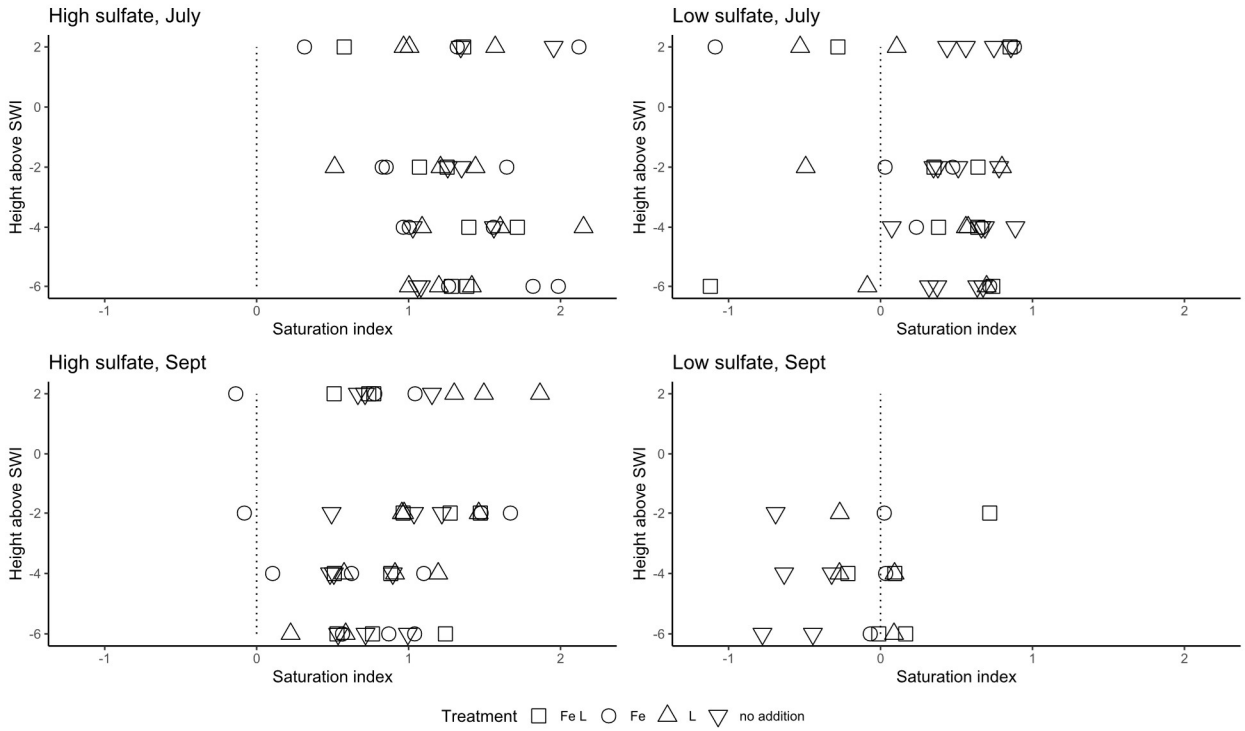

Figure S10. Saturation index with respect to FeS from peeper measurements in July & August 2019 in high sulfate and low sulfate conditions. Include Ksp (10^-3.6).

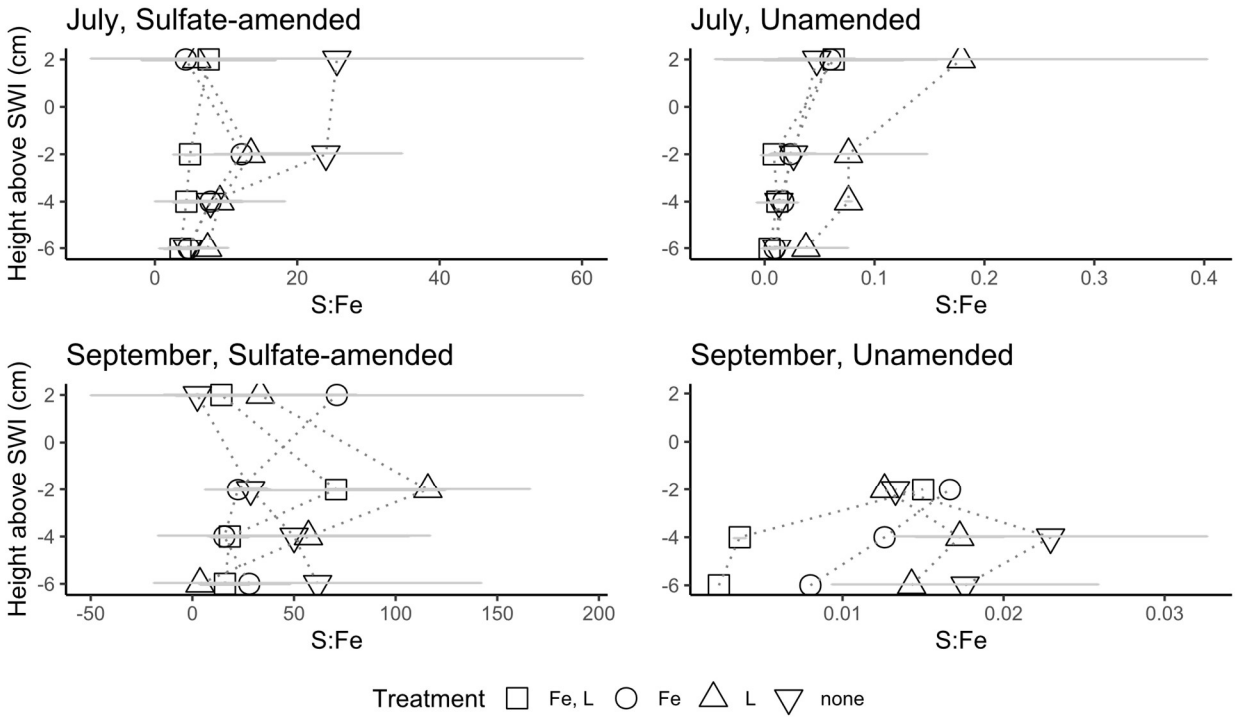

Figure S11. Aqueous HS:Fe ratios in porewater.